NOVEL INSIGHTS INTO BIOMARKER POTENTIAL AND PHYSIOLOGICAL ROLES OF ISOPROSTANES IN DAIRY CATTLE

By

Ashley Kay Putman

A DISSERTATION

Submitted to
Michigan State University
in partial fulfillment of the requirements
for the degree of

Comparative Medicine and Integrative Biology – Doctor of Philosophy

2023

ABSTRACT

Dysregulated inflammation and oxidative stress are major underlying components of dairy cow diseases, such as mastitis, that negatively impact animal health, welfare, and production. These conditions are associated with increased reactive oxygen and nitrogen species (**RONS**) production, which can overwhelm antioxidant defenses and cause severe cellular damage. Indeed, damage to tissue components such as lipids is a defining feature of oxidative stress and leads to the generation of potent inflammatory mediators known as oxylipids. A special class of oxylipid, isoprostanes (**IsoP**), are highly sensitive and specific indicators of lipid damage and are thus considered the gold standard biomarker of oxidative stress in vivo. However, the ability to use IsoP measured at early mammary involution as biomarkers of oxidative stress and to predict postpartum disease in dairy cows was poorly characterized. To address this gap, we determined how oxylipids shift during this time and assess their utility as early biomarkers of disease risk. As the physiological role of IsoP is not fully elucidated, we then developed in vitro models of endothelial inflammation to determine how IsoP influence metabolic, transcriptomic, and proteomic responses to oxidant and endotoxin challenge in endothelial cells (**EC**) and macrophages. We found that different IsoP subtypes show differential expression patterns during times of oxidative stress in dairy cattle. Amongst the IsoP detected, 8-iso-PGA_2 appeared to have the potential to indicate cows at-risk of developing postpartum disease. In our bovine endothelial inflammation model, IsoP have no influence over inflammatory outcomes such as cellular viability, apoptosis, RONS production, barrier integrity, and gene transcription networks. In RAW 264.7 macrophages, however, 15-F_{2t}-IsoP promotes an anti-inflammatory phenotype. This work suggests that IsoP have the potential to be early indicators of postpartum disease risk in dairy cattle. Our data also provides evidence for a novel physiological action in which IsoP may

support healing pathways in late-stage inflammation when they are elevated. Hence, IsoP represent an important biomarker of oxidative stress in dairy cows, especially at early mammary involution. Beyond their role as biomarkers, IsoP also serve as inflammatory modulators to help restore tissue homeostasis during acute inflammation. Establishing stronger associations between oxylipids measured at early mammary involution and specific postpartum diseases should be the focus of future studies. Additionally, further characterization of the mechanisms with which IsoP exert their effects, such as receptor targets, downstream signaling pathways, and functional consequences should be the basis of future work.

I would like to dedicate this dissertation to Dr. Lorraine Sordillo, who provided the exact guidance and mentorship I needed. It is also dedicated to all other mentors in my life, who have given me every chance at success and taught me how to capitalize on my opportunities. Finally, to my family and friends, who have provided support throughout my entire educational journey. I am especially grateful for the countless laughs we have shared. Thank you, earnestly.

ACKNOWLEDGEMENTS

I would like to thank the following entities for supporting this work: Agriculture and Food Research Initiative (AFRI) Competitive Grants Program (2014-68004-21972; 2017-67015-26676; and 2017-38420-26759) from the USDA National Institute of Food and Agriculture, AFRI Predoctoral Fellowship Program (2022-67011-36561) from the USDA National Institute of Food and Agriculture, an endowment from the Matilda R. Wilson Fund (Detroit, MI, USA), and the Michigan Alliance for Animal Agriculture (East Lansing, MI). Thank you to Advanced Animal Diagnostics (Morrisville, NC) for the kind gift of the automated blood leukocyte differential test, QScout BLD. I give many thanks to my guidance committee members: Lorraine Sordillo, G. Andres Contreras, Ángel Abuelo, Vengai Mavangira, and Daniel Langlois. I would also like to thank my extraordinary colleagues in the Meadow Brook laboratory, past and present. Finally, I thank the Michigan State University Mass Spectrometry and Metabolomics Core (East Lansing, MI) and Dr. Matthew Bernard of the Flow Cytometry Core (Institute for Quantitative Health Sciences and Engineering, Michigan State University, East Lansing) for their assistance in liquid chromatography and Luminex analysis, respectively.

TABLE OF CONTENTS

LIST OF ABBREVIATIONS

2,3-dinor-8-iso-$PGF_{2\alpha}$	2,3-dinor-8-isoprostaglandin $F_{2\alpha}$
5-$iPF_{2\alpha}$-VI	5,9α,11α-trihydroxy-(8β)-prosta-6E,14Z-dien-1-oic acid
8,12-iso-$iPF_{2\alpha}$-VI	12-iso-5(R),6E,14Z-prostaglandin $F_{2\alpha}$
8-iso-PGA_1	8-iso-prostaglandin A_1
8-iso-PGA_2	8-iso-prostaglandin A_2
8-iso-PGE_2	8-iso-prostaglandin E_2
8-iso-15-keto-PGE_2	8-iso-15-keto-prostaglandin E_2
8-iso-15 (R)-$PGF_{2\alpha}$	8-iso-15(R)-prostaglandin $F_{2\alpha}$
15-F_{2t}-IsoP	8-iso-prostaglandin $F_{2\alpha}$
AA	Arachidonic acid
AAPH	2,2'-azino-bis-3-ethylbenzothiazoline-6-sulfonic acid
AH	Apparently healthy
ALA	Alpha-linolenic acid
AOP	Antioxidant potential
BCS	Body condition score
BHB	Beta-hydroxybutyrate
BHT	Butylated hydroxytoluene
C +7	7 days after calving
CD	Clinical disease
COX	Cyclooxygenase

CU	Close-up
CYP	Cytochrome-P450
d	Day
DCFH-DiOxyQ	Dichlorodihydrofluorescin DiOxyQ
DHA	Docosahexaenoic acid
DHET	Dihydroxyeicosatrienoic acid
DHIA	Dairy Herd Improvement Association
DiHDPA	Dihydroxydocosapentaenoic acid
DiHETE	Dihydroxyeicosatetraenoic acid
DiHOME	Dihydroxyoctadecenoic acid
DIM	Days in milk
EC	Endothelial cell(s)
ECIS	Electric cell-substrate impedance sensing
EDTA	Ethylenediaminetetraacetic acid
EET	Epoxyeicosatreinoic acid
ELISA	Enzyme-linked immunosorbent assay
EPA	Eicosapentaenoic acid
EpDPE	Epoxydocosapentaenoic acid
EpOME	Epoxyoctadecenoic acid
ES	Effect size
FA	Fatty acid
GC-MS	Gas chromatography-mass spectrometry
GSH	Reduced glutathione

h	Hour
HDoHE	Hydroxydocosahexaenoic acid
HETE	Hydroxyeicosatetraenoic acid
HHTrE	Hydroxyheptadecatrienoic acid
HODE	Hydroxyoctadecadienoic acid
HOTrE	Hydroxyoctadecatrienoic acid
HPLC	High performance liquid chromatography
HPODE	Hydroperoxyoctadecadienoic acid
IsoP	Isoprostanes
LA	Linoleic acid
LC-ESI-MS	Liquid chromatography-electrospray ionization-mass spectrometry
LC-MS	Liquid chromatography-mass spectrometry
LC-MS/MS	Liquid chromatography-tandem mass spectrometry
LC/LC-MS/MS	Tandem liquid chromatrography-tandem mass spectrometry
LOX	Lipoxygenase
LPS	Lipopolysaccharide
mo	Month
MUFA	Monosaturated fatty acid
n-3	Omega-3
n-6	Omega-6
NADPH	Nicotinamide adenine dinucleotide phosphate
NEFA	Nonesterified fatty acid

OSi	Oxidative stress index
oxoETE	Oxoeicosatetraenoic acid
oxoODE	Oxooctadecadienoic acid
PG	Prostaglandin
PhytoP	Phytoprostane
PUFA	Polyunsaturated fatty acid
qRT-PCR	Quantitative reverse transcriptase polymerase chain reaction
RFU	Relative fluorescence unit
RNS	Reactive nitrogen species
RONS	Reactive oxygen and nitrogen species
ROS	Reactive oxygen species
SCC	Somatic cell count
SFA	Saturated fatty acid
TE	Trolox equivalents
TMR	Total mixed ration
TP	Thromboxane receptor
TPP	Triphenylphosphine
TX	Thromboxane
wk	week

INTRODUCTION

The incidence and severity of several economically-important diseases, such as mastitis, are greatest during major physiological transitions in dairy cattle. Perturbations in immune system function and redox balance during these transitions result in dysregulated inflammation and oxidative stress, which are principal underlying components of mastitis pathophysiology (Mavangira and Sordillo, 2018). For instance, copious milk production after calving necessitates enhanced production of reactive oxygen and nitrogen species (**ROS** and **RNS**, respectively or **RONS**, collectively) from the mitochondria. Yet, decreased feed intake at the same time results in insufficient consumption of antioxidants that defend against RONS (Mavangira and Sordillo, 2018). Cows entering early mammary involution can be expected to experience analogous changes in redox balance given stressors they face are comparable to early lactation animals. Such disruptions can lead to oxidative stress, where RONS overtake antioxidant defenses and result in damage to tissue components such as proteins, DNA, and lipids (Lushchak, 2014). Several cell types, including endothelial cells (**EC**) and macrophages, function as immune regulators and can be affected by oxidative stress.

Functioning EC and macrophages are crucial for appropriate inflammatory responses. For instance, EC form the single cell interface between blood and tissue that is vital for activities such as maintaining barrier integrity (Dalal et al. 2020). Macrophages are intimately associated with the vascular endothelium and exhibit a range of pro- and anti-inflammatory phenotypes to help control inflammation by first promoting it, then switching functions to support resolution (Viola et al., 2019). Dysfunctional EC and macrophages allow for sustained dysregulated inflammation that can contribute to impaired immunity and increased disease susceptibility. For instance, RONS are produced excessively by these cells during inappropriately-regulated

inflammation and contribute to the severity of diseases like coliform mastitis (Mavangira et al., 2016; Mavangira and Sordillo, 2018). During increased reactive metabolite generation, both cell types produce potent lipid mediators known as oxylipids, which promote, maintain, and terminate inflammatory responses (Sordillo, 2018).

Isoprostanes (**IsoP**) are a specialized oxylipid formed nonenzymatically when RONS react with polyunsaturated fatty acids (**PUFA**) in lipid membranes (Morrow et al., 1990). Due to this mechanism of formation, IsoP are regarded as highly sensitive and specific biomarkers of oxidative stress. Indeed, increased 15-F_{2t}-IsoP concentrations have been associated with coliform mastitis and early lactation in dairy cows, times that are both associated with overwhelming amounts of RONS (Mavangira et al., 2016; Kuhn et al., 2018). In addition to their role as biomarkers, evidence supports IsoP activity during inflammation at the level of the vasculature. For instance, 15-F_{2t}-IsoP decreased monocyte adhesion to human microvascular EC (Kumar et al., 2005). However, the ability of IsoP to mitigate oxidative stress and inflammation in dairy cattle remains poorly characterized.

Given oxidative stress remains a predominate problem for dairy producers, there is a need to identify and mitigate the condition in dairy cows. As highly-sensitive and specific oxidative stress biomarkers with reported vascular effects in other species, IsoP can potentially allow dairy producers to do both. However, the oxidant status of cows entering early mammary involution has not been clarified, and therefore, the utility of IsoP as biomarkers at this transition is poorly defined. Furthermore, the specific roles IsoP have in mitigating oxidative stress at the level of the vasculature in dairy cows is unclear. This dissertation will discuss IsoP in the context of veterinary medicine, followed by our evaluation of oxylipids to be potential biomarkers of

oxidative stress and as early predictors of disease risk in dairy cattle, and ends with a description of effects IsoP have on EC and macrophages in models of inflammation.

CHAPTER 1

Published in Antioxidants: Putman, A. K., G. A. Contreras, and L. M. Sordillo. 2021. Isoprostanes in Veterinary Medicine: Beyond a Biomarker. Antioxidants (Basel). 10(2). doi: 10.3390/antiox10020145.

INTRODUCTION

Oxidative stress, the imbalance between oxidants and antioxidants leading to tissue damage, has been associated with many diseases in both humans and animals (Lykkesfeldt et al., 2007). Oxidants are chemically reactive molecules that are responsible for the tissue damage associated with oxidative stress and are composed of reactive oxygen species (**ROS**) and reactive nitrogen species (**RNS**). Produced in moderate amounts as a byproduct of energy generation, oxidants are used in numerous cell signaling and immune pathways under physiologic conditions (Mavangira and Sordillo, 2018). Antioxidants are designed to counter oxidants and maintain homeostasis, contributing to what is termed redox balance. However, a disruption in the balance that favors excessive oxidant accumulation leads to oxidative stress (Mavangira and Sordillo, 2018). Examples of human diseases with an oxidative stress-related component in their pathophysiology include Alzheimer's disease, type II diabetes, and heart failure (Butterfield et al., 2001; Polidori et al., 2004; Rehman and Akash, 2017). In veterinary species, oxidative stress has been associated with similar disorders such as canine counterpart of senile dementia of the Alzheimer type, metabolic stress in dairy cattle, and congestive heart failure in dogs (Skoumalová et al., 2003; Contreras, Strieder-Barboza, and Raphael, 2017; and Freeman et al., 2005). Despite the evidence supporting oxidative stress as an important contributor to numerous pathologies, no clinical signs of the process are displayed (Abuelo et al., 2013). Furthermore, it can be challenging to distinguish between redox balance and unchecked oxidants, thereby making it

necessary to use specific measurements to determine if oxidative stress is occurring. In fact, the need for reliable oxidative stress biomarkers and an understanding of any physiologic roles they may play in disease pathogenesis has become a priority in the research community.

Broadly, a biomarker can be described as "a defined characteristic that is measured as an indicator of normal biological processes, pathogenic processes or responses to an exposure or intervention" (FDA-NIH Biomarker Working Group, 2016). Several biomarkers of oxidative stress can be identified due to the tissue damage that occurs as a function of increased interactions between ROS and biological molecules. Common biomarkers generated from the reactions between ROS and nucleic acids, proteins, and lipids include 8-hydroxydeoxyguanosine, protein carbonyls, and isoprostanes (**IsoP**), respectively (Dalle-Donne et al., 2006; Fenga et al., 2017). However, the most favorable biomarkers must be more than merely measurable; they should also show specificity for a particular process, have prognostic value, or correlate with pathology (Frijhoff et al., 2015).

Since their discovery in the early 1990s, IsoP have become one of the most widely used biomarkers of in vivo oxidative stress because they are highly sensitive and specific, can be measured noninvasively from numerous biological tissues and fluids, and are chemically stable (Milne et al., 2005; Janicka et al., 2010). In addition to IsoP themselves, IsoP metabolites are also valuable biomarkers. The metabolite 2,3-dinor-5, 6-dihydro-8-iso-prostaglandin $F_{2\alpha}$, for instance, is only generated in the liver from plasma IsoP and has a longer half-life than its parent compound. Therefore, its presence is considered an accurate representation of systemic oxidative stress over time (Roberts and Morrow, 2000). Indeed, increased IsoP and IsoP metabolites have been associated with many human oxidative stress-related pathologies, including metabolic syndrome and cardiovascular disease (Van 't Erve et al., 2017). However, while IsoP

continuously become more popular in human medicine, studies regarding their potential role in disease pathogenesis remain sparse. Furthermore, literature of IsoP in veterinary species is relatively limited. This review will discuss the history, biosynthesis, and detection of IsoP, followed by current use and knowledge gaps regarding their role in veterinary medicine. Finally, the review will conclude with thoughts on future considerations for IsoP to be used successfully in veterinary medicine.

HISTORY

Isoprostanes are a relatively new oxidative stress biomarker, having only been characterized in vivo in the last 30 years. However, the earliest evidence of IsoP formation surfaced from in vitro work completed by Pryor and Stanley in the 1970s. They found that when methyl linolenate was autoxidized, a bicyclic endoperoxide was formed as a precursor to prostaglandin-like compounds (Pryor and Stanley, 1975). In the 1980s, it was shown that the lower side chains of prostaglandin D_2 (**PGD_2**) will isomerize in aqueous solutions to form isomers of 9α,11β-$PGF_{2\alpha}$ when reduced by 11-ketoreductase (Wendelborn et al., 1988). Later attempts to describe the presence of these compounds in vivo lead to the discovery of what are now termed isoprostanes (Roberts and Fessel, 2004). In the early 1990s, Morrow and colleagues used mass spectrometry to characterize the 9α,11β-$PGF_{2\alpha}$ isomers discovered by Wendelborn et al. (1988). They were prompted by the fact that the peaks generated by the 9α,11β-$PGF_{2\alpha}$ isomers increased around 50-fold when the plasma was analyzed after several months of storage at −20 °C when compared to the plasma that was analyzed immediately after collection (Morrow et al., 1990). Furthermore, the authors found that the addition of antioxidants to the plasma samples would reduce the formation of F-ring prostaglandin-like compounds. This suggested that the molecules were generated independently of enzymatic pathways. First was the discovery of prostaglandin (**PG**) F_2-like

compounds, termed the F_2-isoprostanes (Morrow et al., 1990). Shortly thereafter, Morrow et al. determined that PGE- and PGD-isoprostanes could be generated in vivo as well (1994). Although these earliest discovered IsoP were derived from arachidonic acid, it was soon determined that other polyunsaturated fatty acids could also generate IsoP in the face of interactions with free radicals. Later in the 90s, the omega-3 fatty acids eicosapentaenoic acid (**EPA**) and docosahexaenoic acid (**DHA**) were found to produce F_3-IsoP and F_4-neuroprostanes, respectively (Nourooz-Zadeh, 1997; Nourooz-Zadeh et al., 1998; Roberts et al., 1998). Within a decade of the omega-3 IsoP discoveries, the omega-6 fatty acid, adrenic acid, was found to produce its own class of IsoP when undergoing interactions with free radicals (VanRollins et al., 2008). Furthermore, IsoP are not exclusive to animals. Indeed, the plant-based omega-3 fatty acid α-linolenic acid will generate phytoprostanes (**PhytoP**) (Parchmann and Mueller, 1998). As the name suggests, IsoP are isomers of PG; however, they are synthesized by different mechanisms.

BIOSYNTHESIS

Isoprostanes are formed from interactions between free radicals and plasma membranes. Free radicals are molecules that contain an unpaired electron and are comprised of ROS and RNS (Weidinger and Kozlov, 2015). ROS consist of many diverse molecules, including lipid peroxides, hydrogen peroxide, hydroxyl radical ($OH^{\bullet}$), and superoxide anion ($O_2^{\bullet -}$) (Lushchak, 2014). Production of ROS is part of redox signaling in physiological processes in eukaryotes with the majority being formed by the mitochondria during cellular respiration or as a result of nicotinamide adenine dinucleotide phosphate (**NADPH**) stimulation (Lushchak, 2014; Sordillo and Aitken, 2009). However, ROS are highly reactive and capable of significant damage to biological molecules such as proteins, DNA, and lipids (Sordillo and Aitken, 2009). For instance,

the hydroxyl radical can generate more ROS, alter protein amino acids, and cause lipid peroxidation (Halliwell and Gutteridge, 2006).

Membrane phospholipids are particularly prone to oxidation (Sordillo, 2013). Polyunsaturated fatty acids (**PUFA**) are a major component of membrane phospholipids, and contain methylene groups flanked by double bonds known as bisallylic groups (Else and Kraffe, 2015). Bisallylic groups are readily oxidized because their electrons are pulled to either side by the adjacent double bonds, resulting in weakened bond energies (Johnson and Decker, 2015). There are 3 events involved in the free radical-mediated lipid peroxidation chain mechanism: initiation, propagation, and termination (Figure 1.1) (Milne et al., 2011). The first step to IsoP formation involves radical abstraction of a bisallylic hydrogen, or a hydrogen bound to the methylene carbon adjacent to double bonds, from PUFA (Rund et al., 2018). The abstraction of the bisallylic hydrogen, which results in the formation of a pentadienyl radical, is followed by the addition of oxygen. At this point, a peroxyl radical is formed, which is capable of propagating more free radical-mediated lipid peroxidation (Milne et al., 2011). Sequential rounds consisting of two 5-exo-cyclizations of the peroxyl radical followed by another addition of oxygen and the reduction of the hydroperoxide side chain results in the generation of a bicyclic endoperoxide intermediate that resembles prostaglandin H (**PGH**) (Figure 1.2). Due to their instability, the PGH-like bicyclic endoperoxides rapidly react with reducing agents or isomerize to form F-ring IsoP or D- and E-ring IsoP, respectively (Figure 1.3) (Rund et al., 2018). Lipid peroxidation is ceased when antioxidants quench the free radical reactions (Milne et al., 2011).

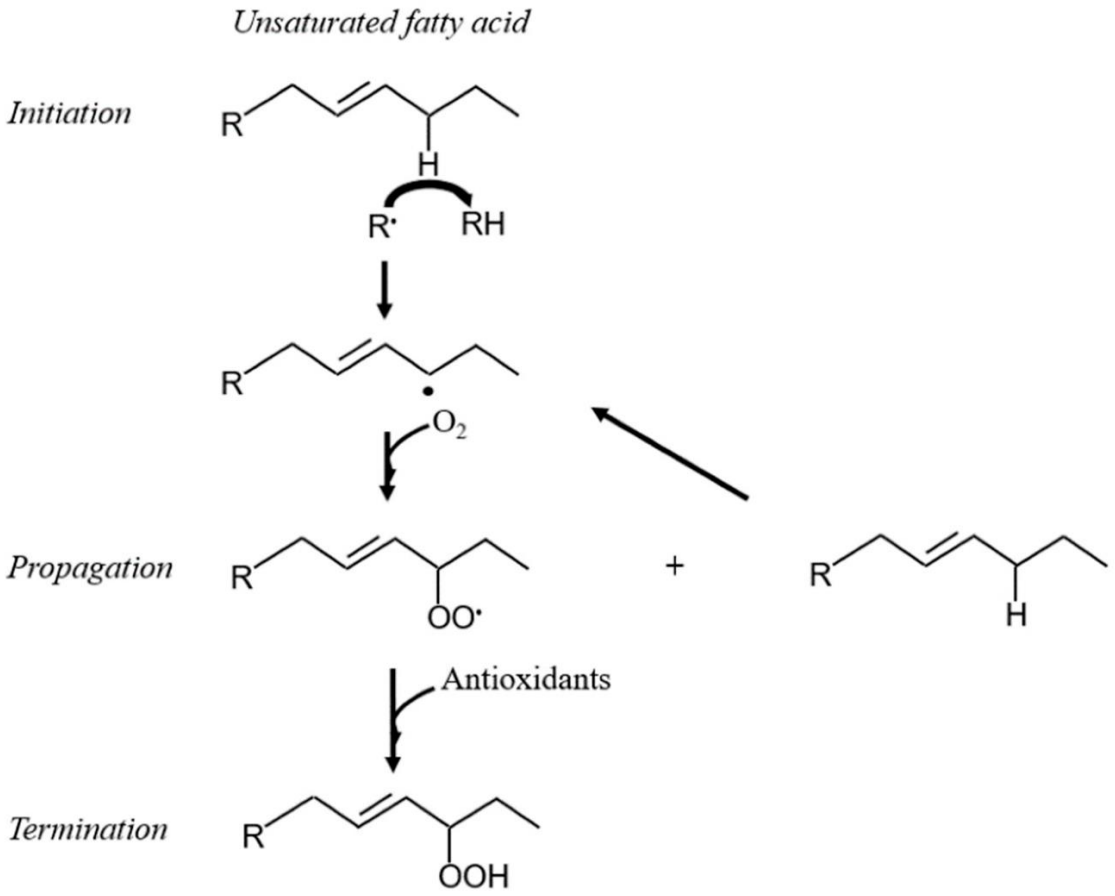

Figure 1.1. Example of initiation, propagation, and termination pathways during lipid peroxidation. R• = free radical.

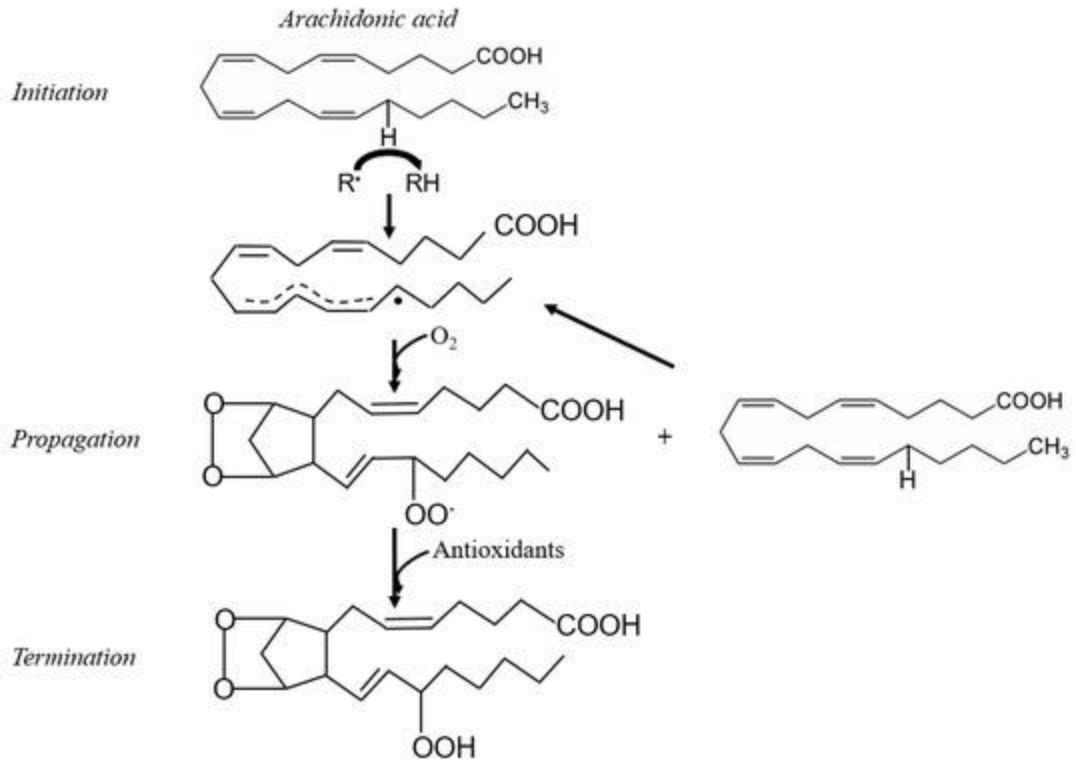

Figure 1.2. Auto-oxidation of arachidonic acid resulting in the formation of the isoprostane (IsoP) precursor, prostaglandin H (PGH)-like bicyclic endoperoxide. R• = free radical.

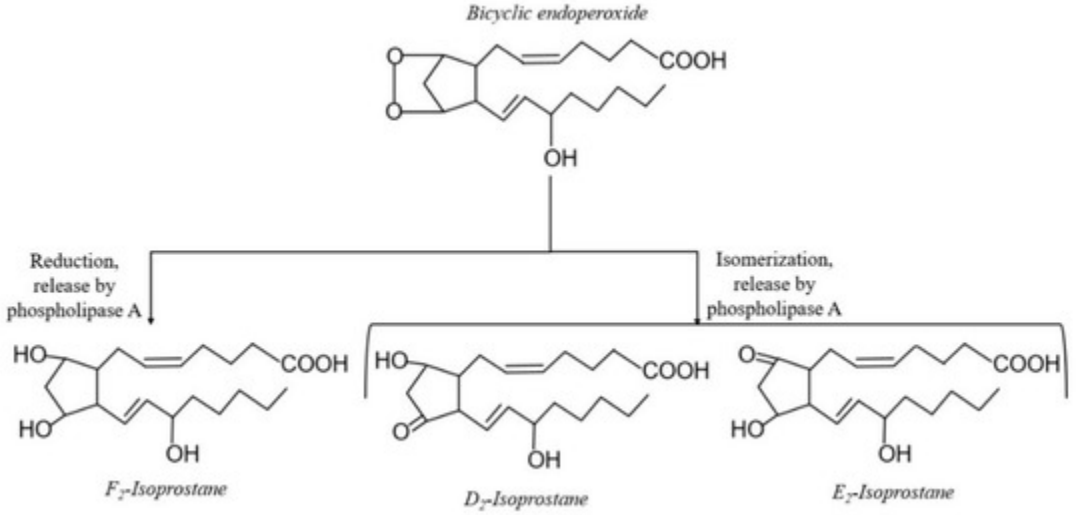

Figure 1.3. Formation of D-, E-, and F-ring isoprostanes (IsoP) from a prostaglandin H (PGH)-like bicyclic endoperoxide intermediate.

The initiation step has an equal chance of occurring at any bisallylic hydrogen when multiple bisallylic groups exist in a PUFA. Polyunsaturated fatty acids that contain more bisallylic

methylenes have more potential to be oxidized. Therefore, docosahexaenoic acid has the most oxidation potential of the common fatty acids, followed in descending order by eicosapentaenoic acid, arachidonic acid, and finally linoleic acid (Milne et al., 2011). Indeed, it has been suggested that docosahexaenoic acid is at an increased susceptibility of oxidative stress in the absence of α-tocopherol and that decreased susceptibility of mitochondrial membranes to oxidative stress may be conferred by the high percentage of linoleic acid in mitochondrial membranes relative to docosahexaenoic acid or eicosapentaenoic acid (Song et al., 2000; Tsalouhidou et al., 2006). As all of the biologically important PUFA can be oxidized and any of the available bisallylic hydrogens can be involved in the initiation step, a diverse array of oxidized products can be formed (Milne et al., 2011). Primary products of free radical-mediated lipid peroxidation include peroxides and hydroperoxides, which are unstable compounds that often degrade into secondary products (Pratt et al., 2011). Secondary lipid peroxidation products include aldehydes, ketones, and IsoP (Milne et al., 2011; Pratt et al., 2011). Prostaglandins are another lipid peroxidation product that are quite similar to IsoP in structure; however, a few key differences distinguish the two. Generation of IsoP is through a nonenzymatic mechanism, unlike prostaglandin formation which occurs via cyclooxygenase enzymes. In contrast to prostaglandins, in which the PUFA is first released by phospholipase and then oxidized, IsoP are oxidized in situ and then released from the plasma membrane (Morrow et al., 1992). The pathways of 15-F_{2t}-IsoP metabolism are much like that of prostaglandins and involve the rapid formation of β-oxidation products that will ultimately be excreted primarily in the urine (Basu and Helmersson, 2005).

A multitude of regioisomers and stereoisomers of IsoP can theoretically be formed. Considering F_2-IsoP, 4 regioisomers are generated (5-, 8-, 12-, and 15-series), with the 5-series and 15-series being the most abundant (Milne et al., 2011). As the number of bisallylic hydrogens present in a

PUFA increases, the number of possible regioisomers and stereoisomers also increases (Galano et al., 2018). Indeed, those IsoP derived from DHA, known as F_4-IsoP or neuroprostanes, can form 8 regioisomers with 128 theoretical stereoisomers (Signorini et al., 2018). With the rapidly expanding number of IsoP classes, it was pertinent to develop a nomenclature system to distinguish all the molecules. Unfortunately, a consistent nomenclature scheme has been elusive despite 3 major classification systems coming to the forefront by Rokach et al., Taber et al., and Mueller (Rokach et al., 2017; Taber et al., 1997; Mueller, 2010). The rationale of each system is beyond the scope of this review, but the details are discussed in an article by Mueller (2010).

MEASUREMENT METHODS

Due to its relevance in many diseases, there is a desire to reliably measure oxidative stress. Logically, it would make sense to measure ROS and antioxidants individually as oxidative stress occurs due to an imbalance of the two. Thorough reviews of both ROS and antioxidants exist in the literature and therefore will not be discussed extensively herein (Sordillo and Aitken, 2009; Valko et al., 2007; Celi, 2010). Although it is possible to measure ROS and antioxidants to evaluate oxidative stress, these indicators do not provide any information regarding if tissue damage has occurred in the host. Therefore, IsoP have become an important and reliable assessment of oxidative stress because they indicate lipid damage in a sensitive and specific manner (McMichael, 2007). Furthermore, they have been found in all tissues and fluids assessed, which means noninvasive detection is possible (Moore and Roberts, 1998).

As mentioned previously, IsoP are esterified on membrane phospholipids and then subsequently released by phospholipases. Therefore, 2 populations of IsoP exist in any given unaltered sample: one that has been esterified and released (free, unesterified) and one that has been esterified but remains attached to lipids (esterified). The sum of both the free and esterified

populations are termed total IsoP, with the majority of IsoP being in the esterified form (Briskey et al., 2014). Free IsoP are readily measured by many assays but do not account for the IsoP still attached to lipids (Sodergren et al., 2000). In plasma, for instance, esterified IsoP are formed on lipoproteins such as low-density lipoprotein (Lynch et al., 1994). An increased amount of esterified IsoP in plasma samples despite steady concentrations of free IsoP suggests compartmentalization of lipid peroxidation (Signorini et al., 2008; Mavangira et al., 2015). Additional sample preparation in the form of hydrolysis can be completed to ensure all IsoP are being measured (Briskey et al., 2014).

Biological samples that contain lipids have the potential to undergo peroxidation ex vivo (Morrow et al., 1990). Therefore, precautions must be taken when assessing IsoP concentrations from these samples. Some considerations for evaluating IsoP concentrations that were not analyzed immediately post-collection include storage conditions. For instance, measuring plasma IsoP concentrations immediately after collection is ideal, but if that is not possible, the use of antioxidants such as butylhydroxytoluene (**BHT**) can prevent some autoxidation (Morrow et al., 1990). Indeed, one study found that plasma collected into tubes containing a mixture of 1 mg/mL EDTA, 40 µg/mL BHT, and 1 mg/mL reduced glutathione (**GSH**) had significantly less oxidation than those collected in EDTA vacutainers. The same study also documented that F_2-IsoP concentrations in samples stored at −20 °C and −80 °C for 6 months post-collection prior to analysis were significantly elevated compared to those stored at the same temperatures for 1 month. Additionally, the concentrations of F_2-IsoP were significantly higher in samples stored at −20 °C than those stored at −80 °C, regardless of the amount of time they were stored or if antioxidants were present. One factor that did not seem to significantly alter the concentrations

of F_2-IsoP, however, was if samples were kept at room temperature or 4 °C for up to 4 h prior to sample processing as long as the antioxidant mixture was present (Barden et al., 2014). Although IsoP are detectable in all fluids and tissues of mammals, certain samples offer advantages over others. Measuring urine IsoP is advantageous because it is not invasive like other methods, but it is still important to consider that urine IsoP concentrations may not truly reflect systemic IsoP due to rapid clearance and production from the kidney (Morrow and Roberts, 2002). Recognizing this predicament, Roberts et al. identified the major 15-F_{2t}-IsoP metabolite, 2,3-dinor-5, 6-dihydro-8-iso-prostaglandin $F_{2\alpha}$, and found it to be a valuable integrative index of in vivo oxidative stress (1996). As mentioned previously, 2,3-dinor-5, 6-dihydro-8-iso-prostaglandin $F_{2\alpha}$ is more stable than its parent compound and is formed exclusively in the liver, thereby eliminating the concern of confounding contributions from the kidney (Roberts and Morrow, 2000).

Although urine IsoP metabolite may be the most advantageous tool for assessing systemic oxidative stress compared to IsoP in certain circumstances, IsoP still remain as the gold standard in most instances. Mavangira and colleagues investigated the ability of 15-F_{2t}-IsoP to be used as a biomarker of oxidative stress in acute bovine coliform mastitis, concluding that free 15-F_{2t}-IsoP concentrations in plasma were the most ideal sample because they correlated positively with systemic oxidant status and negatively with glutathione. Moreover, it was determined that free 15-F_{2t}-IsoP concentrations in urine and milk were not reflective of systemic or local mammary oxidative stress (Mavangira et al., 2015). This study demonstrated that the most ideal sample for IsoP quantification may not be the most intuitive one. Indeed, it was surprising that free 15-F_{2t}-IsoP in milk were inversely correlated with mammary reactive metabolites given that oxidative stress damages mammary tissue and that metabolites are increased during coliform mastitis

(Mavangira et al., 2015a; Mavangira et al., 2015b). The unexpected findings in the Mavangira et al. (2015) study support the argument that appropriate sample considerations must be taken into account for each individual case. For example, free 15-F_{2t}-IsoP were not correlated with milk oxidant status but total milk 15-F_{2t}-IsoP were positively correlated, suggesting that hydrolysis may be required for milk samples prior to IsoP quantification (Mavangira et al., 2015). In addition to sample considerations, selection of an appropriate detection method is equally important in IsoP measurement. Two major detection methods available for IsoP measurement include immunological methods and chromatography coupled with mass spectrometry.

Immunologic Methods

Immunoassays such as enzyme immunoassays and enzyme-linked immunosorbent assays (**ELISA**) both rely on the basic immunological principle of antibodies binding to a specific antigen (Gan and Patel, 2013). Immunoassays are popular choices when measuring IsoP because they are relatively uncomplicated, relatively inexpensive, and are high-throughput. However, there are many drawbacks to immunoassays used to measure IsoP. One such drawback is that the nature of immunoassays such as ELISA allows for consistent overestimation of IsoP concentrations due to cross-reactivity with related compounds such as alternative IsoP isomers and prostaglandins (Il'Yasova et al., 2004). In a study comparing gas chromatography-mass spectrometry (**GC-MS**) and an ELISA method, the ELISA mean and median concentrations of urine 2,3-dinor-5, 6-dihydro-8-iso-prostaglandin $F_{2\alpha}$ were 30-fold higher than those of GC-MS. Furthermore, the Pearson correlation coefficient between ELISA and GC-MS in the study was 0.55, suggesting poor correlation (Il'Yasova et al., 2004). Similarly, Klawitter and colleagues found that 3 different ELISA kits overestimated the concentration of 15-F_{2t}-IsoP in human plasma and urine when compared to tandem liquid chromatography-tandem mass spectrometry

(**LC/LC-MS/MS**). The 3 different ELISA not only had poor agreement with LC/LC-MS/MS, but also with each other, suggesting that results from studies using different assay kits cannot be compared (Klawitter et al., 2011).

The inconsistent performance of immunoassays also translates to studies conducted in veterinary species. An investigation conducted in dairy cows found that different ELISA kits (Cell Biolabs versus Cayman Chemical) used on the same samples yielded different results. For instance, the Cell Biolabs ELISA kit (San Diego, CA, USA) detected significant differences between free and total 15-F_{2t}-IsoP concentrations, while the Cayman Chemical ELISA (Ann Arbor, MI, USA) did not (Mavangira et al., 2015a). In dogs, horses, and cattle, 2 separate ELISA assays had very poor correlations to GC-MS and had substantial bias (Soffler et al., 2010). Thus, while immunoassays represent a convenient option, lack of specificity and consistency in both humans and veterinary species ultimately make them a poor candidate for accurate IsoP measurement. It is, therefore, prudent to interpret results with caution when evaluating literature using immunoassays to measure IsoP concentrations.

Chromatography

Chromatography methods are one of the forerunners of lipid detection and characterization, thereby making them a preferred choice for IsoP measurement (Rustam and Reid, 2018). Chromatographic methods are advantageous in that they are capable of sensitive and specific identification of multiple IsoP isomers, even distinguishing both regioisomers and diastereomers (Rund et al., 2018). Morrow and Roberts first used GC-MS to quantify urine F_2-IsoP in the 90s. However, this protocol required the burdensome steps consisting of 2 rounds of thin-layer chromatography along with chemical derivation (Dahl and van Breemen, 2010). Indeed, not only

is the multi-step GC process labor-intensive, but it also is complicated by potential contamination, artifact generation, and poor recovery (Sircar and Subbaiah, 2007). Therefore, much work was invested into improving IsoP detection with chromatography. For example, an assay was developed using liquid chromatography-electrospray ionization (**LC-ESI**)-MS, where samples were first treated by solid-phase extraction followed by liquid-liquid extraction. With the use of MS/MS, IsoP isomers of the same mass are able to be distinguished based on their specific fragmentation patterns (Ohashi and Yoshikawa, 2000). Sircar and Subbaiah made further improvements on previous attempts and developed a method in 2007 that combined the simplicity of immunoassay preparation with the sensitivity and specificity of LC-MS, along with quantifying total IsoP as opposed to free IsoP only. Indeed, Sircar and Subbaiah's (2007) method required fewer steps than GC-MS, resulting in less sample losses, and was able to be performed at a decreased cost due to use of single quadrupole equipment. Finding methods that decrease the expense of chromatography-MS are important as cost is one of the largest limitations (Sheng and Zhou, 2017). Adding to the expense of chromatographic methods is the expanding number of IsoP isomers to be measured in each sample, provoking the need for distinguishing multiple IsoP isomers during a single run. Rund et al. (2018) developed a method to accomplish this task, resulting in the ability to separate 25 F-ring IsoP, 2 PhytoP, and 8 isofurans (IsoF) derived from multiple PUFA precursors in a single sample. Through the constant quest to improve IsoP quantification methods, LC-MS has become the method of choice because it circumvents the variability of immunoassays and the tedious derivatization steps of GC-MS (Janicka et al., 2013; Aszyk et al., 2017). Indeed, LC-MS/MS has relatively short run times, is sensitive and specific, and is capable of detecting very low concentrations of IsoP when

using non-radioactive isotope-labeled standards (Janicka et al., 2013). Development of improved detection methods has contributed to the widespread use of IsoP in the scientific community.

USE AND PHYSIOLOGICAL ROLES

Biomarkers of Lipid Peroxidation

An ongoing challenge in veterinary medicine lies in the ability to diagnose disease promptly so that best management and treatment recommendations can be made. Isoprostanes may be a valuable tool to clinical practice in this capacity because current literature regarding the use of IsoP is largely based on their advantageous nature as biomarkers of oxidative stress-related disorders. At this time, a handful of literature can be found associating a subset of relevant veterinary diseases with altered IsoP concentrations affecting major domestic species (Freeman et al., 2005; Mavangira et al., 2015a; McMichael et al., 2006; Noschka et al., 2011; Viviano and VanderWielen, 2013; Whitehouse et al., 2017). These studies provide important insights as there is a dearth of information regarding threshold IsoP concentrations that may distinguish between health and disease. Mavangira et al. (2015) found that plasma and urine free 15-F_{2t}-IsoP were higher in cows afflicted with coliform mastitis when compared to control cows, while milk 15-F_{2t}-IsoP concentrations were lower in coliform mastitis cows as assessed by LC-MS/MS. In contrast, hydrolyzed samples analyzed with a Cell Biolabs ELISA yielded higher total milk 15-F_{2t}-IsoP in coliform mastitis cows than in controls (Mavangira et al., 2015a). Colic is a common condition of horses that may result in veterinary intervention in the form of medical therapy or surgery. However, the numerous causes of colic present a challenge in terms of finding a single biomarker that can reliably determine which treatment may be most beneficial and predict prognosis in affected horses. Noschka and colleagues (2011) set out to determine if IsoP and the IsoP metabolite 2,3-dinor-5, 6-dihydro-8-iso-prostaglandin $F_{2\alpha}$ from urine samples would be

suitable prognostic predictors in various causes of equine colic. After normalizing urine IsoP and 2,3-dinor-5, 6-dihydro-8-iso-prostaglandin $F_{2\alpha}$ concentrations to urine creatinine, the authors found that both increased in horses with colic compared to healthy control horses. Furthermore, urine 2,3-dinor-5, 6-dihydro-8-iso-prostaglandin $F_{2\alpha}$ concentrations were significantly higher in horses that underwent surgical correction and those that did not survive. Therefore, the authors proposed that 2,3-dinor-5, 6-dihydro-8-iso-prostaglandin $F_{2\alpha}$ may be a useful biomarker for determining if a horse with colic will require surgery or will be less likely to survive (Noschka et al., 2011). Concentrations of urine IsoP were predictive in a different way. Urine IsoP concentrations were significantly higher in medical colic cases compared to control horses, but surgical cases were not significantly different from controls nor medical colic cases. Additionally, urine IsoP concentrations were significantly higher in horses that survived compared to control, while no difference was detected between nonsurvivors and controls or survivors (Noschka et al., 2011).

Small animals are afflicted with a variety of oxidative stress-related disorders, presenting an opportunity for use of IsoP. Viviano and Van der Wielen (2013) supported that dogs with systemic illness undergo more oxidative stress than healthy controls through the use of biomarkers such as urine F_2-IsoP concentrations. Spinal cord and cardiovascular disease, common conditions seen in veterinary medicine, are associated with oxidative damage (McMichael et al., 2006). Dogs with intervertebral disk disease undergoing surgery had increased urine F_2-IsoP:creatinine ratios compared to healthy dogs undergoing surgery, both before and after the surgical procedure. Interestingly, dogs that had more severe neurological signs as a result of their disc disease had lower urine F_2-IsoP concentrations than those with less severe neurologic signs (McMichael et al., 2006). Dogs with congestive heart failure had

significantly higher 15-F_{2t}-IsoP than healthy controls (Freeman et al., 2005). Chronic kidney disease is also a common ailment in small animals, but can be difficult to diagnose in its early stages due to lack of a sensitive biomarker that can detect the disease before significant organ damage has occurred (Chen et al., 2019). Furthermore, oxidative stress has been implicated in the progression of human chronic kidney disease, but had not been thoroughly investigated in cats prior to a study completed by Whitehouse and colleagues (Whitehouse et al., 2017). Cats with stage 1 chronic kidney disease had significantly higher urine F_2-IsoP concentrations than cats in stages 2-4. In contrast to the increased concentrations of IsoP that are associated with more advanced stages of chronic kidney disease in humans, cats in the more severe stages 3 or 4 had lowest urinary IsoP concentrations, even when compared to healthy controls (Whitehouse et al., 2017). Differences between human and animal studies illustrate the need to understand species-specific IsoP concentrations so that IsoP may be used effectively in veterinary medicine. As generation of ROS occurs during normal physiological processes, hence leading to lipid peroxidation, IsoP are also produced routinely in clinically healthy individuals (Downey et al., 2018). However, only a few studies describe basal IsoP concentrations in apparently healthy animals. The modern dairy cow undergoes major physiological transitions throughout a typical lactation cycle, especially at the onset and cessation of lactation. For instance, tremendous amounts of energy are required for the copious milk synthesis typical of a modern dairy cow at the onset of lactation, suggesting a necessary increase in ROS production via the mitochondria (Abuelo et al., 2014). A concurrent decrease in antioxidant intake during early lactation can thereby lead to ROS accumulation and lipid peroxidation. Kuhn et al. (2018) documented dynamic concentrations of 15-F_{2t}-IsoP throughout the lactation cycles of clinically healthy cattle. Indeed, plasma and urine concentrations of the IsoP were significantly lower in mid-lactation

cows compared to those in either early or late lactation. However, milk concentrations were significantly lower during early lactation compared to mid- or late lactation (Kuhn et al., 2018). Additional work completed by our lab demonstrated that clinically healthy Holstein cows experience changes in IsoP concentrations throughout the physiological transition from lactating to non-lactating as well. In fact, each of the 7 detected IsoP exhibited its own unique expression profile throughout the transition. Intriguingly, the most well-studied IsoP, 15-F_{2t}-IsoP, did not reach statistical significance after adjusting for multiple comparisons, although a relative increase in concentrations was noted for 2 d after abrupt cessation of lactation (Putman et al., 2018). Our study demonstrated that other IsoP besides 15-F_{2t}-IsoP may be biologically relevant and deserve further study investigating their role in the host. During times of intense exercise, and therefore increased oxygen consumption, Hinchcliff et al. (2000) unsurprisingly determined that healthy sled dogs completing 58 km runs on 3 consecutive days had significantly higher plasma concentrations of IsoP than healthy control dogs that did not run at all. Determining the concentrations that may be seen during both disease and health in animals provides a first step in understanding how changes in the concentrations may be impacting the host.

Vascular Regulation

Although IsoP are sensitive and specific biomarkers of oxidative stress, research also is focused on determining potential physiological roles in the host. Vascular endothelium dysfunction is a primary component of oxidative stress and as such, the interaction between IsoP and the vasculature has gathered a considerable amount of research attention (Verma et al., 2003). Most of the research supports that a predominant role of IsoP is vasoconstriction, which has been demonstrated in numerous species and tissue types (Bauer et al., 2014). Early evidence of vasoconstriction was established by directly infusing rat kidneys with 15-F_{2t}-IsoP, which

revealed a substantial dose-dependent decrease in glomerular filtration rate and renal plasma flow in vivo, both at the whole kidney and single nephron level (Takahashi et al., 1992). Both 15-F_{2t}-IsoP and 15-E_{2t}-IsoP were shown to cause sustained and dose-dependent coronary vasoconstriction in isolated guinea pig hearts, sometimes decreasing coronary flow by 50% (Möbert et al., 1997). Vasoconstriction can be strongly attenuated by infusing or treating cells concomitantly with a thromboxane A_2 receptor (**TP**) antagonist (SQ29548), suggesting that IsoP exert their action through TP (Takahashi et al., 1992; Möbert et al., 1997). In fact, numerous studies have supported IsoP as a ligand for TP and Figure 1.4 summarizes proposed biological consequences as a result of IsoP-TP interaction (Audoly et al., 2000; Benndorf et al., 2008). Isoprostanes are also capable of vasodilation, although this biological effect is often eclipsed by vasoconstriction and is dependent on many factors including the IsoP isomer, concentration, species, vascular bed, and whether or not a ligand is bound to TP (Bauer et al., 2014; Villamor and González-Luis, 2010). For example, 15-E_{2t}-IsoP relaxed porcine pulmonary and coronary arteries that had been pre-treated with the TP agonist U46619. Conversely, none of the 6 IsoP tested (including 15-E_{2t}-IsoP) relaxed pulmonary veins pre-constricted by U46619 (Villamor and González-Luis, 2010). Table 1.1 summarizes the effects of IsoP in various tissues and species.

Table 1.1. Putative roles of IsoP on the vasculature of veterinary species from selected literature.

Tissue	Species	IsoP	Biological Effect	Source
Kidney	Rat	15-F_{2t}-IsoP	Decreased glomerular filtration rate & renal plasma flow (vasoconstriction)	Takahashi et al. 1992
Lung	Pig	15-E_{2t}-IsoP	Vasodilation when vessels precontracted with a thromboxane receptor agonist; vasoconstriction when precontracted with endothelin-1	Villamor and Gonzalez-Luis, 2010
		8-iso-PGE_1 & 15-F_{2t}-IsoP	Modest vasodilation when vessels precontracted	Villamor and Gonzalez-Luis, 2010
	Chicken	15-F_{2t}-IsoP & 15-E_{2t}-IsoP	Vasoconstriction; vasodilation when vessels were precontracted with thromboxane agonist	van der Sterrer and Villamor 2011
Heart	Guinea pig	15-F_{2t}-IsoP & 15-E_{2t}-IsoP	Vasoconstriction	Mobert et al 1997
	Pig	8-iso-PGE_1, 15-E_{2t}-IsoP, & 15-F_{2t}-IsoP	Vasodilation when precontracted with thromboxane receptor agonist	Villamor and Gonzalez-Luis, 2010
		15-F_{2t}-IsoP	Vasoconstriction	Kromer and Tippins 1996
	Cow	15-F_{2t}-IsoP	Vasoconstriction	Kromer and Tippins 1996
Ductus arteriosis; femoral artery	Chicken	15-F_{2t}-IsoP & 15-E_{2t}-IsoP	Vasoconstriction; vasodilation when vessels were precontracted with thromboxane agonist	van der Sterrer and Villamor 2011

Although vascular tone is one aspect that TP modulate, platelet function regulation is another. Through their action on TP, IsoP impact platelet function in a complex way. For instance, early studies indicated that 15-F_{2t}-IsoP increased platelet adhesion in a dose-dependent manner, an effect that could be significantly reduced in the presence of a TP antagonist (Minuz et al, 1998). Another study conducted by Cranshaw and colleagues (2001) found that out of 11 studied IsoP (including 15-F_{2t}-IsoP), none induced platelet aggregation in human whole blood on their own. However, the pro-aggregatory responses induced by the TP agonist U46619 were inhibited by 15-F_{2t}-IsoP, 8-isoPGE$_1$, 15-E_{2t}-IsoP, and 8-isoPGF$_{3\alpha}$ in the same study. A more recent study indicated that platelets produce 15-F_{2t}-IsoP in the presence of free radicals and that 15-F_{2t}-IsoP was important for platelet recruitment (Pignatelli et al, 2011). Therefore, IsoP appear to play an important role in mediation of vascular effects, at least in part through actions on TP (Figure 1.4).

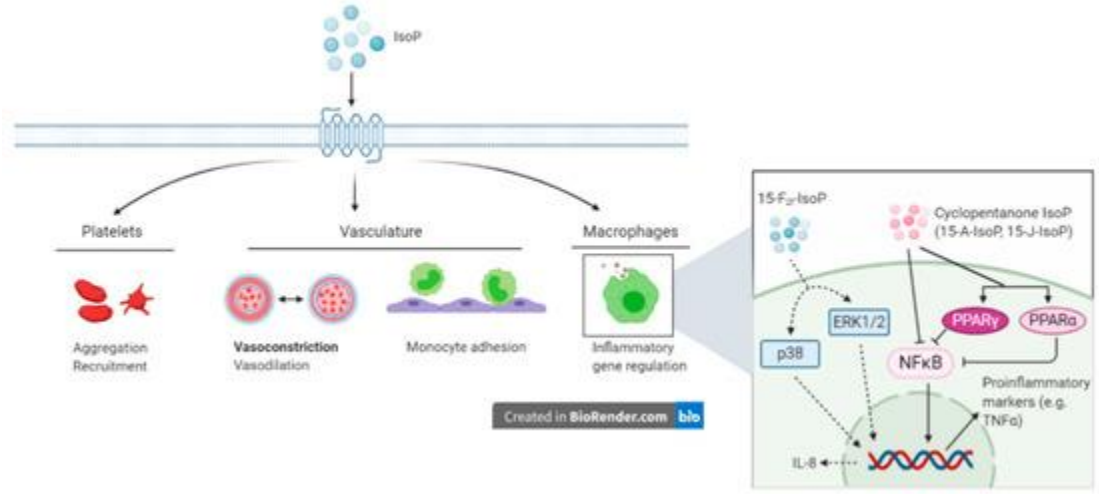

Figure 1.4. Putative actions of isoprostanes (IsoP) through the thromboxane receptor. Isoprostanes participate in vascular regulation and inflammation through their actions on platelets, the vasculature, and macrophages. During inflammation, IsoP affect monocyte adhesion to the endothelium and alter macrophage inflammatory genes. Insert box: 15-F2t-isoprostane modifies monocyte adhesion and increases interleukin-8 production via p38 and ERK1/2. Anti-inflammatory effects of IsoP are mediated by signaling through nuclear factor kappa B and peroxisome proliferator-activated receptor. IsoP = isoprostane;

Figure 1.4 (cont'd)
ERK = extracellular-signal-regulated kinase; NFκB = nuclear factor kappa B; PPAR = peroxisome proliferator-activated receptor; IL = interleukin. Created with BioRender.com.

The TP is a G-protein-coupled receptor distributed widely throughout the body and among various cells, having been described in platelets, EC, and smooth muscle cells, along with others (Miggin and Kinsella, 1998). Ligand binding to TP can result in coupling to a wide range of G proteins, ultimately leading to downstream effects that impact coagulation, inflammation, and oxidative stress (Xu et al., 2006; Woodward et al., 2011; Capra et al., 2013). For instance, oxidative stress was mitigated when animals were treated with the TP antagonist S18886 as demonstrated by decreased urinary 15-F_{2t}-IsoP and evidence of renal pathology in a murine model of diabetic nephropathy (Xu et al., 2006). The diversity of TP provides a possible explanation for the divergent effects of IsoP on the vasculature between different species and tissue beds. For instance, work performed by Ogletree and Allen questioned whether both intraspecies and interspecies differences existed between TP of artery, vein, and airway smooth muscles. Although TP appeared to be the same within a species, TP antagonists had significantly divergent potencies between the smooth muscles of rats and guinea pigs (Ogletree and Allen, 1992). From this early study, the authors concluded that there may not be different subtypes of TP, but there is likely significant variation between species. However, more recent studies have supported the existence of TP heterogeneity. This is exemplified in humans, where there are 2 subtypes of TP commonly termed TPα (placental) and TPβ (endothelial) (Raychowdhury et al., 1994). Although these subtypes are encoded by a single gene, their cytoplasmic tails are alternatively spliced, they are expressed to varying degrees in tissues, and have shown to exert differential signaling and downstream effects (Miggin and Kinsella, 1998; Yukawa et al., 1997). For instance, TPα is down-regulated in fibroblasts that have prolonged stimulation with a TP

agonist while TPβ is up-regulated (Yukawa et al., 1997). It is not true, however, that every species expresses 2 subtypes of TP. In fact, cattle express only one whose amino acid sequence most closely resembles that of the human TPα isoform (Muck et al., 1997). Investigating IsoP-TP interaction and the downstream effects in each species represents an area of opportunity to gain a more thorough understanding of how IsoP exert biological actions.

Inflammatory Effects

Outside the scope of vascular regulation, a limited number of studies have investigated other biological roles of IsoP. The intimate relationship between inflammation and oxidative stress suggests that IsoP may serve as an inflammatory mediator. Indeed, 15-F_{2t}-IsoP is capable of inhibiting monocyte adhesion to human dermal microvascular EC, with maximal inhibition being noted at a concentration of 1 μM. However, in human umbilical vein EC, 15-F_{2t}-IsoP enhanced monocyte adhesion at 10^{-10} to 10^{-8} M (Kumar et al., 2004). To characterize the mechanism by which 15-F_{2t}-IsoP caused the suppression of monocyte adhesion to EC, the authors investigated several direct and indirect effects the IsoP may have. Of the proposed mechanisms, 15-F_{2t}-IsoP inhibited monocyte adhesion induced by tumor necrosis factor alpha (**TNFα**), had inhibitory effects comparable to those seen with a TP agonist, and appeared to be working through the p38 and c-Jun N-terminal kinases (**JNK**) pathway via a TP-mediated mechanism. Furthermore, 15-F_{2t}-IsoP appears to encourage the production of a secondary inhibitor of monocyte adhesion, which acts in a TP-independent manner (Kumar et al., 2004). Scholz and coworkers (2003) discovered that 8-isoP also increase interleukin-8 expression in human macrophages. Cyclopentenone IsoP (15-A_2-IsoP and 15-J_2-IsoP) are also capable of modulating macrophage inflammatory actions. The cyclopentenone IsoP abrogated inflammatory responses in both RAW 264.7 murine macrophages and primary macrophages via blocking translocation of nuclear factor

kappa B (**NFκB**) to the nucleus. Downstream effects of this blockade included inhibition of nitrite production, which was abrogated by performing glutathione adduction (Musiek et al., 2005). Interestingly, F_2-IsoP does not inhibit nitrite production, which implicates the cyclopentenone moiety as being responsible for the anti-inflammatory responses. The cyclopentenone IsoP diverge in their actions under some circumstances though, highlighted by the potent activation of PPARγ by 15-J_2-IsoP but not 15-A_2-IsoP (Musiek et al., 2005). Additional evidence for the anti-inflammatory effects of IsoP has been offered for 15-A_{3t}-IsoP, 14-A_{4t}-NeuroP, and 4-F_{4t}-NeuroP (Bosviel et al., 2017; Brooks et al., 2011). Given the impact IsoP have demonstrated in macrophages, it would likely be beneficial to investigate their effects on other cells that participate in the inflammatory response, such as other leukocytes and EC.

CONCLUSIONS AND FUTURE DIRECTIONS

Oxidative stress continues to be a cornerstone of numerous disorders in both humans and animals. Lipids readily succumb to oxidation damage, thereby introducing IsoP as the gold standard measurement of oxidative stress. In the last 30 years, studies have established the mechanism of IsoP formation and several measurement methods, along with building some evidence for their physiological role in the host. Large deficits remain, however, in maximizing the use of IsoP in veterinary medicine. For instance, although sufficient methods exist to do so, detecting the presence and concentrations of IsoP in a patient will be of little benefit if there is not an understanding of threshold concentrations that indicate disease or an understanding of how altered IsoP concentrations may be impacting the host.

To use IsoP most-effectively in veterinary medicine, it will be critical to first establish IsoP concentrations in healthy animals so that a basis for disease detection can occur. Then, measurement of IsoP during various relevant diseases can be performed to elucidate conditions

in which IsoP may indicate a disease process. Concurrently, it will also be necessary to determine which sample and processing method is most ideal for each case. In association with changing IsoP concentrations, whether during health or disease, many opportunities remain in determining actions of IsoP in the host. Additionally, it is prudent to perform species-specific studies as IsoP have proven to be complex and incredible amounts of variation have been demonstrated between humans and numerous domestic species. Ultimately, however, learning how IsoP actions benefit or harm the host will be of little use in veterinary medicine without the development of reliable, convenient assays that do not depend on complicated sample preparation or expensive laboratory equipment. If these conditions can be improved upon, both human and veterinary species stand to reap the benefits of a highly sensitive and specific oxidative stress biomarker capable of exerting important, complex physiological effects.

CHAPTER 2

Published in Journal of Dairy Science: Putman, A. K., J. L. Brown, J. C. Gandy, L. Wisnieski, and L. M. Sordillo. 2018. Changes in biomarkers of nutrient metabolism, inflammation, and oxidative stress in dairy cows during the transition into the early dry period. J. Dairy Sci. 101:9350–9359. doi: 10.3168/jds.2018-14591.

INTRODUCTION

The dry period is the critical time between lactations in which a cow's mammary gland remodels and regenerates in preparation for the ensuing lactation. During this time, high-producing dairy cows are subject to stressors such as an abrupt cessation in milking, mammary gland discomfort, and physiological imbalances such as altered energy, immune, and hormonal states (Zobel et al., 2015). For instance, intramammary pressure increases when the udder becomes engorged with milk after abrupt milking cessation, leading to discomfort. Acute involution also follows abrupt milking cessation and elicits an inflammatory response, further causing cattle distress (Zobel et al., 2015). Early involution is a critical transition for dairy cows; however, most retrospective and prospective studies have focused instead on health risk factors associated with the peri-parturient period such as metabolic stress (Sordillo and Mavangira, 2014).

Metabolic stress is a cluster of risk factors in periparturient cows that leads to an increased susceptibility to certain health disorders, such as metritis and mastitis (Sordillo and Mavangira, 2014). Metabolic stress of periparturient cows is analogous to metabolic syndrome in humans and results from a combination of aberrant nutrient metabolism leading to dyslipidemia, chronic inflammation, and oxidative stress (Sordillo et al., 2009; Sordillo and Mavangira, 2014; Mbata et al., 2017). For instance, early-lactation cows that cannot meet energy demands through dry matter intake experience aberrant nutrient metabolism, indicated by biomarkers of fat

mobilization such as nonesterified fatty acids (NEFA; Bell, 1995). While lipid mobilization is a normal physiological response to help the cow adapt in these situations, excessive fat mobilization can be problematic. For instance, overproduction of ketones such as BHB occurs during times of high circulating NEFA concentrations when there is not a sufficient amount of Kreb's cycle intermediates to appropriately oxidize the acetyl coenzyme A produced by NEFA (Kuhla et al., 2016; Han van der Kolk et al., 2017). Additionally, increased concentrations of certain biomarkers, such as NEFA and BHB, have been linked to early-lactation disease and altered immune competence (Erdmann et al., 2018). Furthermore, the presence of aberrant nutrient metabolism, chronic inflammation, or oxidative stress can intensify the other factors that can cause metabolic stress, causing further problems (Trevisi et al., 2012; Esposito et al., 2014; Sordillo and Mavangira, 2014). For instance, increased plasma NEFA can lead to an increase in reactive oxygen species, which can exacerbate oxidative stress when present in excess. Oxidative stress can then contribute to dysregulated inflammatory responses and dyslipidemia (Sordillo et al., 2009). Cows entering the dry period may also experience dyslipidemia, chronic inflammation, or oxidative stress; however, assessments of these biomarkers have not been made during the physiological transition from late lactation to involution.

Cows undergoing the major physiological transition from lactating to nonlactating experience many stressors that may compromise their health and well-being. For instance, a cow entering the dry period is in her last trimester of pregnancy, when fetal growth is most rapid, milk production rapidly declines, and social stressors may occur due to moving to new pens with a new group of cows (Schirmann et al., 2011). Due to the similarities of potential stressors imposed on high-producing cows entering both the early dry period and early lactation, it can be anticipated that the cows will experience some changes in biomarkers of nutrient metabolism,

oxidative stress, and inflammation that collectively may contribute to metabolic stress. Understanding changes in biomarkers associated with metabolic stress will give valuable insight into how the early dry period may affect animal health and welfare. Therefore, the goal of this study was to document changes in biomarkers of nutrient metabolism, oxidative stress, and inflammation present during the early dry period of dairy cows.

MATERIALS AND METHODS

Animals

This study was approved by the Michigan State University Institutional Animal Care and Use Committee. Animals were enrolled 56 d before the expected calving date with owner consent. Blood samples were collected from 29 Holstein dairy cows (326 ± 5 DIM; range: 299–390 DIM) from a commercial herd that was free from clinical disease with SCC $<250 \times 10^3$ cells/mL. Cows had an average milk production of 34 kg/d (range: 17.8–52.3 kg of milk/d) in the previous lactation. Parity ranged from 1 to 5, and cows had an average BCS of 3.0 at the time of dry-off (range: 2.6–4.0). Cows had ad libitum access to a TMR and water. At d−6, cows were fed a late-lactation diet and switched to a far-off dry cow diet at d 0 (Table 2.1). Cows remained on the far-off dry cow diet for the remainder of the study. Before drying off, cows were milked 2 times/d and were treated with a standard intramammary dry cow antimicrobial therapy to protect against new intra-mammary infections. All cows were housed in a freestall barn that was cooled via fans and grouped according to stage of lactation. As cows were dried off, they were moved from a late-lactation pen to a dry cow pen with a new group of animals. Animals were sampled in 4 cohorts based on dry-off date. Group 1 (n = 13), group 2 (n = 9), and group 3 (n = 5) were all sampled during the summer over a 6-wk period, whereas group 4 (n = 2) was sampled in the fall.

Table 2.1. Diet of late-lactation and early dry cows for the study period.

Item	Late Lactation	Far-Off Dry
NEL[1] (Mcal/kg)	1.5	1.15
Crude Protein (%)	19	11
Fat (%)	5.3	2.3
Non-fiber Carbohydrate (%)	38	17
Calcium (%)	0.75	0.51
Phosphorus (%)	0.69	0.36
Magnesium (%)	0.78	0.31
Potassium (%)	1.4	2.5
Sodium (%)	0.29	0.34
Chloride (%)	0.53	0.99
Sulfur (%)	0.3	0.18
Selenium (ppm)	6.2	23
Vitamin E (IU/animal)	290	1064

[1]Estimated energy of lactation for an animal consuming 3× its requirement.

Sample Collection and Processing

Samples were collected aseptically in the morning between 0800 and 1000 h from the coccygeal vein in evacuated tubes containing serum separator and EDTA. Six collection time points were chosen as d −6, 0, +1, +2, +6, and +12 relative to the dry-off date. Samples were immediately stored on ice throughout the collection and processing stages. Serum was harvested after centrifugation at 1,449 ×g for 15 min at 4°C and aliquoted. A serum aliquot from each cow was sent to Michigan State University's Veterinary Diagnostic Laboratory (Lansing, MI), where commercially available assays were used to quantify calcium, NEFA [HR Series NEFA-HR(2), Wako Life Sciences, Mountain View, CA], BHB (Catachem Inc., Bridgeport, CT), albumin (Beckman Coulter Inc., Brea, CA), and cortisol concentrations on each collection day. An autoanalyzer (Olympus AU 640e, Beckman Coulter Inc.) was used to visualize the colorimetric measurements, and appropriate controls were used for quality control. Additional aliquots of serum were flash frozen in liquid nitrogen and stored at −80°C pending analysis within 1 mo of collection for oxidative stress indicators and acute phase proteins.

Whole-blood samples collected in EDTA evacuated tubes were kept refrigerated at 4°C immediately upon returning from the farm until blood leukocyte differential analysis could be performed. A 4-way leukocyte differential was performed to quantify total leukocyte, neutrophil, lymphocyte, eosinophil, and monocyte concentrations on collection day using an automated blood leukocyte differential test (QScout BLD, Advanced Animal Diagnostics, Morrisville, NC).

Haptoglobin

A commercially available photometric colorimetric assay (Phase haptoglobin assay kit, Tridelta Development LLC., Boonton, NJ) was used to determine haptoglobin concentrations in serum following the manufacturer's instructions. Absorbance was read at 600 to 630 nm on an Infinite 200 Pro plate reader (Tecan, Männedorf, Switzerland). The intra- and interassay coefficients of variation were 2.47 and 0.74%, respectively.

Oxidative Stress

Commercial assays were used to quantify oxidative stress indices following the manufacturer's instructions. Reactive oxygen and nitrogen species (**RONS**) concentrations were quantified in serum using an OxiSelect in vitro reactive oxygen species/RNS assay kit (Cell BioLabs Inc., San Diego, CA). In brief, free radicals that exist in the sample will attach to a dichlorodihydrofluorescin DiOxyQ probe, converting dichlorodihydrofluorescin to a product that fluoresces (2',7'-dichlorodihydrofluorescein). Thus, fluorescence is proportional to the amount of RONS in the sample. All 96-well microtiter plates (Black Isoplate-96, Perkin-Elmer, Waltham, MA) were read using an Infinite 200 Pro plate reader (Tecan). Dichlorofluorescent dye fluorescence was determined at 480 nm of excitation and 530 nm of emission. A standard curve (0–10,000 nM) was created to ensure fluorescence at various concentrations. Background

fluorescence was eliminated by subtracting blank values from sample values (Abuelo et al., 2013). Units were measured as relative fluorescence units (**RFU**) per microliter.

Antioxidant potential (**AOP**) concentrations were determined in serum using trolox (synthetic vitamin E analog) equivalents (**TE**) antioxidant capacity as previously described (Re et al., 1999). Antioxidant components interact in serum, and it is difficult to measure each antioxidant separately. As such, this method accounts for all antioxidants present in a sample, such as albumin, thiols, bilirubin, and superoxide dismutase. In short, a known amount of trolox standard concentration will result in a similar reduction of the radical 2,2'-azino-bis-3-ethylbenzothiazoline-6-sulfonic acid (Sigma-Aldrich, St. Louis, MO) based on the standard curve (0–25 mg/mL). Shifts in oxidative balance can result from an increase in RONS, a decrease in AOP, or changes in both parameters. Thus, an oxidant status index (**OSi**) was calculated as RONS/AOP to characterize shifts in oxidative balance (Abuelo et al., 2013).

Targeted analyses of plasma isoprostanes (**IsoP**), which are highly sensitive and specific products of lipid peroxidation associated with oxidative stress, were quantified using liquid chromatography–tandem MS. The specific isomers analyzed were 5,9α,11α-trihydroxy-(8β)-prosta-6E,14Z-dien-1-oic acid (**5-iPF$_{2\alpha}$-VI**), 12-iso-5(R),6E,14Z-prostaglandin F$_{2\alpha}$ (**8,12-iso-iPF$_{2\alpha}$-VI**), 8-iso-prostaglandin E$_2$ (**8-iso-PGE$_2$**), 8-iso-15-keto-prostaglandin E$_2$ (**8-iso-15-keto-PGE$_2$**), 8-iso-15(R)-prostaglandin F$_{2\alpha}$ [**8-iso-15(R)-PGF$_{2\alpha}$**], 8-iso-prostaglandin A$_1$ (**8-iso-PGA$_1$**), 8-iso-prostaglandin A$_2$ (**8-iso-PGA$_2$**), 15-F$_{2t}$-Iso (formerly 8-iso-prostaglandin F$_{2\alpha}$), and 2,3-dinor-8-iso prostaglandin F$_{2\alpha}$ (**2,3-dinor- 8-iso-PGF$_{2\alpha}$**). Samples were collected, extracted, and batch analyzed using methods published previously by Mavangira et al. (2016) with slight modification. Briefly, 1 mL of flash-frozen plasma was thawed on ice and mixed with an antioxidant-reducing agent and cyclooxygenase inhibitor mixture at 4 µL/mL to prevent

degradation of preformed oxylipids and prevent ex vivo lipid peroxidation. The antioxidant-reducing agent mixture consisted of 50% methanol, 25% ethanol, and 25% water with 0.9 mM butylated hydroxytoluene, 0.54 mM EDTA, 3.2 mM tetraphenylporphyrin, and 5.6 mM indomethacin. Samples were combined with a 15-µL mixture of deuterated internal standards containing 0.25 µM 5(S)-hydroxyeicosatetraenoic acid-d_8, 0.25 µM 15(S)-hydroxyeicosatetraenoic acid-d_8, 0.5 µM 8(9)-epoxyeicosatrienoic acid-d_{11}, 0.5 µM prostaglandin E_2-d_9, and 0.25 µM 8,9-dihydroxyeicosatrienoic acid-d_{11}. Afterward, methanol was added to yield a 60% methanol solution. Samples were vortexed for 2 min, incubated at room temperature for 15 min, and centrifuged at 4,816 ×g for 20 min at 4°C. Supernatant was diluted with HPLC water to yield a 20% methanol solution. Solid phase extraction was carried out using Phenomenox (Torrance, CA) Strata-X 33-µm polymeric reversed-phase 200 mg/3 mL columns preconditioned with 3 mL of methanol followed by 3 mL of HPLC water. Supernatants were loaded into the columns and then washed with 20% methanol and eluted with a 50:50 mixture of methanol and acetonitrile with 2% formic acid. Volatile solvents were dissolved using a Savant SpeedVac (ThermoFisher Scientific, Waltham, MA), and residues were reconstituted in methanol, mixed at a 2:1 ratio with HPLC water, and stored in chromatography vials at −80°C until analysis. Quantification of IsoP was carried out on a Waters (Milford, MA) Xevo TQ-S tandem quadrupole mass spectrometer using multiple reaction monitoring. Chromatography separation was performed with a Waters Acquity UPLC BEH C18 column (1.7 µm, 2.1 × 150 mm) held at 50°C and autosampler held at 10°C. Mobile phase bottle A was water containing 0.1% acetic acid, mobile phase bottle B was acetonitrile, and mobile phase bottle C was methanol; the flow rate was 0.3 mL/min. Liquid chromatography separation took 10 min/sample. Concentrations of IsoP were detected using electrospray ionization in negative-ion mode. Cone

voltages and collision voltages were optimized for each analyte using Waters QuanOptimize software, and data analysis was carried out with Waters TargetLynx software.

Statistical Analyses

Repeated-measures linear mixed effects models were constructed using the PROC MIXED procedure in SAS 9.4. (SAS Institute Inc., Cary, NC) to assess trends in concentrations of metabolic biomarkers over the study period. The biomarkers included calcium, NEFA, BHB, albumin, haptoglobin, cortisol, total leukocytes, neutrophils, lymphocytes, eosinophils, monocytes, RONS, AOP, OSi, and IsoP. Each biomarker was tested in a separate model that included the fixed effect of time point and a random intercept for cow, which accounted for the dependence between samples taken from the same cow. A spatial covariance residual matrix was used to account for unequal spacing between time points. Normality of residuals was visually assessed with quantile-quantile plots and histograms. Data that violated the normality assumption were transformed by either the log or square root function. Levene's test and graphs of predicted residuals were used to assess heteroscedasticity, which is when the variance of the residuals is unequal. Degrees of freedom were estimated using the Kenward-Roger approximation if heteroscedasticity was present. Differences in concentrations of biomarkers between different time points were tested using multiple group comparisons with a Bonferroni adjustment. Statistical significance was set at $P < 0.05$.

RESULTS

Many of the biomarkers indicative of altered nutrient metabolism varied over the sampling period from d −6 to d +12. Table 2.2 depicts the mean and standard error for altered nutrient metabolism biomarkers over the sampling period. Calcium concentrations were higher at d +2 (mean = 2.58 mmol/L) than the other time points ($P < 0.01$). Mean concentrations of NEFA were

0.15 mmol/L at d −6 and reached highest mean concentrations of 0.59 mmol/L at d +1 ($P < 0.1$). After d +1, NEFA concentrations began to decrease and approached those seen before dry-off by d +12 (mean = 0.18 mmol/L). Lowest concentrations of BHB were 0.48 mmol/L at d 0, and highest concentrations were 0.72 mmol/L at d +2 ($P < 0.001$).

Table 2.2. Changes in biomarkers of nutrient metabolism during the dry-off period in 29 healthy Holstein cows.

	Day Relative to Dry-Off						
Biomarker	D-6	D0	D+1	D+2	D+6	D+12	SE
Calcium***(mg/dL)	9.67^{bc}	9.43^{cd}	9.91^{b}	10.3^{a}	9.83^{b}	9.33^{d}	0.07
NEFA[1]*** (mEq/L)	0.15^{c}	0.24^{bc}	0.59^{a}	0.33^{b}	0.22^{c}	0.18^{c}	0.03
BHB[2]*** (mg/dL)	7.04^{ab}	5.0^{c}	6.93^{ab}	7.52^{a}	5.32^{c}	5.82^{bc}	0.36

[a-d]Means within a row with different superscripts are different ($P < 0.05$).
[1]NEFA=nonesterified fatty acids
[2]BHB=beta-hydroxybutyrate
[***]ANOVA *P*-value <0.001

Almost all indicators of inflammation changed over the sampling period, as shown in Table 2.3. The negative acute phase protein albumin generally remained consistent, but a decrease was noted at d +12 with a mean concentration of 32.5 g/L ($P < 0.01$). Haptoglobin is a positive acute-phase protein that increased at d +12 to a mean concentration of 0.32 g/L ($P < 0.01$). Similarly, cortisol concentrations peaked at d +1 with a concentration of 13.8 mmol/L. Cortisol concentrations were lower at d +6 and +12 with concentrations of 4.91 and 3.68 mmol/L, respectively, than d +1 ($P < 0.01$). Table 2.4 indicates changes in blood leukocytes over the sampling period. Lowest total leukocyte concentrations were reached at d +1 and +2 (8.23 and 8.39 × 10^3 cells/µL, respectively). Neutrophil concentrations were lower at d +1 (mean = 3.88 × 10^3 cells/µL) and d +2 (mean = 3.94 × 10^3 cells/µL) compared with d −6 (mean = 4.79 × 10^3 cells/µL; $P < 0.01$). The lowest concentrations of lymphocytes were 4.07 and 4.08 × 10^3 cells/µL at d +2 and +12, respectively, which differed from d −6 (mean = 4.85 × 10^3 cells/µL; $P < 0.01$).

Eosinophil concentrations steadily increased from a mean concentration of 0.07×10^3 cells/μL at d −6 to 0.24×10^3 cells/μL at d +12 ($P < 0.01$). Monocyte concentrations were higher at d −6 and 0 (mean = 0.27 and 0.25×10^3 cells/μL, respectively) compared with the other sampling points except d +6, which had a mean of 0.23×10^3 cells/μL ($P < 0.05$).

Table 2.3. Changes in inflammatory indicators during the dry-off period in 29 healthy Holstein cows.

	Day Relative to Dry-Off						
Biomarker	D-6	D0	D+1	D+2	D+6	D+12	SE
Albumin*** (g/dL)	3.50^{abc}	3.49^{bc}	3.56^{a}	3.52^{ab}	3.43^{c}	3.25^{d}	0.04
Haptoglobin[1]*** (mg/mL)	0.05^{b}	0.06^{b}	0.06^{b}	0.07^{b}	0.04^{b}	0.32^{a}	0.001
Cortisol[1]*** (mmol/L)	9.8^{ab}	7.0^{abc}	13.8^{a}	10.1^{ab}	4.9^{bc}	3.68^{c}	0.08

[a-c]Means within a row with different superscripts are different ($P < 0.05$).
[1]Data transformed by square root function. Back-transformed values are shown.
*** ANOVA *P*-value <0.001

Table 2.4. Changes in blood leukocyte counts during the dry-off period in 29 healthy Holstein cows.

	Day Relative to Dry-Off						
Biomarker	D-6	D0	D+1	D+2	D+6	D+12	SE
Total Leukocytes*** (10^3/μL)	10.0^{a}	9.46^{ab}	8.29^{c}	8.39^{c}	9.27^{ac}	8.69^{bc}	0.53
Neutrophils*** (10^3/μL)	4.79^{a}	4.43^{ac}	3.88^{b}	3.94^{bc}	4.48^{abc}	4.13^{abc}	0.23
Lymphocytes*** (10^3/μL)	4.85^{a}	4.68^{ab}	4.13^{bc}	4.07^{c}	4.37^{abc}	4.08^{c}	0.34

Table 2.4 (cont'd)

Eosinophils*** (10^3/μL)	0.07^{bc}	0.06^{c}	0.07^{bc}	0.14^{abc}	0.17^{ab}	0.24^{a}	0.03
Monocytes*** (10^3/μL)	0.27^{a}	0.25^{ab}	0.17^{c}	0.19^{bc}	0.23^{abc}	0.19^{bc}	0.02

[a-c]Means within a row with different superscripts are different ($P < 0.05$).
*** ANOVA P-value <0.001

All biomarkers of oxidant status varied over the sampling period. Table 2.5 represents changes in direct measures of oxidant status. Reactive oxygen and nitrogen species concentrations were lowest at d +2 (mean = 12.0 RFU/μL), which was lower than all other time points ($P < 0.01$) except d −6. Concentrations of AOP were lower at d +2 (mean = 14.4 TE/μL) and d +12 (mean = 13.5 TE/μL) compared with the other sampling points ($P < 0.05$ and < 0.01, respectively). The OSi tended to increase from the previous time point at all sampling times except d +2. The lowest OSi was observed at d −6 and d +2 compared with the highest OSi at d +12 ($P < 0.001$). The different IsoP isomers measured in this study had varied responses through the sampling period. The isomers 8-iso-PGE_2 and 2,3-dinor-8-iso-$PGF_{2\alpha}$ were undetectable throughout the study. Concentrations of 8,12-iso-$PGF_{2\alpha}$-VI, 8-iso-15(R)-$PGF_{2\alpha}$, and 8-iso-15-keto-PGE_2 did not differ over the sampling period and are shown in Table 2.6. In contrast, other IsoP did change over the sampling period. Concentrations of 5-i$PF_{2\alpha}$-VI remained relatively stable from d −6 to +6 but increased to the highest concentrations at d +2 ($P < 0.01$; Figure 2.1). Concentrations of 15-F_{2t}-Iso gradually increased following the abrupt cessation of lactation and reached highest concentrations of the study (0.69 nM) at d +2 before returning to baseline amounts (0.2 nM) by d +6 (Figure 2.2). Although the ANOVA detected differences for 15-F_{2t}-Iso ($P < 0.01$), no pairwise comparisons differed between sampling points after Bonferroni adjustment. The dehydration IsoP products of 8-iso-PGE_2, 8-iso- PGA_1, and 8-iso-PGA_2 both differed over the

sampling period (Figure 2.3). Concentrations of 8-iso-PGA_1 were higher at d +12 (0.59 nM) than all other sampling points ($P < 0.01$), whereas 8-iso-PGA_2 was lower at d +12 (1.51 nM) compared with d +2 (3.24 nM; $P < 0.05$).

Table 2.5. Changes in biomarkers of oxidant status during the dry-off period in 29 healthy Holstein cows.

	Day Relative to Dry-Off						
Biomarker	D-6	D0	D+1	D+2	D+6	D+12	SE
RONS[1***] (RFU/µL)	14.8[bc]	19.4[a]	19.6[a]	12.0[c]	17.2[ab]	17.5[ab]	2.1
AOP[2***] (TE/µL)	15.9[b]	18.7[a]	18.0[a]	14.4[c]	17.4[a]	13.5[c]	0.44
OSi[3***] (RFU/TE)	1.02[b]	1.12[ab]	1.16[ab]	0.89[b]	1.09[ab]	1.33[a]	0.18

[a-c]Means within a row with different superscripts are different ($P < 0.05$).
[1]RONS=Reactive oxygen and nitrogen species
[2]AOP=Antioxidant potential
[3]OSi=Oxidant status index
[***] ANOVA *P*-value <0.001

Table 2.6. Changes in select indicators of arachidonic acid peroxidation during the dry-off period in 10 healthy cows.

	Day Relative to Dry-Off						
Biomarker	D-6	D0	D+1	D+2	D+6	D+12	SE
8, 12-iso-iPF$_{2\alpha}$-VI	0.12	0.19	0.14	0.14	0.1	0.14	0.004
8-iso-15(R)-PGF$_{2\alpha}$	0.12	0.12	0.13	0.1	0.02	undetectable	0.003
8-iso-15-keto-PGE$_2$[1]	0.24	0.25	0.3	0.27	0.15	0.13	0.004

[1] Data transformed by square root function. Back transformed values are shown.

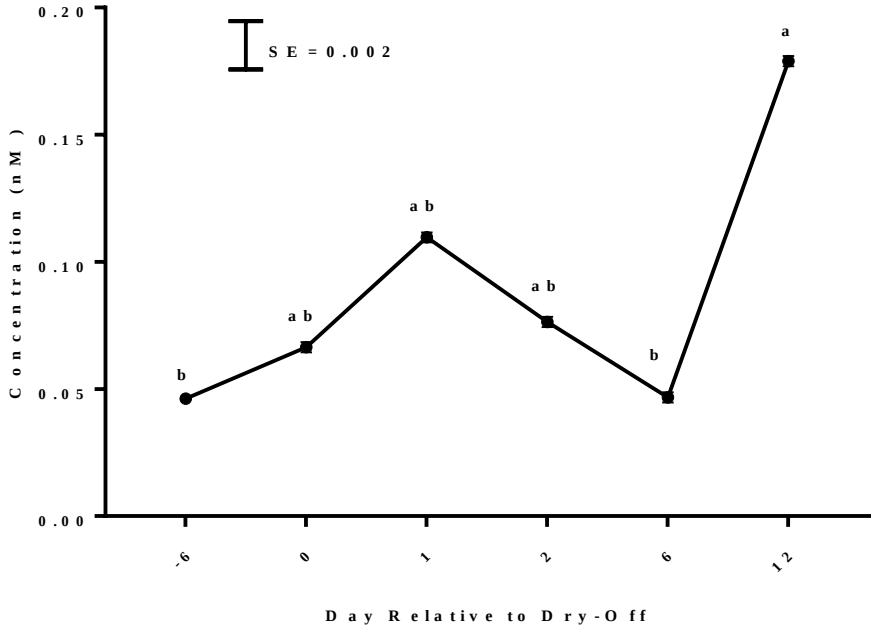

Figure 2.1. Changes in plasma 5,9α,11α-trihydroxy-(8β)-prosta-6E,14Z-dien-1-oic acid (5-iPF$_{2\alpha}$-VI) concentrations from baseline (d−6) to d +12 after dry-off in healthy cows (n = 10). Means with different letters (a,b) are different ($P < 0.05$). Data are presented as means ± SE. Error bars are partially obscured by data points due to small SE.

Figure 2.2. Changes in 15-F_{2t}-Iso from baseline (d −6) to d +12 after the cessation of lactation in healthy cows (n = 10). Data are presented as means ± SE. Error bars are partially obscured by data points due to small SE.

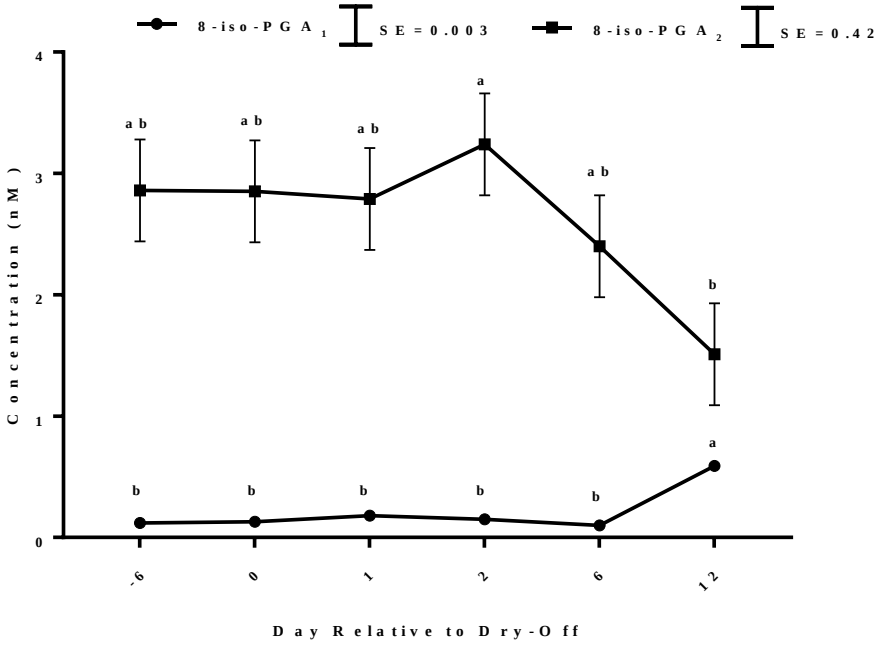

Figure 2.3. Changes in dehydration products of 8-iso-prostaglandin E_2 (8-iso-PGE_2) throughout the sampling period (n = 10). Mean concentrations with different letters (a,b) are different ($P < 0.05$).

Figure 2.3 (cont'd).
Data are presented as means ± SE. Error bars for 8-iso-prostaglandin A_1 (8-iso-PGA_1) are obscured by data points due to small SE. 8-iso-PGA_2 = 8-iso-prostaglandin A_2.

DISCUSSION

This study highlighted that biomarkers of nutrient metabolism, inflammation, and oxidative stress indeed changed throughout the transition into the early dry period, particularly in the first 2 d after abrupt milking cessation. Altered nutrient metabolism is related to many metabolic and inflammatory conditions in periparturient cows (Sordillo and Mavangira, 2014). In the present study, mean calcium concentrations varied between many of the sampling points and approached the upper reference limit of 2.6 mmol/L during the first several days after dry-off. In the past, a proposed treatment for hypocalcemia was to increase pressure in the mammary gland via insufflation, which increased blood calcium concentrations (Marshak, 1956). This treatment was successful for 2 potential reasons: calcium demands decreased after milking cessation, and milk accumulation in the mammary gland led to weakening of tight junctions between mammary epithelial cells, resulting in increased paracellular transport of calcium into the blood (Aslam and Tucker, 1998). Similarly, cows in early involution have decreased calcium demands and increased intramammary pressure when milking is ceased, which may explain the increased concentrations noted in the present study.

Elevated concentrations of NEFA and BHB are indicators of negative energy balance (Abdelli et al., 2017). The peak NEFA concentration noted in this study occurred during the first day of involution. Early involution was previously shown to involve inflammatory processes that may cause an increase in NEFA concentrations (Kushibiki et al., 2003). Increased NEFA concentrations also occur in a fasting state, causing some lipid mobilization (Sordillo and Mavangira, 2014). The increase in NEFA concentration observed in this study may also be due

to reduced feed intake as a result of displacement of cows from the feed bunk when they were mixed with a new group of cows in the first few days of dry-off. A previous study suggests that herd NEFA concentrations >0.4 mEq/L prepartum or >0.7 mEq/L postpartum are indicative of increased risk of developing diseases and production losses such as displaced abomasum (Ospina et al., 2010). Although NEFA concentrations noted in this study approached this level at 1 sampling point, the concentrations were lower than the accepted prepartum disease risk concentrations of 0.4 mEq/L at all other sampling points (Ospina et al., 2010). To date, there is no information on what the NEFA concentrations would be around the time of dry-off that would indicate increased risk of early-lactation disease incidence. The ability to use alerted NEFA concentrations during the early dry period as a potential tool for predicting disease risk in the ensuing lactation may allow for sufficient time to adjust nutritional management practices to optimize health in periparturient cows.

Similar to NEFA, BHB concentrations tend to increase as cows approach calving and as glucose concentrations decrease (Farahani et al., 2017). In the present study, BHB concentrations decreased as the dry-off date approached. The differences can be attributed to cows being in an improved energy balance as lactation ends and therefore having more carbohydrate available to fully oxidize NEFA as opposed to shifting to ketone synthesis via incomplete oxidation. Previous studies suggest that a herd prepartum concentration for BHB of at least 12 mg/dL is associated with increased risk of early-lactation diseases (Ospina et al., 2010). None of the samples collected in our study reached the 12 mg/ dL of BHB threshold that was associated with increased risk for certain postcalving diseases and production losses seen in periparturient cows. It is important to note, however, that sampling occurred immediately after the cows were fed, which could have an effect on the BHB concentrations due to butyrate conversion to BHB by

rumen epithelia cells (Remling et al., 2014). Therefore, the variations in BHB concentrations noted in the present study may correspond to physiological changes associated with feeding. Moreover, no studies have been conducted to date that would suggest that increases in either NEFA or BHB concentrations around the time of dry-off would have any effect on disease incidence in periparturient cows. There is evidence, however, that NEFA concentrations representative of those found in healthy cows can still affect immune competence. Lacetera et al. (2004) found that NEFA concentrations as low as 0.25 mmol/L could decrease IgM secretion and that concentrations as low as 0.125 mmol/L could suppress interferon gamma secretion in peripheral blood mononuclear cells. Thus, it can be reasoned that cows at dry-off may also be subject to these immunosuppressive effects because the NEFA concentrations noted in the present study were consistently higher than 0.125 mmol/L. Due to the complex interactions between altered nutrient metabolism and inflammatory indices that contribute to metabolic stress and disease occurrence (Trevisi et al., 2012), it would be beneficial to investigate whether there are any correlations between NEFA or BHB concentrations at dry-off and periparturient disease risk.

Dysfunctional inflammation contributes to metabolic disturbances of dairy cows (Sordillo et al., 2009; Esposito et al., 2014). Certain blood proteins, known as the acute phase proteins, are considered to be highly sensitive indicators of inflammation because serum concentrations change >25% during an inflammatory response (Eckersall and Bell, 2010). Albumin is considered to be a negative acute phase protein associated with the resolution of inflammation (Zou et al., 2017). Brscic et al. (2015) reported albumin concentrations of 36.3 g/L for healthy dry cows, which is similar to the concentrations noted in this study. Serum haptoglobin has been stated as a valid biomarker that can distinguish diseased animals from healthy animals (Eckersall

and Bell, 2010). Additionally, it has been reported that healthy cattle have serum haptoglobin concentrations <20 mg/L (Eckersall and Bell, 2010). The mean concentrations of haptoglobin in this study were consistently higher than 20 mg/L. In contrast to the cows in the Eckersall and Bell (2010) study that were not undergoing any known inflammatory processes; however, mammary gland involution involves inflammation as the tissue remodels and may explain the higher concentrations during the present study. The effect of increased concentrations of haptoglobin during the transition into the early dry period on subsequent health and well-being of the cow is still unknown, although an argument could be made that the presence of haptoglobin in the mammary gland during this time would be beneficial. Arslan et al. (2013) demonstrated that haptoglobin was important for appropriate matrix remodeling after myocardial infarction in mice, and dairy cows in early involution also experience matrix remodeling of the mammary gland.

Cortisol is a hormone paramount to daily functions and the stress response in cows (Locatelli et al., 1989; Hannibal and Bishop, 2014). Past work has indicated that cows regrouped into a high-density stocked pen have an increased cortisol response when stimulated with adrenocorticotropic hormone (Friend et al., 1977). The cows in our study were regrouped into a pen stocked to full capacity, which may explain the increased cortisol concentrations noted after dry-off. Additionally, past studies have shown that NEFA concentrations increase with increased cortisol concentrations (Locatelli et al., 1989). Therefore, a peak of NEFA concentrations at d +1 in this study may be related in part to the peak of cortisol concentrations observed at the same time. Under normal conditions in the periparturient cow, plasma cortisol concentrations begin increasing a few days before parturition until the calf is born. Baseline levels of cortisol are then reached within 24 h of calving (Hydbring et al., 1999). The differences noted between the

animals in this study and periparturient cows can be attributed to the time at which stress occurs in the respective animals. Stress associated with labor can cause the increased cortisol concentrations of the periparturient cow (Hydbring et al., 1999), whereas animals entering the dry period experience stressors such as changing their social group at dry-off that can cause increased cortisol concentrations until the herd dynamics are established.

In general, total blood leukocytes, neutrophils, and lymphocytes followed similar patterns of changes throughout the study. It is well documented that leukocytes increase in the bovine mammary gland during acute involution (Sordillo and Nickerson, 1988). Therefore, the decrease of immune cells immediately following dry-off can be attributed to cells migrating from blood and into tissue (Atabai et al., 2007). Interestingly, eosinophils tended to steadily increase throughout the study. Typically associated with allergies and parasites, eosinophils have been shown to exist in healthy tissues, although their role is unclear (Gouon-Evans et al., 2000). For instance, Gouon-Evans et al. (2000) proposed that eosinophils are important for postnatal ductal branching of the mammary gland in mice. However, it is still unknown what role, if any, eosinophils may play in the involuting bovine mammary gland. Additionally, an autoallergy to the milk protein casein has been described in dairy cattle and develops within hours of dry-off (Peek and Divers, 2008). Therefore, the increased eosinophil concentrations may represent a subclinical hypersensitivity to the milk retained in the udder upon cessation of lactation. Alternatively, the combination of increased eosinophil and haptoglobin concentrations with decreased concentrations of albumin at d +12 could be indicative of an inflammatory response. Inflammation plays a pertinent role in metabolic stress in early-lactation cows (Sordillo and Mavangira, 2014); therefore, future studies should investigate how these changes may affect the health and well-being of cows during dry-off.

Oxidative stress occurs when there is an imbalance between RONS and antioxidant defenses and is a common disorder during periods of increased metabolic demands (Sordillo and Aitken, 2009; Abuelo et al., 2013). In accordance with the concept that antioxidants are produced in an attempt to minimize the damage induced by RONS (Sordillo and Aitken, 2009; Saeed-Zidane et al., 2017), concentrations of AOP generally followed the same pattern as RONS in the present study. However, OSi was highest at d +12 compared with all other sampling points, suggesting that this time point was when antioxidant defenses were lowest relative to RONS exposure. In an attempt to maintain antioxidant defense against increasing RONS, it is common to add antioxidant supplements to periparturient cow diets (Abuelo et al., 2013). However, it is unknown whether this practice would benefit cows entering the dry period and should be the focus of future investigations. Evaluating OSi, the ratio between RONS and AOP, has been indicated to provide a more accurate depiction of cow oxidant status compared with evaluating RONS or AOP concentrations alone (Abuelo et al., 2013). In our study, the OSi remained around 1 RFU/TE, which suggests a balanced redox status for the animals. Based on this measurement alone, one might assume that the cows were unlikely to experience oxidative stress because changes in RONS appeared to be matched by changes in AOP. However, it is also important to consider macromolecule damage that can occur due to free radical production before making this conclusion.

Although oxidative status changed during the sampling period, direct measures of macromolecule damage, such as quantification of IsoP concentrations, must be assessed to determine potential harmful effects on host tissues (Sordillo, 2018). Isoprostanes are prostaglandin-like compounds that are produced by oxidation of PUFA such as arachidonic acid through interactions with free radicals such as RONS (Lawson et al., 1999). Measures of

elevated 15-F_{2t}-Iso concentrations in particular are a valid biomarker of lipid peroxidation damage during severe oxidative stress in both humans and dairy cattle (Mavangira et al., 2016; Mavangira and Sordillo, 2018; Sordillo, 2018). The higher concentration of plasma 15-F_{2t}-Iso observed at d +2 in this study may be a consequence of the gradual increase in RONS exposure leading up to this sampling time point. Indeed, the RONS at d +1 was higher compared with baseline measures observed before the abrupt cessation of lactation. Although oxidative stress is known to adversely affect the immune and inflammatory responses of dairy cows (Sordillo and Aitken, 2009), the consequence that elevated 15-F_{2t}-Iso concentrations may have on important host defenses during the early dry period has yet to be determined. Furthermore, it is still unknown whether there is significance to having differential IsoP isomer production throughout the early dry period. In our study, for instance, 8-iso- PGA_1 isomer increased at d +12, whereas 8-iso-PGA_2 was decreased at this time (Figure 1.2). Although it is known that E_2- and D_2-IsoP will preferentially be produced over F_2-IsoP when reducing agents such as α-tocopherol are depleted (Milne et al., 2011), there is still a paucity of knowledge regarding why certain isomers of related IsoP do not always get produced to the same magnitude at any given time. For instance, perhaps 8-iso-PGA_1 is a proinflammatory IsoP and 8-iso-PGA_2 may be anti-inflammatory, and thus they would have opposite responses at the same time point. Therefore, further studies into the biological activities of IsoP may provide answers to these questions.

CONCLUSIONS

This study evaluated for the first time key biomarkers of altered nutrient metabolism, inflammation, and oxidative stress during the transition from late lactation and into the early dry period. Although many of the biomarkers changed during the initial stages of involution, the changes were not always equivalent with respect to magnitude and duration to those seen during

the periparturient period. The data obtained from this study provide insight into alterations of nutrient metabolism, inflammation, and oxidative stress biomarkers during the major transition from a lactating state to a nonlactating state. However, it remains unknown whether the magnitude of these changes merely represents a physiological response, whether they are negatively affecting cow health, or whether there is a threshold at which these biomarkers would predict disease. Therefore, future studies are necessary to elucidate specific causes and potential effects of these changes on the health of cows throughout the dry period and into early lactation.

CHAPTER 3

Published in Journal of Dairy Science: Putman, A. K., J. L. Brown, J. C. Gandy, Á. Abuelo, and L. M. Sordillo. 2019. Oxylipid profile of dairy cattle vary throughout the transition into early mammary gland involution. J. Dairy Sci. 102(3):2481-2491. doi: 10.3168/jds.2018-15158.

INTRODUCTION

Within a typical lactation cycle, the period of time in which a cow is not producing milk is known as the dry period. During this critical stage, the mammary gland remodels and regenerates in preparation for the ensuing lactation. In fact, omitting the dry period can lead to production losses ranging from 12 to 25% in the subsequent lactation (Rastani et al., 2005). The first 15 d after dry-off, which are a part of acute involution, are particularly important to the health and productivity of the cow (Smith et al., 2017). During this time, the mammary gland is highly susceptible to new infections, partially because abrupt cessation of milking results in a relatively compromised streak canal that is no longer being flushed to aid in the removal of bacteria (Bradley and Green, 2004). Furthermore, early involution is coupled with major hormonal, nutritional, and physiological changes as the mammary gland undergoes a change from a lactating to nonlactating state. For example, the mammary gland becomes engorged with milk, leading to cattle discomfort and is infiltrated with immune cells to remove residual milk and debris during this time (Sordillo and Nickerson, 1988; Zobel et al., 2015). Recruitment of inflammatory cells to the mammary gland is one of several important processes involved in mammary tissue remodeling (Atabai et al., 2007) and depends upon an appropriate inflammatory response.

An important component of the innate immune response is inflammation. When regulated properly, inflammation is capable of resolving tissue insults, both infectious and otherwise,

without causing further tissue damage. For instance, when mastitis-causing pathogens are recognized by the host, an immune response will occur that facilitates the neutralization of the organisms without compromising milk or tissues in a noticeable way (Sordillo, 2018). If inflammation is not controlled appropriately, however, mammary gland tissue damage can occur that may lead to negative effects on production. For example, the immune cells recruited during an inflammatory response can cause damage to mammary gland epithelial cells, leading to decreased milk production (Akers and Nickerson, 2011). Due to the potential damage inflammation can cause to host tissues, the onset and resolution of inflammation is tightly regulated and orchestrated by many mediators. One such class of mediators are oxylipids, which are derived from phospholipid membrane fatty acids (**FA**) via enzymatic or nonenzymatic pathways (Buczynski et al., 2009). Enzymatic pathways include cyclooxygenase (**COX**), lipoxygenase (**LOX**), and cytochrome-P450 (**CYP**), whereas nonenzymatic oxidation can occur when FA interact with reactive metabolites, such as reactive oxygen species (**ROS**; Buczynski et al., 2009). Oxylipids are capable of regulating all aspects of inflammation, possessing both pro-inflammatory and anti-inflammatory functions (Gabbs et al., 2015).

The FA substrate that oxylipids are derived from is a major determinant of their function. For instance, those that are derived from n-6 PUFA, such as arachidonic acid and linoleic acid (**LA**), tend to contribute to a pro-inflammatory state. On the other hand, those derived from n-3 PUFA, such as eicosapentaenoic acid (**EPA**) and docosahexaenoic acid (**DHA**), are generally considered anti-inflammatory (Calder, 2009). Products of PUFA peroxidation, including hydroperoxyoctadecadienoic acid and hydroperoxyeicosatetraenoic acid, typically are reduced immediately into more stable hydroxyls, such as hydroxyoctadecadienoic acid (**HODE**) and hydroxyeicosatetraenoic acid (**HETE**; Raphael et al., 2014). Although some oxylipids act

primarily as anti-inflammatory substances, such as those derived from n-3 PUFA, others may have multiple effects depending on cell type and location. For instance, HODE can be pro-inflammatory via adhesion molecule activation on EC (Friedrichs et al., 1999). However, HODE can also be anti-inflammatory by decreasing tumor necrosis factor-α-induced inflammatory responses in human epithelial cells (Altmann et al., 2007). Sources of oxylipids and their putative roles are depicted in Figure 3.1.

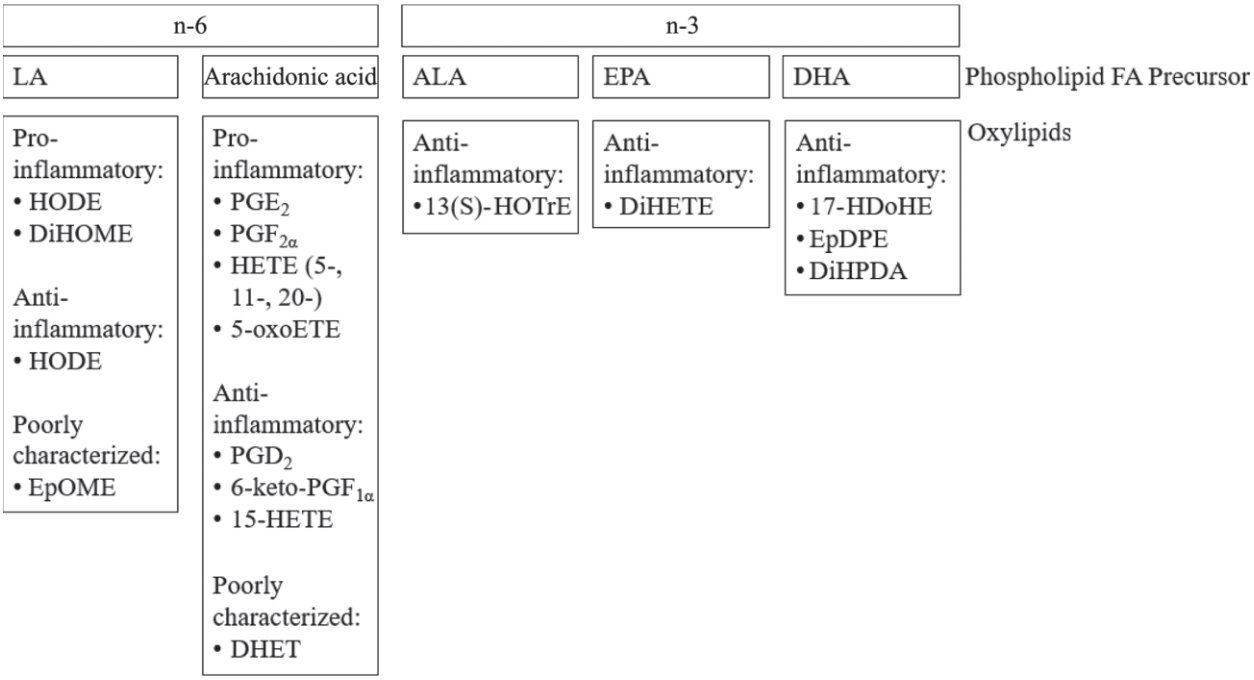

Figure 3.1. Sources and putative roles for oxylipids described in the present study. FA = fatty acid; LA = linoleic acid; ALA = α-linolenic acid; EPA = eicosapentaenoic acid; DHA = docosahexaenoic acid; HODE = hydroxyoctadecadienoic acid; DiHOME = dihydroxyoctadecenoic acid; EpOME = epoxyoctadecaenoic acid; HETE = hydroxyeicosatetraenoic acid; oxoETE = oxoeicosatetraenoic acid; DHET = dihydroxyeicosatrienoic acid; HOTrE = hydroxyoctadecatrienoic acid; DiHETE = dihydroxyeicosatetraenoic acid; HDoHE = hydroxydocosahexaenoic acid; EpDPE = epoxydocosapentaenoic acid; DiHPDA = dihydroperoxydocosahexaenoic acid.

The relative amount and potency of pro-inflammatory to anti-inflammatory oxylipids generates a profile that can influence inflammatory outcomes (Raphael et al., 2014). Previous work characterizing the complex oxylipid profile of dairy cattle has involved the periparturient and

lactating cow during health and disease, such as mastitis. Given that cows entering the dry period experience a major physiological change like that of periparturient cows, it can be anticipated that the oxylipid profile of dry cows would also be complex in nature. However, the oxylipid profile of dairy cattle entering the early dry period has not been explored. Determining the oxylipid profile of cows during this time provides further insight into the physiology of the dry period, leading to new hypotheses on how cow health and productivity may be affected. Therefore, this study aimed to document for the first time changes in these potent inflammatory mediators during the transition from late lactation to the early dry period.

MATERIALS AND METHODS

Animals

This study was approved by the Michigan State University Institutional Animal Care and Use Committee. Holstein cows (n = 10) from a commercial dairy herd were enrolled 56 d before expected calving date with owner consent, were free from clinical disease, and had SCC <250 × 10^3 cells/mL at their last DHIA test date. All cows were housed in a freestall barn, were grouped according to stage of lactation, and were milked 2 times/d before abrupt cessation of milking. At the time of dry-off, cows were treated with a standard intramammary antimicrobial treatment. Average milk production at the last DHIA test day was 31.7 kg/d (range: 17.8–39.5 kg/d), and the average DIM was 315 (range: 291–357). The average BCS was 3.2 out of 5 (range: 2.7–3.9), and parity ranged from 1 to 5 (average = 2.8 ± 1.5). Cows had ad libitum access to a TMR and water. Animals sampled at d −6 were fed a late lactation diet, whereas those sampled for the remainder of the study were fed a far-off dry cow diet (Table 3.1). Cows were sampled between the summer and fall of 2017.

Table 3.1. Diet of late lactation and early dry cows for the study period on a DM basis.

Item	Late Lactation	Far-Off Dry
NEL[1] (Mcal/kg)	1.5	1.15
Crude Protein (%)	19	11
Fat (%)	5.3	2.3
Non-fiber Carbohydrate (%)	38	17
Calcium (%)	0.75	0.51
Phosphorus (%)	0.69	0.36
Magnesium (%)	0.78	0.31
Potassium (%)	1.4	2.5
Sodium (%)	0.29	0.34
Chloride (%)	0.53	0.99
Sulfur (%)	0.3	0.18
Selenium (ppm)	6.2	23
Vitamin E (IU/animal)	290	1064

[1]HMSC = high-moisture shelled corn.
[2]NEL = the estimated energy of lactation for an animal consuming 3× its requirement

Sample Collection and Processing

Blood samples were collected aseptically into EDTA-containing evacuated tubes via coccygeal venipuncture between 0800 and 1000 h. Sampling occurred at 6 time points: d −6, 0, +1, +2, +6, and +12 relative to the dry-off date. Samples were immediately stored on ice during transportation and processing. Upon returning to the laboratory, blood samples were centrifuged at 1,449 × g for 15 min at 4°C, and plasma was subsequently harvested, aliquoted, and flash-frozen in liquid nitrogen. Plasma samples were stored at −80°C pending analysis via liquid chromatography (LC)-MS or LC-MS/MS within 1 mo.

Targeted Lipidomics

Targeted MUFA, PUFA, and SFA were analyzed with LC-MS, and oxylipids were quantified using LC-MS/MS (Table 3.2). Plasma samples (1 mL) were mixed with an antioxidant reducing agent mixture of 50% methanol, 25% ethanol, 25% water, butylhydroxytoluene (0.9 mM; Acros, Thermo Fisher Scientific, Waltham, MA), EDTA (0.54 mM; Sigma-Aldrich, St. Louis, MO), triphenylphosphine (3.2 mM; Sigma-Aldrich), and indomethacin (5.6 mM; Cayman Chemical,

Ann Arbor, MI) to prevent ex vivo lipid peroxidation and oxidation of preformed oxylipids (Mavangira et al., 2015).

Table 3.2. Lipids and corresponding abbreviations analyzed in the study.

Lipid	Abbreviation
Arachidonic acid	AA
Adrenic acid	-
α-Linolenic acid	ALA
Docosahexaenoic acid	DHA
Docosapentaenoic acid	DPA
Eicosapentaenoic acid	EPA
Dihomo-γ-linolenic acid	Dihomo-GLA
Linoleic acid	LA
Lauric acid	-
Myristic acid	-
Oleic acid	-
Palmitic acid	-
Palmitoleic acid	-
Stearic acid	-
Thromboxane B_2	TXB_2
Prostaglandin D_2	PGD_2
Prostaglandin E_2	PGE_2
Prostaglandin $F_{2\alpha}$	$PGF_{2\alpha}$
6-Keto-prostaglandin $F_{1\alpha}$	6-keto-$PGF_{1\alpha}$
5-Hydroxyeicosatetraenoic acid	5-HETE
5-Oxoeicosatetraenoic acid	5-oxoETE
8, 9-Dihydroxyeicosatrienoic acid	8, 9-DHET
9, 10-Epoxyoctadecenoic acid	9, 10-EpOME
9,10-Dihydroxyoctadecenoic acid	9,10-DiHOME
9-Hydroxyoctadecadienoic acid	9-HODE
9-Oxooctadecadienoic acid	9-oxoODE
11, 12-Dihydroxyeicosatrienoic acid	11, 12-DHET
11-Hydroxyeicosatetraenoic acid	11-HETE
12, 13-Epoxyoctadecenoic acid	12, 13-EpOME
12, 13-Dihydroxyoctadecenoic acid	12, 13-DiHOME
13-Oxooctadecadienoic acid	13-oxoODE
14, 15-Dihydroxyeicosatetraenoic acid	14, 15-DiHETE
15-Hydroxyeicosatetraenoic acid	15-HETE
17, 18-Dihydroxyeicosatetraenoic acid	17, 18-DiHETE
20-Hydroxyeicosatetraenoic acid	20-HETE
17-Hydroxydocosahexaenoic acid	17-HDoHE
19, 20-Dihydroperoxydocosahexaenoic acid	19, 20-DiHPDA
19, 20-Epoxydocosapentaenoic acid	19, 20-EpDPE
13-Hydroxyoctadecadienoic acid	13-HODE

Table 3.2 (cont'd)

13-Hydroxyoctadecatrienoic acid	13(S)-HOTre

Deuterated internal standards in the following concentrations were added to each sample: 5(S)-hydroxyeicosatetraenoic acid-d_8 (0.25 μM), 15(S)-hydroxyeicosatetraenoic acid-d_8 (0.25 μM), 8(9)-epoxyeicosatrienoic acid-d_{11} (0.5 μM), prostaglandin E_2-d9 (0.5 μM), 8,9 dihydroxyeicosatrienoic acid-d_{11} (0.25 μM), arachidonic acid-d_8 (50 μM), 2-arachidonoyl glycerol-d_8 (2 μM), and arachidonoyl ethanolamide-d_8 (0.25 μM) in the amount of 15 μL. For FA, solid phase extraction was carried out using Waters (Milford, MA) OASIS Prime HLB 3cc 150 mg Extraction Cartridges. Samples were passed through the columns, then washed with 5% methanol and eluted with acetonitrile:methanol (95:5). Solid phase extraction for oxylipids was carried out using Phenomenox (Torrance, CA) Strata-X 33 μm polymeric reversed-phase 200 mg/3 mL columns preconditioned with 3 mL of methanol followed by 3 mL of HPLC water. Supernatants were loaded into the columns, then washed with 20% methanol and eluted with a 50:50 mixture of methanol and acetonitrile with 2% formic acid. Removal of volatile solvents was performed with a Savant SpeedVac (Thermo Fisher Scientific) followed by reconstitution of the residues in a 2:1 methanol:HPLC-grade water mixture. To remove any particulates, samples were passed through Waters Acrodisc GHP 13 mm GHP 0.2-μm syringe filters. The samples were then stored in glass chromatography vials with glass inserts and kept at −80°C until quantification within 1 mo of collection. A 7-point standard curve was created with a mix of standards and the internal standards mentioned above for quantification.

All FA were quantified using a modified version of a previously described technique (Ryman et al., 2017). Briefly, reverse-phase LC on a Waters Acquity UPLC utilizing a Supelco (State College, PA) Ascentis Express C18 10 cm × 2.1 mm, 2.7 μm column was used with a flow rate

of 0.35 mL/min at 50°C. The single quadrupole MS was in electrospray negative ionization mode, and voltage was −3 kV with the turbo ion spray source temperature at 450°C. The gradient mobile phase was programmed in the following manner (A/B/D ratio): time 0 to 0.2 min (45/22/33), to (80/19/1) at 4.0 min and held until 5.0 min, to (45/22/33) at 6.0 min and held until 8.0 min. In this gradient mobile phase A = acetonitrile, B = methanol, and D = 0.1% formic acid. Fatty acids were quantified by matching mass-1 and retention time with corresponding deuterated internal standard abundance and calibrated to a linear 7-point standard curve (R2 > 0.99) using Waters Empower 3 software (Milford, MA).

The LC-MS/MS protocol has also been reported previously by Mavangira et al. (2015). Metabolites were quantified by a Waters Acquity UPLC connected to a Waters Xevo-TQ-S tandem quadrupole mass spectrometer using multiple reaction monitoring. Chromatography separation was performed with an Ascentis Express C18 HPLC column (Sigma-Aldrich), held at 50°C, and autosampler held at 10°C. Mobile phase bottle A was water containing 0.1% formic acid, and mobile phase bottle B was acetonitrile. The flow rate was 0.3 mL/min. Liquid chromatography separation took 15 min with linear gradient steps programmed as follows (A:B ratio): time 0 to 0.5 min (99:1), to (60:40) at 2.0 min, to (20:80) at 8.0 min, to (1:99) at 9.0 min, 0.5 min held at (1:99) until min 13.0; then returned to (99:1) at 13.01 min, and held at this condition until 15.0 min. All oxylipids were detected using electrospray ionization in negative-ion mode. Cone voltages and collision voltages were optimized for each analyte using Waters QuanOptimize software, and data analysis was carried out with Waters TargetLynx software.

Statistical Analysis

Repeated measures linear mixed effects models were constructed using the PROC MIXED procedure in SAS 9.4. (SAS Institute Inc., Cary, NC) to assess trends in concentrations of

MUFA, PUFA, SFA, and oxylipids over the study period. Each MUFA, PUFA, SFA, and oxylipid was tested in a separate model that included the fixed effect of sampling point and a random intercept for cow to account for the dependence between samples taken from the same cow. A spatial covariance residual matrix was used to account for unequal spacing between time points. Normality of residuals was visually assessed with Q-Q plots and histograms. Data were transformed either by the log or square root function that violated the normality assumption. Estimated least squares means were then back-transformed and presented as geometric means. Levene's test and graphs of predicted residuals were used to assess heteroscedasticity, which is when the variances of the residuals are unequal. Degrees of freedom were estimated using the Kenward-Rogers approximation if heteroscedasticity was present. Differences in concentrations of FA and oxylipids between different time points were tested using multiple pairwise comparisons with a Bonferroni adjustment. Statistical significance was set at $P < 0.05$.

RESULTS

Table 3.3 shows mean concentrations of targeted MUFA, PUFA, and SFA, which are precursors to oxylipids. The MUFA analyzed in this study, oleic and palmitoleic acid, attained their respective highest concentrations at d +2 and +1. All PUFA, with the exception of EPA, analyzed in this study saw numerically highest concentrations at d +2, whereas all PUFA except ALA reached numerically lowest concentrations at d +12. The SFA lauric acid, myristic acid, palmitic acid, and stearic acid attained the highest concentrations of the study at d +12, +6, +2, and +2, respectively.

Table 3.3. Select plasma fatty acid substrates in healthy cows (n = 10)[1].

	Day Relative to Dry-Off							
Fatty acid[1] (µM)	d-6	d0	d+1	d+2	d+6	d+12	SE	*P*
AA[2]	0.96[b]	5.18[b]	5.86[ab]	26.2[a]	5.15[b]	0.25[b]	0.38	0.02
Adrenic Acid	0.4[b]	0.96[b]	1.76[ab]	6.56[a]	1.04[b]	0.01[b]	0.53	0.04
LA[2]	290	1087	2860	5067	697	120	5	0.04
ALA[2]	10.8[c]	19.5[bc]	39[ab]	50.2[a]	24.9[abc]	23.2[bc]	0.3	0.04
Dihomo-GLA[2]	1.6[b]	5.5[b]	4[ab]	25.7[a]	5.64[b]	0.13[b]	8.38	0.03
DHA[2]	0.01[b]	0.03[b]	0.24[a]	0.38[a]	0.03[b]	0.01[b]	0.03	0.0001
DPA[2]	0.5[c]	0.85[bc]	2.89[ab]	4.67[a]	0.71[c]	0.03[d]	0.07	0.0001
EPA	0.27[b]	0.43[b]	2.0[a]	1.88[a]	0.79[b]	0.11[b]	0.12	0.0003
Lauric acid[2]	6.88[b]	9.75[b]	19.1[b]	14[b]	15.6[b]	199[a]	0.06	0.0001
Myristic acid	94	266	592	268	631	135	66.6	0.12
Oleic acid[2]	158[bc]	451[ab]	1174[a]	2162[a]	46[c]	47[c]	0.09	0.0002
Palmitic acid[2]	114[c]	176[c]	995[ab]	1329[a]	192[bc]	859[a]	0.09	0.01
Palmitoleic acid	4.26[b]	14.4[b]	105[a]	66.7[a]	10.3[b]	22.1[b]	4.33	0.0001
Stearic acid[2]	117	49.6	86.6	268	86.2	31.5	1.1	0.1

[a-d]Means within a row with different superscripts are different ($P < 0.05$).

Table 3.3. (cont'd)
[1]Standard error and *P*-values listed for each row represents the SE and *P*-value for the overall ANOVA. LA = linoleic acid; ALA = α-linoleic acid; DHA = docosahexaenoic acid; DPA = docosapentaenoic acid; EPA = eicosapentaenoic acid.
[2]Data log or square root transformed. Back-transformed values are shown.

Out of the 63 oxylipid species targeted, 27 were detected in this study. Of those, the majority varied over the sampling period ($P < 0.05$). Prostaglandins, a thromboxane (TXB_2), and 11-HETE were representatives of the COX-derived oxylipids (Table 3.4). After the cessation of lactation, the prostaglandin E_2 had the lowest concentrations at d +12, which were different than all other sampling points ($P < 0.01$). Concentrations of $PGF_{2\alpha}$ were highest at d +1. This sampling point was higher than d −6, +2, and +6 ($P < 0.05$). The COX derivatives prostaglandin D_2, 6-keto-prostaglandin $F_{1\alpha}$ (a stable metabolite of prostaglandin I_2), and TXB_2 (a stable metabolite of TXA_2) did not vary over the sampling period. The mean concentrations of 11-HETE at d +1 were the highest of the sampling period ($P < 0.01$).

Table 3.4. Plasma cyclooxygenase-derived oxylipids in healthy cows (n = 10)[1].

	Day Relative to Dry-Off							
Oxylipid[1] (nM)	d-6	d0	d+1	d+2	d+6	d+12	SE	*P*
PGD_2[2]	0.48	0.33	0.43	0.2	0.35	0.3	0.02	0.46
PGE_2[2]	49[a]	48[a]	75[a]	126[a]	84[a]	0.41[b]	2.44	0.0001
$PGF_{2\alpha}$	0.35[b]	0.7[ab]	1.67[a]	0.65[b]	0.23[b]	0.88[ab]	0.22	0.0005
6-Keto-$PGF_{1\alpha}$[2]	0.07	0.13	0.48	0.57	0.36	0.25	0.02	0.1
TXB_2[2]	0.48	0.57	0.93	0.96	0.63	0.14	0.02	0.07

Table 3.4 (cont'd)

11-HETE[2]	0.23[c]	0.48[bc]	1.45[a]	0.76[b]	0.67[b]	0.36[bc]	0.005	0.0001

[a–c]Means within a row with different superscripts are different ($P < 0.05$).
[1]Standard error and *P*-values listed for each row represent the SE and *P*-value for the overall ANOVA. TX = thromboxane; HETE = hydroxyeicosatetraenoic acid.
[2]Data log or square root transformed. Back-transformed values are shown.

The LOX-derived oxylipid concentrations for the sample period are listed in Table 3.5. Several LOX-derived oxylipids reached highest concentrations of the study at 1 d after dry-off, including 5-HETE, 5-oxoETE, 9-HODE, 13-HODE, 13-oxoODE, and 15-HETE. In contrast, the ketone derivative of 9-HODE, 9-oxoODE, reached the highest concentrations at d +2 and did not vary over the sampling period. The highest concentrations of 13(S)-HOTrE were seen at d +12, which were higher compared with all other time points ($P < 0.01$). The precursor to the anti-inflammatory oxylipid protectin D_1, 17-HDoHE, did not show changes throughout the study ($P < 0.13$), achieving its numerically higher mean concentrations at d +6.

Table 3.5. Plasma lipoxygenase-derived oxylipids in healthy cows (n = 10)[1].

	Day Relative to Dry-Off							
Oxylipid[1] (nM)	d-6	d0	d+1	d+2	d+6	d+12	SE	*P*
5-HETE[2]	0.52[d]	1.36[bcd]	3.27[a]	2.48[ab]	1.42[bc]	1.08[cd]	0.01	0.0001
5-oxoETE[2]	0.42[ab]	0.31[ab]	0.67[a]	0.2[ab]	0.32[ab]	0.15[b]	0.01	0.04
9-HODE	7.9[bc]	12.5[ab]	19[a]	13[ab]	9.6[bc]	2.19[c]	1.96[3]	0.0001
9-oxoODE[2]	4.35	5.8	7.19	9.45	7.66	8.57	0.06	0.06
13-HODE[2]	33.9[a]	42.3[a]	50.1[a]	43.1[a]	31.2[a]	4.2[b]	0.11[3]	0.0001

Table 3.5 (cont'd)

13-oxoODE	1.69^{bc}	2.46^{ac}	4.56^{a}	4.34^{ab}	2.63^{abc}	0.41^{c}	0.62	0.0001
13(S)-HOTrE[2]	29.5^{c}	36.3^{bc}	35.6^{bc}	53.6^{b}	44.8^{bc}	122^{a}	0.16	0.0001
15-HETE	0.4^{b}	0.74^{b}	2.25^{a}	1.2^{ab}	0.99^{b}	0.72^{b}	0.28	0.0002
17-HDoHE[2]	1.19	0.9	1.53	1.42	1.84	0.76	0.03	0.13

[a–d]Means within a row with different superscripts are different ($P < 0.05$).
[1]Standard error and *P*-values listed for each row represent the SE and *P*-value for the overall ANOVA. HETE = hydroxyeicosatetraenoic acid; oxoETE = oxoeicosatetraenoic acid; HODE = hydroxyoctadecadienoic acid; oxoODE = oxooctadecadienoic acid; HOTrE = hydroxyoctadecatrienoic acid; HDoHE = hydroxydocosahexaenoic acid.
[2]Data log or square root transformed. Back-transformed values were used.
[3]The SE for d +1 differed from the other sampling points and are as follows: 9-HODE (SE = 2.07) and 13-HODE (SE = 0.14).

Table 3.6 shows the concentrations of CYP-derived oxylipids through the sampling period. Some oxylipids produced by this pathway reached highest concentrations of the study at d +12, whereas others reached the lowest concentrations of the study at this time. For instance, 8,9-DHET, 11,12-DHET, 14,15-DHET, 20-HETE, 17,18-DiHETE, 19,20-EpDPE, and 19,20-DiHPDA attained the highest concentrations at d +12, whereas the EpOME and DiHOME stereoisomer concentrations were lowest at this time ($P < 0.05$). Finally, the highest concentrations of 14,15-DiHETE were seen at d +2.

Table 3.6. Plasma cytochrome P450-derived oxylipids in healthy cows (n = 10)[1].

	Day Relative to Dry-Off							
Oxylipid[1] (nM)	d-6	d0	d+1	d+2	d+6	d+12	SE	*P*
8, 9-DHET[2]	0.14^{c}	0.2^{c}	0.7^{ab}	0.37^{bc}	0.24^{c}	1.0^{a}	0.01	0.0001
11, 12-DHET[2]	1.39^{c}	2.64^{bc}	5.89^{a}	3.16^{b}	2.4^{bc}	7.96^{a}	0.03	0.0001
14, 15-DHET	2.21^{c}	4.05^{bc}	5.77^{b}	5.06^{b}	4.54^{b}	8.85^{a}	0.52	0.0001
9, 10-EpOME[2]	2.12^{c}	3.0^{bc}	8.21^{a}	8.28^{ab}	3.34^{ac}	0.02^{d}	0.11	0.0001
9, 10-DiHOME	51^{b}	94^{a}	47^{b}	35^{bc}	26^{bc}	4.8^{c}	7.1	0.0001
12, 13-EpOME[2]	9.83^{b}	18.3^{ab}	24.9^{ab}	27.6^{a}	14^{ab}	0.25^{c}	0.34[3]	0.0001
12, 13-DiHOME	31.6^{a}	41.5^{a}	31^{a}	28.4^{a}	28.5^{a}	0.96^{b}	4.6[3]	0.0001
20-HETE[2]	0.8^{c}	0.87^{c}	3.77^{ab}	1.61^{bc}	1.25^{c}	4.17^{a}	0.03[3]	0.0001
14, 15-DiHETE	12.2^{ab}	16.7^{ab}	22.3^{a}	23.7^{a}	19.8^{a}	5.88^{b}	3.8[3]	0.002
17, 18-DiHETE	129^{b}	174^{ab}	226^{ab}	178^{ab}	194^{ab}	292^{a}	34[3]	0.01
19, 20-EpDPE	0.33^{b}	0.46^{b}	0.43^{b}	0.38^{b}	0.29^{b}	1.25^{a}	0.13	0.0001
19, 20-DiHPDA	0.67^{b}	1.1^{b}	1.95^{ab}	0.94^{b}	1.37^{b}	2.42^{a}	0.49[3]	0.007

$^{a–d}$Means within a row with different superscripts are different ($P < 0.05$).

[1]Standard error and *P*-values listed for each row represent the SE and *P*-value for the overall ANOVA. DHET = dihydroxyeicosatrienoic acid; EpOME = epoxyoctadecenoic acid; DiHOME = dihydroxyoctadecenoic acid; HETE = hydroxyeicosatetraenoic acid; DiHETE = dihydroxyeicosatetraenoic acid; DiHPDA = dihydroperoxydocosahexaenoic acid; EpDPE = epoxydocosapentaenoic acid.

[2]Data log or square root transformed. Back-transformed values are shown.

Table 3.6 (cont'd)
[3]The SE for d +1 differed from the other sampling points and are as follows: 12,13-EpOME (SE = 0.38); 12,13-DiHOME (SE = 4.7); 20-HETE (SE = 0.04); 14,15-DiHETE (SE = 3.9); 17,18-DiHETE (SE = 38); and 19,20-DiHPDA (SE = 0.51).

DISCUSSION

The availability of FA substrates is a major determinant of oxylipid biosynthesis. Before oxylipid biosynthesis, FA are released from the sn-2 esterification site in the phospholipid glycerol backbone by phospholipase A_2 (Mavangira et al., 2015). Phospholipase A_2 is activated in many circumstances, including after cytokine stimulation during inflammation (Schmiel and Miller, 1999). Therefore, the inflammation that occurs with mammary gland remodeling can be the inciting cause of phospholipase A_2-mediated release of PUFA, leading to increased oxylipid biosynthesis at the same time. High concentrations of oleic acid throughout our study correspond to previous studies that found it to be one of the most abundant FA found in the digestive tract and blood of dairy cows (Yanting et al., 2018). The high concentrations of LA throughout the sample period are also not surprising as it has been reported as the most abundant PUFA in milk and plasma throughout lactation (Kuhn et al., 2017). Linoleic acid and other UFA are extensively hydrogenated in the rumen to produce MUFA and SFA. In fact, oleic acid was found to increase linearly with increasing concentrations of LA in vitro (Honkanen et al., 2012). Therefore, the increased concentrations of some MUFA and SFA at times of increased PUFA concentrations is anticipated.

Furthermore, the enzymatic pathways of oxylipid production show substrate preference, often preferring to oxidize n-3 PUFA over n-6 PUFA if they are available. The relative amounts of n-6 and n-3-derived oxylipids in the present study may therefore be a reflection of the concentrations of their respective PUFA precursors. Previous work has documented the alteration of oxylipid profiles in tissues by changing the dietary supply of PUFA (Raphael and Sordillo, 2013). In dairy

cattle, dietary PUFA have been shown to influence the inflammatory outcomes of infectious diseases such as mastitis (Raphael and Sordillo, 2013). However, the effect of supplementing dietary n-3 PUFA on the oxylipid profile of cattle during the transition into the dry period has not been investigated and should serve as the basis for future studies.

In the present study, many of the quantified plasma oxylipids varied throughout the sample period. This is in contrast to a previous study performed on healthy cows 14 d prepartum to 84 d postpartum, which found that only 3 of the 23 measured plasma oxylipids differed throughout the sampling period (Raphael et al., 2014). However, previous work in dairy cattle has shown that oxylipid biosynthesis is complex, varying within a lactation. For instance, PUFA and total oxylipids in bovine milk were lower in early lactation than during mid or late lactation (Kuhn et al., 2017). In fact, it would be reasonable to think that the oxylipid profile of high-producing cows may differ from that of low-producing cows. However, our group found no differences in concentrations of other serum inflammatory biomarkers, such as acute phase proteins, between high- and low-producing cows during the early dry period (Putman et al., 2018). Therefore, we suggest that milk production may not affect oxylipid concentrations in the early dry period as they are also related to inflammation. Additionally, pro- and anti-inflammatory oxylipids were not altered to the same degree. Whereas the pro-inflammatory 20-HETE was increased in the periparturient period, other pro-inflammatory oxylipids like 9,10-DiHOME and 5-oxoETE were decreased compared with mid and late lactation (Kuhn et al., 2017). That being said, many of the oxylipids in the present study reached their highest concentrations at d +1, +2, or +12, regardless of being typically considered pro- or anti-inflammatory (Figure 3.2). This pattern may be explained by the inflammation that occurs during early involution to adjust the mammary gland from a lactating to a nonlactating state because oxylipid production follows the onset of

inflammation (Sordillo, 2018). This is supported by the fact that other biomarkers of inflammation in serum, such as nonesterified FA, albumin, and haptoglobin, suggested that dairy cattle undergo inflammation in the early dry period at d +1 and +12 in a previous study completed by our group (Putman et al., 2018). Additional support that the inflammation required by mammary involution may be related to oxylipid concentrations is provided because neutrophils and macrophages are abundant in the mammary gland during acute involution (Sordillo and Nickerson, 1988). Indeed, the inflammatory cells present during acute involution are likely contributing to the oxylipid profile noted in the present study as they are known to produce oxylipids, including prostaglandins (Dennis and Norris, 2015), 15-HETE (Sordillo, 2018), and EpOME (Thompson and Hammock, 2007). The influence cell type has on oxylipid biosynthesis is partially due to the enzymes they possess. For example, platelets are capable of producing thromboxanes from arachidonic acid because they contain COX enzymes whereas reticulocytes can produce certain HETE due to the presence of LOX (Kuhn et al., 2002; Courtois et al., 2018). Under the influence of different pathways, a given substrate can be metabolized into a variety of oxylipids that can perform diverse functions.

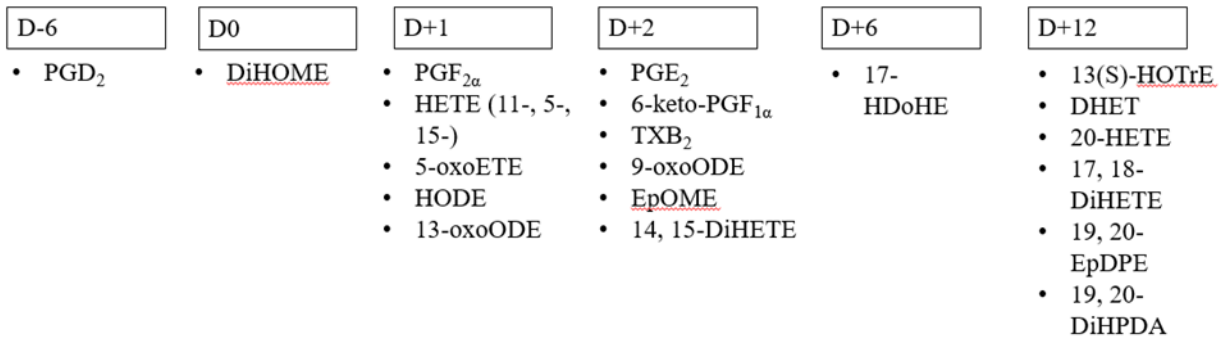

Figure 3.2. Sampling point at which each oxylipid attained their respective highest concentration. DiHOME = dihydroxyoctadecenoic acid; HETE = hydroxyeicosatetraenoic acid; oxoETE = oxoeicosatetraenoic acid; HODE = hydroxyoctadecadienoic acid; oxoODE = oxooctadecadienoic acid; TX = thromboxane; DiHETE = dihydroxyeicosatetraenoic acid; DHET = dihydroxyeicosatrienoic acid; HOTrE = hydroxyoctadecatrienoic acid;

Figure 3.2 (cont'd)
EpOME = epoxyoctadecaenoic acid; HDoHE = hydroxydocosahexaenoic acid; EpDPE = epoxydocosapentaenoic acid; DiHPDA = dihydroperoxydocosahexaenoic acid.

Oxylipids produced via the COX pathway include numerous prostaglandins and thromboxanes that are capable of a wide range of biological activities. For instance, prostaglandin D_2 is associated with significant anti-inflammatory actions, whereas prostaglandin E_2 is associated with pro-inflammatory actions in the gastrointestinal tract (Wallace, 2018). In a mouse model of lung cancer, some prostaglandins were increased at earlier time points than others. Poczobutt et al. (2013) found that $PGF_{2\alpha}$ and prostaglandin E_2 were increased at 2 wk after cancer cell injection, whereas prostaglandin D_2 and TXB_2 were increased 3 wk after injection. The authors suggested this time dependency could be due to changing phenotypes of inflammatory cells, such as macrophages, during tumor progression (Poczobutt et al., 2013). Similarly, COX-derived oxylipids in the present study were increased at different times. In mice, the phenotype of macrophages and mammary epithelial cells transforms to the M2 phenotype during mammary involution (Hughes et al., 2012). Therefore, the phenotype of the cells present in the early dry period of dairy cows may be affecting the timing of oxylipid biosynthesis in this study as well. Although 11-HETE can be produced via COX enzymes, it is typically associated with nonenzymatic production through interactions between lipid membranes and ROS. The effects of 11-HETE have been reported as potently pro-inflammatory, vasoconstrictive, and immunosuppressive (Ferreiro-Vera et al., 2011). In the present study, 11-HETE was increased at d +1, which is a sampling point where our previous study found that ROS production was also increased (Putman et al., 2018), and therefore may be a result of increased nonenzymatic production at this time.

Likewise, LOX-derived oxylipids display a wide range of biological actions. For instance, 15-HETE has been associated with anti-inflammatory effects, whereas 9- and 13-HODE have been associated with anti-thrombotic effects in humans (Wolfer et al., 2017). In accordance with a study performed by Raphael et al. (2014), plasma concentrations of 9- and 13-HODE followed a similar trend in healthy cows across the sample period. However, the concentrations of 13-HODE were at least 2-fold higher than 9-HODE at all sampling points in the present study, which is in contrast to the Raphael et al. (2014) study where 9-HODE concentrations were at least 2-fold higher than 13-HODE. Many functions have been attributed to HODE, both pro- and anti-inflammatory. For example, HODE has been implicated in pro-inflammatory actions via the induction of adhesion molecule expression on human vascular tissue but also in the activation of peroxisome proliferator-activated receptors, which serves as an anti-inflammatory action (Ricote et al., 1998; Friedrichs et al., 1999). However, the role of 9- and 13-HODE during the early dry period in dairy cattle is still unknown and needs to be investigated further. Both 9- and 13-HODE can be oxidized to form the ketone derivatives 9- and 13-oxoODE, which also have shown both pro-inflammatory effects by activating pain receptors and anti-inflammatory effects by acting as a ligand for peroxisome proliferator-activated receptors (Mattmiller et al., 2014). Two LOX-derived oxylipids associated with anti-inflammatory outcomes, 13(S)-HOTrE and 17-HDoHE (a precursor to an anti-inflammatory oxylipid, protectin D_1), were increased at differing time points in the present study. Both 13(S)-HOTrE and 17-HDoHE were found to increase in a mouse model during the recovery phase of inflammatory bowel disease (Hamabata et al., 2018). Although the presence of these compounds in our study suggests anti-inflammatory properties, the differential times at which they were increased further supports that oxylipid biosynthesis is complex and more research needs to be completed to determine the cause of differential oxylipid

production during early involution. For instance, it is still difficult to distinguish if and when oxylipids are the cause of or merely a consequence of inflammation and this would be beneficial to investigate in the future. Such studies may involve noting if an inflammatory response occurs upon stimulation with certain oxylipids.

Following suit with the other enzymatic pathways, CYP-derived oxylipids can also exert a wide range of biological effects. For instance, the epoxy metabolites of n-3 PUFA have demonstrated potent anti-inflammatory effects and play an important role in vascular homeostasis (Heemskerk et al., 2014). The DHA-derived oxylipid, 19,20-EpDPE, exemplifies this point as it has been found to have potent vasodilatory effects. Furthermore, the epoxy metabolites can be further metabolized into corresponding vicinal diols, such as 19,20-DiHPDA, via soluble epoxide hydrolase (Fischer et al., 2014). The diols produced often have differing potencies and functions than their epoxy substrate. For instance, DHET and 19,20-DiHPDA are less biologically active than epoxyeicosatrienoic acid and 19,20-EpDPE, respectively (Heemskerk et al., 2014; Duflot et al., 2017). In the present study, the LA-derived epoxide products 9,10- and 12,13-EpOME reached the highest concentrations at d +2 whereas the epoxide hydration products (9,10- and 12,13-DiHOME) had the highest concentrations at d 0. This may suggest that the epoxides are being rapidly converted to their respective diols at d 0, whereas the conversion may be dampened at d +2. Utilizing soluble epoxide hydrolase inhibitors to prolong the availability of the anti-inflammatory epoxides has been proposed as a therapy for pathologies such as inflammatory-related pain, atherosclerosis, and metabolic syndrome in humans (Swardfager et al., 2018). However, these inhibitors have not been investigated in dairy cattle, so whether or not they would be a beneficial therapy for modulating inflammatory responses is unknown. Pro-inflammatory actions are performed by 20-HETE, which is able to increase ROS production

(Han et al., 2013). In bovine cells, 20-HETE has been associated with vasodilation and increased production of superoxide anion and hydrogen peroxide (Bodiga et al., 2010). Additionally, hydrogen peroxide has been shown to activate the Ca^{2+}/calmodulin-dependent protein kinase II/Janus-kinase 2-dependent pathway in bovine aortic EC (Bodiga et al., 2010). Janus-kinase 2 is critical for the proliferation and survival of mammary epithelial cells (Creamer et al., 2010) and perhaps the increased concentrations of 20-HETE in this study are associated with mammary gland remodeling through a similar mechanism. The arachidonic acid-derived 14,15- and 17,18-DiHETE are known for anti-inflammatory actions. For instance, 14,15-DiHETE has been shown to reduce superoxide anion generation (Vachier et al., 2002). The increased concentrations of these oxylipids at d +1 in the study, therefore, may be the result of anti-inflammatory compounds being produced in response to inflammation.

CONCLUSIONS

Overall, oxylipids varied throughout the transition into early mammary gland involution. However, the oxylipid profile of this time diverged from those observed previously at different stages of the lactation cycle or in cows with differing health status. This study documented the oxylipids present during the early dry period for the first time, which contributes valuable knowledge given the diverse actions the potent inflammatory mediators can perform. However, it remains unknown whether the presence or alterations of these oxylipids during this time affect cow health and productivity. Therefore, future studies should be directed toward investigating causes of the changes noted along with determining if these oxylipids have an effect on cow health and productivity throughout the lactation cycle.

CHAPTER 4

Published in Journal of Dairy Science: Putman, A. K., J. C. Gandy, G. A. Contreras, and L. M. Sordillo. 2022. Oxylipids are associated with higher disease risk in postpartum cows. J. Dairy. Sci. 105(3):2531-2543. doi: 10.3168/jds.2021-21057.

INTRODUCTION

Periparturient diseases, which include numerous metabolic and infectious diseases such as ketosis, displaced abomasum, mastitis, and metritis, cause severe animal welfare concerns and economic losses for dairy producers. The incidence and severity of periparturient diseases is associated with dysregulated inflammation (Sordillo and Raphael, 2013). Specific physiological circumstances during the periparturient period, such as uterine involution and adipose tissue remodeling, invoke inflammation without the presence of a pathogen (Chapwanya et al., 2012; Contreras et al., 2017). To avoid periparturient diseases, dairy cows rely on a tightly regulated inflammatory response that is robust enough to promote tissue healing or pathogen elimination but not to an extent that tissue damage occurs (Sordillo, 2016). If inflammation is attenuated, such as when neutrophil function is diminished around the time of calving, it is more likely for diseases such as mastitis and metritis to occur (Cai et al., 1994; Sordillo, 2016). On the other hand, if inflammation is excessive or prolonged, substantial tissue damage may occur as exemplified during certain bovine mastitis cases where upregulation of proinflammatory substances and increased leukocyte infiltration can lead to apoptosis and mammary gland damage (Aitken et al., 2011). Navigating the periparturient period successfully necessitates tight control of every aspect of inflammation from its initiation to its termination, a process facilitated by numerous soluble mediators (Sordillo, 2018).

Oxylipids are potent soluble inflammatory mediators capable of regulating the onset, progression, and resolution of inflammation (Mavangira and Sordillo, 2018). Oxylipids are oxidized products of PUFA and the substrate they are generated from largely determines their biological action during inflammation (Figure 4.1). Oxylipids derived from n-6 PUFA, such as AA, are most commonly associated with proinflammatory actions. In contrast, oxylipids derived from n-3 PUFA, including EPA and DHA, tend to exert anti-inflammatory effects (Innes and Calder, 2018). For example, PGE_2 is a metabolite of AA with well-documented proinflammatory effects such as mast cell degranulation and increased vascular permeability (Morimoto et al., 2014). The DHA-derived 17-hydroxydocosahexaenoic acid (**17-HDoHE**) is a precursor to inflammation-resolving metabolites and has been associated with decreased nuclear factor kappa B and proinflammatory cytokine expression in models of adipose tissue inflammation (Neuhofer et al., 2013). The biological action of oxylipids also depends on the pathway with which they are produced. Enzymatic production occurs through COX, LOX, and CYP pathways while nonenzymatic production occurs via mechanisms mediated by free radicals [e.g., hydroxyl radical, $OH^{-\bullet}$ (Mavangira and Sordillo, 2018)]. Reactions with free radicals form specialized oxylipids known as IsoP, which are highly sensitive and specific biomarkers of lipid peroxidation (Milne et al., 2015). Given the diverse substrates and pathways available for biosynthesis, hundreds of oxylipids have been identified to date, each with its own unique but interrelated effect on inflammation (Wang et al., 2014). Thus, it is not merely the presence of any particular oxylipid but rather the relative abundance, potency, and timing of production of all oxylipids that influences inflammatory outcomes (Kuhn et al., 2017).

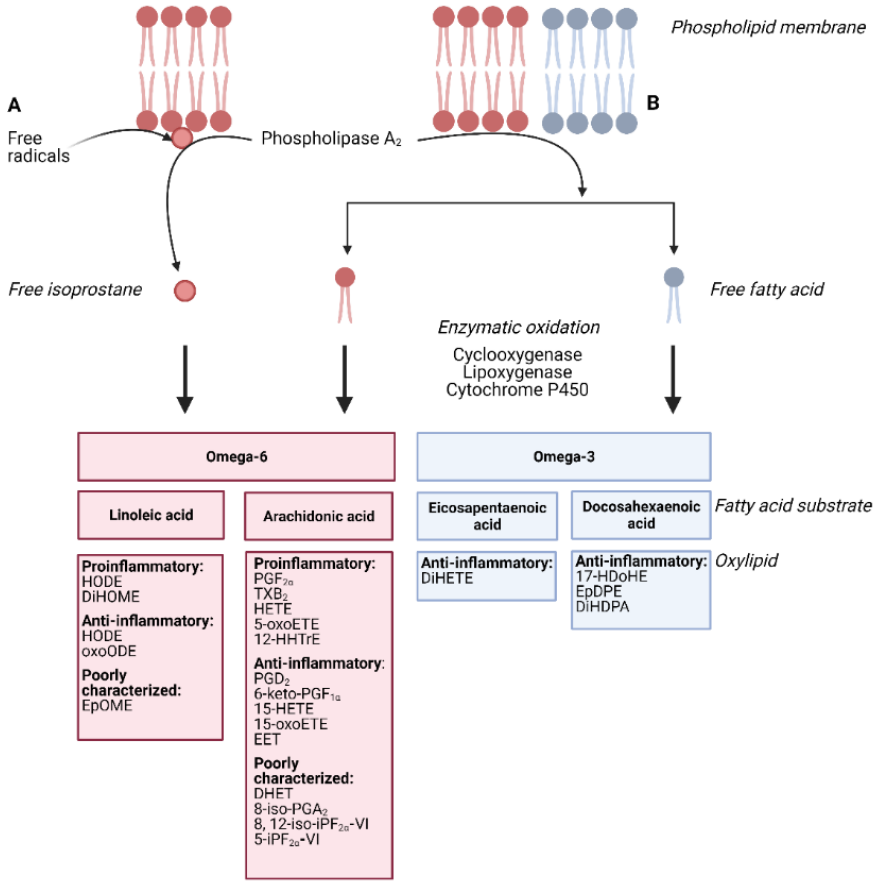

Figure 4.1. Formation of the oxylipids detected in Chapter 4. A. Free radicals interact directly with PUFA in lipid membranes to form esterified isoprostanes, which are then released by phospholipases to generate free (unesterified) isoprostanes. B. Phosopholipases release PUFA from lipid membranes, which can then undergo enzymatic oxidation to produce a variety of oxylipid species. HODE=hydroxyoctadecadienoic acid; oxoODE=oxooctadecadienoic acid; DiHOME=dihydroxyoctadecenoic acid; EpOME=epoxyoctadecenoic acid; PG=prostaglandin; TX=thromboxane; HETE=hydroxyeicosatetraenoic acid; oxoETE=oxoeicosatetraenoic acid; HHTrE=hydroxyheptadecatrienoic acid; EET=epoxyeicosatrienoic acid; DHET=dihydroxyeicosatrienoic acid; 8-iso-PGA_2=8-isoprostane-PGA_2; 8, 12-iso-$iPF_{2\alpha}$-VI=8, 12-iso-Isoprostane-$F_{2\alpha}$-VI; 5-$iPF_{2\alpha}$-VI=5-iso prostaglandin $F_{2\alpha}$-VI; DiHETE=dihydroxyeicosatetraenoic acid; HDoHE=hydroxydocosahexaenoic acid; DiHDPA=dihydroxydocosapentaenoic acid; EpDPE=epoxydocosapentaenoic acid. Created with biorender.com.

While the dysregulated inflammation that occurs around the time of calving is well-recognized to contribute to risk of periparturient diseases, the early dry period is often overlooked. However, many of the factors that underlie clinical illnesses around parturition may begin weeks earlier when lactation is abruptly ceased, such as inflammation resulting from mammary involution

(Putman et al., 2018; Wisnieski et al., 2019). For instance, previous work demonstrates that the oxylipid profile of clinically healthy dairy cattle is variable throughout the first 2 wk of the dry period (Putman et al., 2019). However, the potential of measuring oxylipids shortly after the day of dry-off to assess disease risk after calving has yet to be investigated. Therefore, this study aimed to characterize the oxylipid profile from the early dry period through early lactation in both cattle without detected disease and those that developed periparturient diseases.

MATERIALS AND METHODS

Animals

This study was approved by the Michigan State University Institutional Animal Care and Use Committee. Holstein cows from a commercial dairy herd were free from clinical disease at enrollment, had SCC $<250 \times 10^3$ cells/mL at their last DHIA test date, and were enrolled 56 d before expected calving date with owner consent. All cows were housed in a freestall barn, grouped according to stage of lactation, and lactating cows were milked 2 times/d. At the time of dry-off, cows were treated with intramammary cephapirin benzathine (ToMORROW, Boehringer Ingelheim, Lyon, France) in all milking quarters. Average milk production at enrollment was ascertained from the last DHIA test day and was 32.5 kg/d (range: 17.8–40.4 kg/d), with the average DIM being 318 (range: 291–357). The average BCS at dry-off was 3.4 ± 0.3 out of 5 (range: 3–4), and average parity was 2 (range 1-4). Cows had ad libitum access to a TMR and water. Animals were fed diets based on their lactation status (Table 4.1). Briefly, cows sampled at d -6 were fed a late lactation diet, those sampled at d 0, d +1, d +2, d +6, and d +12 were fed a far-off dry cow diet, those in the close-up dry period were fed a close-up diet, and finally, animals sampled after calving were fed a fresh cow diet. After calving, herd records were inspected and cows were grouped into those without detectable clinical disease (n=7) or those

with detected disease (n=9) as determined by trained farm staff. Mastitis was diagnosed in 3 cows due to abnormal milk with or without one or more of the following: redness and swelling of the udder, decreased appetite, depressed attitude, or rectal temperature greater than 39 ºC. The mastitis cows were diagnosed at 9, 18, and 16 DIM. Metritis was diagnosed in 1 cow (11 DIM) based on the presence of malodorous uterine discharge and a fluid-filled uterus on rectal palpation within 21 d of calving, with or without decreased appetite, a rectal temperature greater than 39 ºC, and depressed attitude. One cow (11 DIM) developed subclinical hypocalcemia, defined as a serum calcium concentration of <8.4 mg/dl, whereas the development of clinical hypocalcemia would have been defined as a serum calcium concentration of <8.4 mg/dl accompanied by muscle weakness, muscle shaking, or inability to rise. Lameness was detected in 1 cow (39 DIM), being diagnosed based on abnormal gait. Displaced abomasum was diagnosed based on auscultation of a characteristic "ping" in the region between the 9th rib and flank and was seen in 1 cow (8 DIM) of the present study. Finally, 2 cows displayed retained placenta (recorded at 7 DIM and 10 DIM), which was diagnosed when the placenta had not been expelled within 24 h of calving. Other postpartum diseases, such as ketosis, were not diagnosed by farm staff in the present study. Each cow was only diagnosed with 1 disease during the study period according to farm records. For the remainder of the manuscript, cows where clinical disease was not detected after calving may be referred to as the apparently healthy (**AH**) group while those that developed clinical disease postpartum may be referred to as the clinical disease (**CD**) group.

Table 4.1. Late lactation, early dry, close-up, and early lactation diet compositions on a dry matter basis of animals used in this study.

Item	Late Lactation	Far-Off Dry	Close Up	Fresh
Ingredients	Canola	Straw	Dehulled soymeal	Canola
	Corn gluten	Grass silage	Soybean hulls	HMSC[1]
	HMSC[1]	Corn silage	Wheat middlings	Alfalfa
	Alfalfa	Salt	Molasses	Corn silage
	Corn silage	Mineral supplement	Yeast culture	Mineral supplement
	Mineral supplement		Wheat straw	
			Corn silage	
			Salt	
			Mineral supplement	
NE_L[2] (Mcal/kg)	1.5	1.15	1.28	1.29
Crude Protein (%)	19	11	13.31	13.1
Fat (%)	5.3	2.3	2.29	24.8
Non-fiber Carbohydrate (%)	38	17	27.86	21.82
Calcium (%)	0.75	0.51	0.5	0.55
Phosphorus (%)	0.69	0.36	0.34	0.32
Magnesium (%)	0.78	0.31	0.26	0.13
Potassium (%)	1.4	2.5	1.34	0.95
Sodium (%)	0.29	0.34	0.11	0.01
Chloride (%)	0.53	0.99	0.2	0.16
Sulfur (%)	0.3	0.18	0.2	0.16
Selenium (ppm)	6.2	23	0.09	
Vitamin E (IU/animal)	290	1064	1200	540

[1]HMSC=High-moisture shelled corn

[2]NE_L=Net energy requirements for lactation, the estimated energy of lactation for an animal consuming 3X its requirement.

Sample Collection and Processing

All samples were collected between the summer and fall of 2018. Sampling occurred at d −6, 0, +1, +2, +6, and +12 relative to the dry-off date, along with a sample 14 ± 3 d before the expected calving date (**CU**) and 7 ± 2 d after calving (**C+7**). Blood samples were collected aseptically into EDTA-containing vacutainer tubes via coccygeal venipuncture between 0800 and 1000 h. As

lipid-containing biological samples are susceptible to ex vivo peroxidation, a mixture of 50% methanol, 25% ethanol, 25% water, 0.9 mM of butylated hydroxytoluene (**BHT**), 0.54 mM EDTA, 3.2 mM triphenylphosphine (**TPP**), and 5.6 mM indomethacin was added to each blood tube (10 μL/mL of blood) immediately following venipuncture (Morrow et al., 1990; O'Donnell et al., 2009). Samples were immediately stored on ice during transportation and processing. Upon returning to the laboratory, blood samples were centrifuged at 1,449 × *g* for 15 min at 4°C, and plasma was subsequently harvested, aliquoted, and flash-frozen in liquid nitrogen. Plasma samples were stored at −80 °C pending analysis via LC-MS/MS within 1 mo of collection.

Targeted Lipidomics

Plasma was prepared for LC-MS/MS as described in Mavangira et al. (2015). Briefly, 1 mL of flash-frozen plasma was thawed on ice, diluted with 1 mL of 4% formic acid, and mixed with the antioxidant reducing agent listed above at 4 μL/mL to prevent degradation of preformed oxylipids and ex vivo lipid peroxidation (O'Donnell et al., 2009). Samples were combined with a 15 μL mixture of internal standards containing 0.25 μM 5(S)-HETE-d_8, 0.25 μM 15(S)-HETE-d_8, 0.5 μM 8(9)-EET-d_{11}, 0.5 μM PGE_2-d_9, and 0.25 μM 8,9-DHET-d_{11}. Solid phase extraction utilizing Waters Oasis Prime HLB 3 cc (150mg) columns (Waters Corporation, Milford, MA) was performed. Supernatants were loaded into the columns and pushed through with nitrogen. The columns were then washed with 3 mL of 5% methanol. Samples were eluted with 2.5 mL of 90:10 acetonitrile:methanol. Volatile solvents were removed using a Savant SpeedVac (Thermo Fisher Scientific, Waltham, MA) and residues were reconstituted in methanol, mixed at a 2:1 ratio with HPLC water and stored in chromatography vials at -80 °C until analysis. A 6-point standard curve was created with a mix of standards and the internal standards mentioned above for quantification.

The LC-MS/MS protocol also has been reported previously by Mavangira et al. (2015). The quantification of oxylipid metabolites was accomplished on a Waters Xevo-TQ-S tandem quadrupole mass spectrometer using multiple reaction monitoring. Chromatography separation was performed with an Ascentis Express C18 HPLC column (Millipore Sigma, Burlington, MA) held at 50 ^{o}C and autosampler held at 10 ^{o}C. Mobile phase bottle A was water containing 0.1% acetic acid and mobile phase bottle B was acetonitrile with a flow rate of 0.3 mL/min. Liquid chromatography separation took 15 min with linear gradient steps programmed as follows (A:B ratio): time 0 to 0.5 min (99:1), to (60:40) at 2.0 min, to (20:80) at 8.0 min, to (1:99) at 8.01 min until 13.0 min; then returned to (99:1) at 13.01 min, and held at this condition until 15.0 min. Data analysis was performed by generating 6-point linear curves with commercial standards (Cayman Chemical, Ann Arbor, MI) in 5-fold dilutions ranging from 0.01-100 nM. The generated linear curves produced R^2 values of 0.99 with percent deviations of less than 100%. Quantification of isoprostanes (IsoP) was accomplished with a Waters Xevo TQ-S tandem quadrupole mass spectrometer using multiple reaction monitoring. Chromatography separation was performed with a Waters Acquity UPLC utilizing a BEH C18 1.7 μM (2.1 × 150 mm) column, held at 50 ^{o}C and auto sampler held at 10 ^{o}C. Mobile phase bottle A was 0.1% acetic acid, mobile phase bottle B was acetonitrile, and mobile phase bottle C was methanol. The flow rate was 0.3 mL/min. The gradient initial phase (A:B) (80:20) to 1 min, changing to (A:B:C) (50:30:20) to 7 min, changing to (A:B:C) (1:80:19) to 7.01 min, changing back to initial phase and holding until 10 min. All oxylipids and IsoP were detected using electrospray ionization in negative-ion mode. Cone voltages and collision voltages were optimized for each analyte using Waters QuanOptimize software and data analysis was carried out with Waters MassLynx software.

Statistical Analysis

Sample size was calculated a priori with the equation $n_i = 2(\frac{Z\sigma}{ES})^2$ and suggested that 7 animals were needed in each group to detect differences (based on preliminary data of one of the most abundant oxylipids detected in cattle, 13-HODE; n_i=sample size, Z=Z-score for α=0.05, σ=0.94, effect size (ES)=1 (Ott and Longnecker, 2010; Putman et al., 2019). Repeated measures linear mixed effects models were constructed using the PROC MIXED procedure in SAS 9.4. (SAS Institute Inc., Cary, NC) for analysis of oxylipid and IsoP data over the study period. Each oxylipid and IsoP was tested in a separate model that included the fixed effect of sampling point and a random intercept for cow to account for the dependence between samples taken from the same cow. A spatial covariance residual matrix was used to account for unequal spacing between time points. Potential confounders, such as variation that may occur due to variable diets of cows at different stages of the lactation cycle, BCS, environmental factors, or stress related to handling, were accounted for by sampling from only one farm and having the same individuals handle the cattle. Each sampling occurred during the same timeframe to account for any potential variation due to time of day samples were taken. Similar numbers of primiparous and multiparous cows were used to minimize any impact age may have on the results. Normality of residuals was visually assessed with Q-Q plots and histograms. Data that violated the normality assumption were transformed either by the log or square root function. Estimated least square means were then back-transformed and presented as geometric means. Levene's test and graphs of predicted residuals were used to assess heteroscedasticity. Degrees of freedom were estimated using the Kenward-Rogers approximation if heteroscedasticity was present. Differences in concentrations of oxylipids and IsoP over the sampling period and between groups at each sampling point were tested using multiple pairwise comparisons with a Bonferroni adjustment.

Statistical significance for differences between groups over the entire sampling period was set at $P < 0.0016$ to adjust for family-wise error rate due to running multiple models ($P = 0.05/32$). Statistical significance for differences between groups at each sampling point were determined based on adjusted *P* values calculated by SAS in the linear mixed effects model. As such, concentrations were deemed significantly different if the adjusted *P* value on the SAS output was less than 0.05.

RESULTS

Sixty-three oxylipid species were targeted in this study, of which 32 were detectable (Table 4.2). Sampling 16 cows at 8 time points resulted in a total of 128 observations for each oxylipid, presented here as least square means and standard error of the mean. The concentrations of 25 oxylipids were affected by time (from d -6 to C +7) in both AH and CD cows ($P < 0.05$). Of those 25 oxylipids, concentrations of 7 were different between the AH and CD groups ($P < 0.05$). Tables 3-6 indicate the concentrations of oxylipids that did not differ between AH and CD cows. Furthermore, the greatest concentrations of any given oxylipid were often not seen during the same sampling point between AH and CD animals (Figure 4.2).

Table 4.2. Names and corresponding abbreviation for the lipids analyzed in Chapter 4.

Lipid	Abbreviation
Thromboxane B_2	TXB_2
Prostaglandin D_2	PGD_2
Prostaglandin $F_{2\alpha}$	$PGF_{2\alpha}$
6-Keto-prostaglandin $F_{1\alpha}$	6-keto-$PGF_{1\alpha}$
5-Hydroxyeicosatetraenoic acid	5-HETE
5-Oxoeicosatetraenoic acid	5-oxoETE
5, 6- Dihydroxyeicosatetraenoic acid	5, 6-DiHETE
8, 9-Dihydroxyeicosatrienoic acid	8, 9-DHET
8, 9-Epoxyeicosatrienoic acid	8, 9-EET
9, 10-Epoxyoctadecenoic acid	9, 10-EpOME
9,10-Dihydroxyoctadecenoic acid	9,10-DiHOME
9-Hydroxyeicosatetraenoic acid	9-HETE
9-Hydroxyoctadecadienoic acid	9-HODE
9-Oxooctadecadienoic acid	9-oxoODE

Table 4.2 (cont'd)

11, 12-Dihydroxyeicosatrienoic acid	11, 12-DHET
12, 13-Epoxyoctadecenoic acid	12, 13-EpOME
12, 13-Dihydroxyoctadecenoic acid	12, 13-DiHOME
12-Hydroxyheptadecatrienoic acid	12-HHTrE
13-Hydroxyoctadecadienoic acid	13-HODE
13-Oxooctadecadienoic acid	13-oxoODE
14, 15-Dihydroxyeicosatrienoic acid	14, 15-DHET
14, 15-Dihydroxyeicosatetraenoic acid	14, 15-DiHETE
14, 15-Epoxyeicosatrienoic acid	14, 15-EET
15-Hydroxyeicosatetraenoic acid	15-HETE
15-Oxoeicosatetraenoic acid	15-oxoETE
17, 18-Dihydroxyeicosatetraenoic acid	17, 18-DiHETE
17-Hydroxydocosahexaenoic acid	17-HDoHE
19, 20-Dihydroxydocosapentaenoic acid	19, 20-DiHDPA
19, 20-Epoxydocosapentaenoic acid	19, 20-EpDPE
20-Hydroxyeicosatetraenoic acid	20-HETE
8-iso-prostaglandin A_2	8-isoPGA_2
8, 12-iso-Isoprostane-$F_{2\alpha}$-VI	8, 12-iso-i$PF_{2\alpha}$-VI
5-iso Prostaglandin $F_{2\alpha}$-VI	5-i$PF_{2\alpha}$-VI

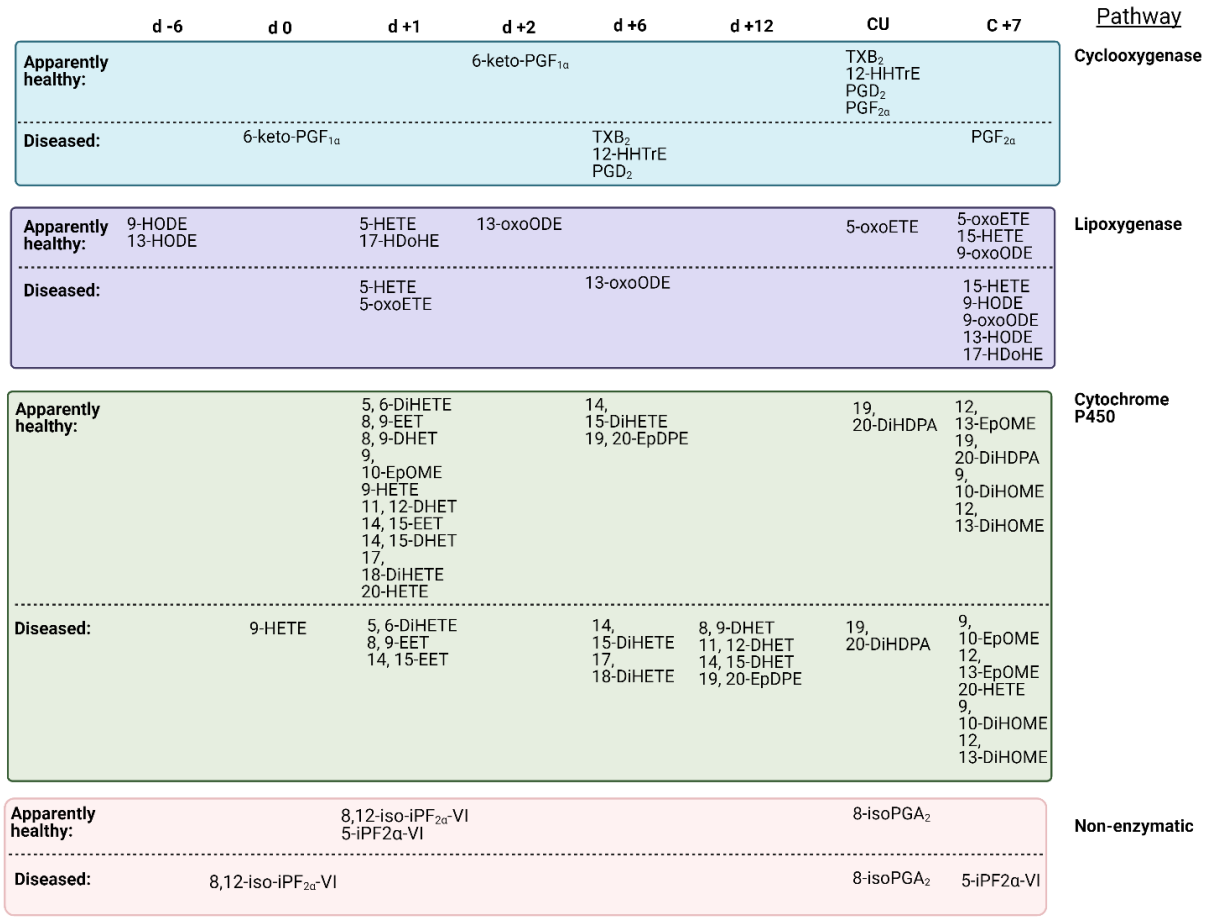

Figure 4.2. Sampling point at which each oxylipid reached peak concentrations for apparently healthy cows (n=7) and those that developed a postpartum disease (diseased; n=9). Sampling points were as follows: d -6=6 d prior to dry-off; d 0=dry-off; d +1, +2, +6, and +12=1, 2, 6, and 12 d after dry-off; CU=14 ± 3 d prior to expected calving date; and C +7=7 ± 2 d post-calving. If an oxylipid is listed twice for the same group, peak concentrations were met at 2 sampling points. Created with biorender.com.

The blood concentrations of COX-derived of TXB_2, 6-keto-$PGF_{1\alpha}$, and 12-HHTrE are listed in Table 4.3. Cyclooxygenase-derived PGD_2 and $PGF_{2\alpha}$, differed between AH and CD cows (Figure 4.3; $P < 0.001$). Apparently healthy cows had the greatest concentrations at CU (PGD_2=0.28 nM; $PGF_{2\alpha}$=0.54 nM) while CD cows had peak concentrations of PGD_2 at d +6 (0.58 nM) and $PGF_{2\alpha}$ at C +7 (0.9 nM).

Table 4.3. Mean plasma concentrations of cyclooxygenase-derived oxylipids in apparently healthy cows (n=7) and those that developed a postpartum disease (diseased; n=9) from 6 d prior to dry-off (d -6) to 7 d after calving (C +7). Standard error (SE) and P-values listed for each row represents the SE and P-value for the treatment effect of undetected disease versus detected disease in the linear mixed model. After Bonferroni's correction to account for family-wise error, statistical significance was set at $P < 0.001$. Cyclooxygenase-derived oxylipids that differed between groups are also shown in Figure 4.3.

	Sampling Point									
Oxylipid[1] (nM)	d -6	d 0	d +1	d +2	d +6	d +12	CU	C +7	SE	*P*
TXB_2[2]										0.08
Apparently healthy	0.75	0.91	1.62	1.92	0.77	0.78	3.81	1.08	0.05	
Diseased	1.79	1.81	1.76	1.83	2.57	1.69	2.19	1.26	0.04	
6-keto-$PGF_{1\alpha}$[2]										0.75
Apparently healthy	0.21	0.09	0.16	1.32	0.19	0.18	0.27	0.19	0.02	
Diseased	0.19	0.44	0.38	0.27	0.36	0.23	0.33	0.17	0.01	
PGD_2[2]										0.0001
Apparently healthy	0.12	0.13	0.27	0.22	0.14	0.08	0.28	0.06	0.006	
Diseased	0.18	0.48	0.57	0.34	0.58	0.3	0.39	0.39	0.004	
$PGF_{2\alpha}$[2]										0.001
Apparently healthy	0.16	0.2	0.19	0.24	0.16	0.27	0.54	0.17	0.01	

Table 4.3 (cont'd)

Diseased	0.52	0.83	0.55	0.41	0.6	0.31	0.33	0.9	0.008	
12-HHTrE[2]										0.53
Apparently healthy	0.21	0.38	0.42	0.54	0.32	0.26	0.75	0.49	0.01	
Diseased	0.5	0.55	0.41	0.38	0.64	0.29	0.53	0.36	0.01	

[1]TX=thromboxane; PG=prostaglandin; HHTrE=hydroxyheptadecatrienoic acid.
[2]Data log or square root transformed. Back-transformed values shown.

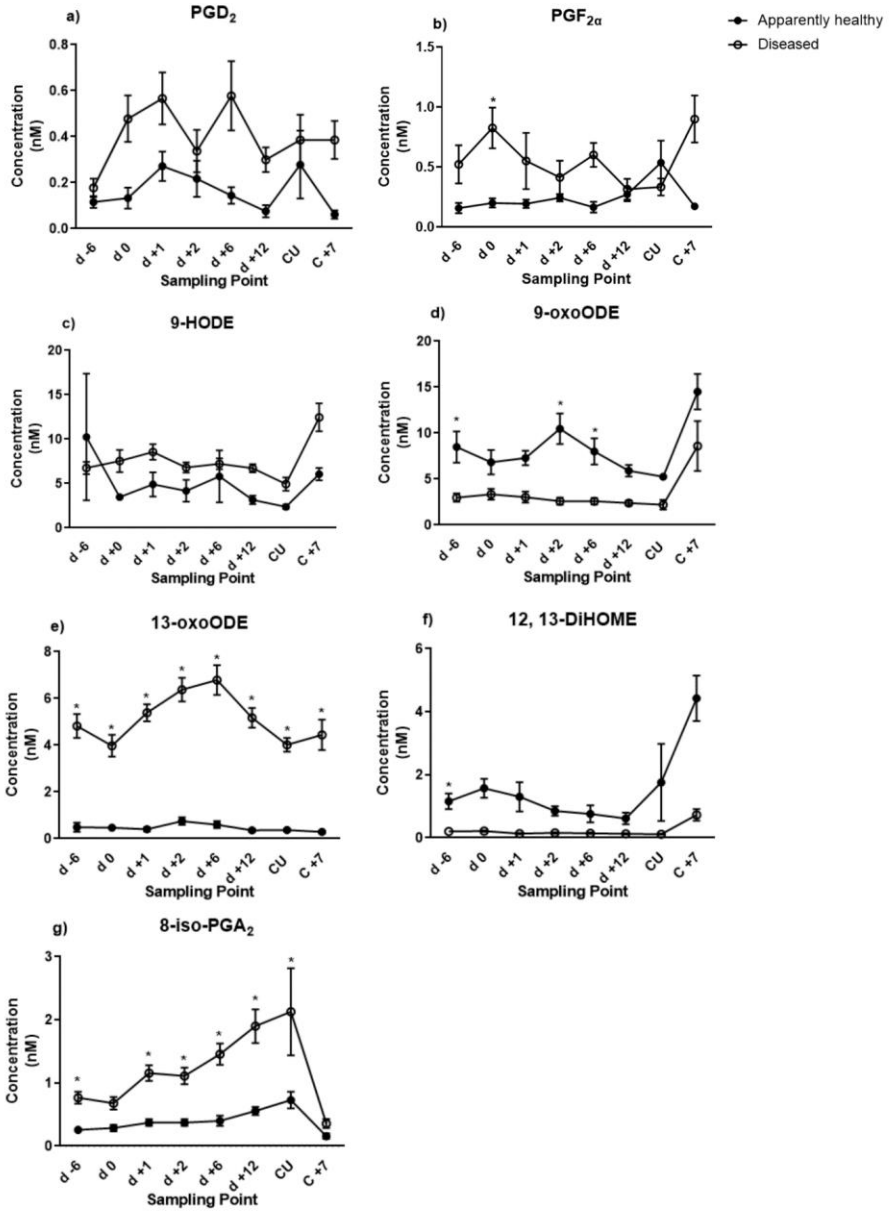

Figure 4.3. Concentrations of oxylipids that differed between apparently healthy cows (n=7) and those that developed a postpartum disease (diseased; n=9) from 6 d prior to dry-off (d -6) to 7 d after calving (C +7). a) Cyclooxygenase (COX)-derived prostaglandin (PG) D_2 ($P < 0.0001$). b) COX-derived $PGF_{2\alpha}$ ($P < 0.001$). c) Lipoxygenase (LOX)-derived 9-HODE ($P = 0.0003$). d) LOX-derived 9-oxoODE ($P < 0.0001$). e) LOX-derived 13-oxoODE ($P < 0.001$). f) Cytochrome P450-derived 12, 13-DiHOME ($P < 0.0001$). g) Non-enzymatically-derived 8-iso-PGA_2 ($P < 0.0001$). Data square root transformed; back-transformed values shown. After Bonferroni's correction to account for family-wise error, statistical significance between groups over the entire sampling period was set at $P < 0.001$. *Pairwise differences between seemingly healthy and sick cows at a given sampling point after Bonferroni's correction for multiple comparisons (Adjusted $P < 0.05$).

Products of the LOX pathway are listed in Table 4.4. Out of 8 LOX-derived oxylipids, the concentrations of 3 differed between AH and CD animals throughout the sampling period (Figure 4.3; $P < 0.001$). Throughout the sampling period, peak concentrations of 9-HODE and its ketone derivative 9-oxoODE were greatest in the CD group at C +7 (12.5 nM and 8.59 nM, respectively). Concentrations of 9-HODE were greater in the CD group than the AH group at every sampling point except d -6. The opposite was true of 9-oxoODE in that concentrations were consistently greater in the AH group throughout the study. In contrast, the concentrations of 13-oxoODE were greater at every sampling point in CD animals compared to AH animals (Figure 4.3; $P < 0.001$).

Table 4.4. Mean plasma concentrations of lipoxygenase-derived oxylipids in apparently healthy cows (n=7) and those that developed a postpartum disease (diseased; n=9) from 6 d prior to dry-off (d -6) to 7 d after calving (C +7). Standard error (SE) and P-values listed for each row represents the SE and P-value for the treatment effect of undetected disease versus detected disease in the linear mixed model. After Bonferroni's correction to account for family-wise error, statistical significance was set at $P < 0.001$. Lipoxygenase-derived oxylipids that differed between groups are also shown in Figure 4.3.

	Sampling Point									
Oxylipid[1] (nM)	d -6	d 0	d +1	d +2	d +6	d +12	CU	C +7	SE	*P*
5-HETE[2]										0.23
Apparently healthy	1.78	1.53	3.47	2.22	1.3	1.25	1.14	1.68	1.27	
Diseased	2.09	2.04	2.92	2.37	2.13	2.07	1.17	2.11	1.24	
5-oxoETE										0.49
Apparently healthy	0.09	0.1	0.14	0.11	0.12	0.11	0.16	0.16	0.03	

Table 4.4 (cont'd)

Diseased	0.09	0.07	0.14	0.11	0.12	0.13	0.12	0.11	0.02	
9-HODE[2]										0.0003
Apparently healthy	10	3.5	4.9	4.2	5.8	3.2	2.4	6.1	1.2	
Diseased	6.8	7.5	8.6	6.8	7.2	6.7	4.9	12	1.18	
9-oxoODE[2]										0.0001
Apparently healthy	8.5	6.8	7.3	11	8.0	5.9	5.3	15	0.05	
Diseased	3.0	3.3	3.0	2.6	2.6	2.4	2.2	8.6	0.04	
13-HODE[2]										0.007
Apparently healthy	8.25	9.64	8.75	8.07	7.84	6.51	5.48	12.6	1.1	
Diseased	11.6	12.6	10.6	8.78	9.86	8.69	7.66	16.3	1.1	
13-oxoODE[2]										0.0001
Apparently healthy	0.49	0.47	0.4	0.75	0.6	0.36	0.37	0.29	0.01	
Diseased	4.8	4.0	5.4	6.4	6.8	5.2	4.0	4.4	0.009	
15-HETE[2]										0.4
Apparently healthy	1.5	1.81	1.97	2.3	1.69	1.61	1.83	2.38	1.21	
Diseased	2	2.22	2.16	1.79	2.17	2.13	1.77	2.44	1.17	

Table 4.4 (cont'd)

17-HDoHE										0.03
Apparently healthy	1.54	1.38	1.82	1.55	1.54	1.35	1.4	1.58	0.13	
Diseased	1.65	1.77	1.81	1.62	1.8	1.72	1.58	1.84	0.11	

[1]HETE=hydroxyeicosatetraenoic acid; oxoETE=oxoeicosatetraenoic acid.
[2]Data log or square root transformed. Back-transformed values shown.

Sixteen CYP-derived oxylipids were detected in this study, of which only 12, 13-DiHOME concentrations differed between the AH and CD group over the study period (Table 4.5). Peak concentrations of 12, 13-DiHOME were reached at C +7 for both groups, with greater concentrations seen in the AH cows (Figure 4.3; $P < 0.0001$).

Table 4.5. Mean plasma concentrations of cytochrome P450-derived oxylipids in apparently healthy cows (n=7) and those that developed a postpartum disease (diseased; n=9) from 6 d prior to dry-off (d -6) to 7 d after calving (C +7). Standard error (SE) and P-values listed for each row represents the SE and P-value for the treatment effect of undetected disease versus detected disease in the linear mixed model. After Bonferroni's correction to account for family-wise error, statistical significance was set at $P < 0.001$. Cytochrome P450-derived oxylipids that differed between groups are also shown in Figure 4.3.

	Sampling Point									
Oxylipid[1] (nM)	d -6	d 0	d +1	d +2	d +6	d +12	CU	C +7	SE	*P*
5,6-DiHETE[2]										0.94
Apparently healthy	3.82	6.21	39.1	8.15	5.86	5.44	6.01	5.18	1.4	
Diseased	4.61	5.45	14.9	14.7	9.64	9.27	5.35	2.41	1.34	
8, 9-EET[2]										0.59

Table 4.5 (cont'd)

Apparently healthy	0.05	0.06	0.29	0.1	0.1	0.09	0.09	0.19	0.003	
Diseased	0.08	0.04	0.17	0.14	0.1	0.15	0.02	0.13	0.003	
8, 9-DHET[2]										0.34
Apparently healthy	0.45	0.49	0.87	0.68	0.6	0.56	0.54	0.62	0.01	
Diseased	0.52	0.63	0.75	0.72	0.79	0.84	0.6	0.71	0.004	
9, 10-EpOME[2]										0.49
Apparently healthy	0.13	0.11	0.24	0.13	0.14	0.1	0.13	0.23	0.001	
Diseased	0.12	0.13	0.15	0.11	0.11	0.11	0.12	0.26	0.001	
9,10-DiHOME[2]									0.004	
Apparently healthy	31.4	29.6	13	9.29	8.79	6.38	12.9	59	1.14	
Diseased	20.8	20	8.55	6.88	6.3	5.51	8.09	33	1.16	
9-HETE[2]										0.22
Apparently healthy	0.22	0.12	0.36	0.14	0.22	0.2	0.14	0.23	0.02	
Diseased	0.22	0.39	0.37	0.32	0.19	0.27	0.27	0.33	0.01	
11, 12-DHET[2]										0.14

Table 4.5 (cont'd)

Apparently healthy	1.84	2.19	2.7	2.02	2.26	2.37	2.31	2.68	1.15	
Diseased	2.38	2.47	2.92	2.96	3.1	3.69	2.58	2.96	1.13	
12, 13-EpOME[2]										0.14
Apparently healthy	5.72	6.3	5.08	5.33	3.49	3.06	3.81	13.3	0.03	
Diseased	6.9	7.45	5.72	4.55	4.59	4.15	6.88	16.7	0.02	
12, 13-DiHOME[2]										0.0001
Apparently healthy	1.2	1.6	1.3	0.85	0.76	0.61	1.8	4.4	1.4	
Diseased	0.2	0.21	0.13	0.16	0.14	0.13	0.11	0.73	1.3	
14, 15-EET[2]										0.39
Apparently healthy	0.11	0.08	0.36	0.19	0.15	0.17	0.14	0.2	0.002	
Diseased	0.15	0.12	0.27	0.21	0.24	0.21	0.1	0.23	0.002	
14, 15-DHET[2]										0.2
Apparently healthy	2.88	3.55	5.19	3.77	3.72	3.87	4.0	4.33	1.12	
Diseased	3.6	3.83	4.93	4.62	4.48	5.23	4.1	4.57	1.1	

Table 4.5 (cont'd)

14, 15-DiHETE										0.4
Apparently healthy	6.41	7.46	9.41	9.45	9.53	8.31	7.81	7.86	1.24	
Diseased	7.38	7.83	10.2	9.94	10.8	10.5	8.69	7.5	1.1	
17, 18-DiHETE										0.16
Apparently healthy	65.9	72.3	132	82.4	83.8	73	67	61.2	14.7	
Diseased	83.9	85.6	114	108	126	125	84.6	59.9	13	
19, 20-DiHDPA[2]										0.19
Apparently healthy	0.94	1.16	1.88	1.12	1.43	1.65	1.9	1.9	0.02	
Diseased	1.9	1.85	2.39	1.65	2.06	1.36	2.65	1.87	0.01	
19, 20-EpDPE[2]										0.33
Apparently healthy	1.53	1.67	1.97	1.9	2.15	1.69	1.69	1.79	0.01	
Diseased	1.59	1.73	1.68	1.63	1.49	1.84	1.49	1.76	0.004	
20-HETE[2]										0.69

Table 4.5 (cont'd)

Apparently healthy	1.15	1.52	5.77	3.72	3.39	3.31	2.79	3.65	0.1
Diseased	1.69	1.64	2.92	2.8	2.92	3.56	1.61	4.58	0.08

[1]DiHETE=dihydroxyeicosatetraenoic acid; EET=epoxyeicosatrienoic acid; DHET=dihydroxyeicosatrienoic acid; EpOME=epoxyoctadecenoic acid; DiHOME= dihydroxyoctadecenoic acid; HETE=hydroxyeicosatetraenoic acid; DiHDPA=dihydroxydocosapentaenoic acid; EpDPE=epoxydocosapentaenoic acid; HETE=hydroxyeicosatetraenoic acid.
[2]Data log or square root transformed. Back-transformed values shown.

Isoprostanes are a specialized oxylipid produced via a non-enzymatic mechanism. Although all 3 detected IsoP showed differences between AH and CD animals, only 8-iso-PGA_2 remained significant after accounting for family-wise error (Table 4.6**;** Figure 4.3). Nonetheless, concentrations of IsoP were most commonly numerically or significantly greater in the CD group compared to AH cows. For 8-iso-PGA_2 in both groups, concentrations steadily rose from the early dry period to CU, where greatest concentrations were noted (AH=0.73 nM; CD=2.13 nM), before decreasing to the smallest concentrations of the study at C +7 (AH=0.16 nM; CD=0.36 nM).

Table 4.6. Mean plasma concentrations of isoprostanes (IsoP), non-enzymatically-derived oxylipids, in apparently healthy cows (n=7) and those that developed a postpartum disease (diseased; n=9) from 6 d prior to dry-off (d -6) to 7 d after calving (C +7). Standard error (SE) and P-values listed for each row represents the SE and P-value for the treatment effect of undetected disease versus detected disease in the linear mixed model. After Bonferroni's correction to account for family-wise error, statistical significance was set at $P < 0.001$. Isoprostanes that differed between groups are also shown in Figure 4.3.

	Sampling Point									
Oxylipid[1] (nM)	d -6	d 0	d +1	d +2	d +6	d +12	CU	C +7	SE	*P*
8-iso-PGA_2[2]										0.0001
Apparently healthy	0.26	0.29	0.37	0.37	0.4	0.56	0.73	0.16	0.004	
Diseased	0.77	0.68	1.2	1.1	1.5	1.9	2.1	0.36	0.003	
8, 12-iso-$iPF_{2\alpha}$-VI										0.04
Apparently healthy	0.3	0.26	0.3	0.19	0.19	0.17	0.23	0.21	0.05	
Diseased	0.39	0.41	0.3	0.24	0.24	0.17	0.29	0.33	0.04	
5-$iPF_{2\alpha}$-VI										0.04
Apparently healthy	0.09	0.07	0.09	0.07	0.07	0.06	0.06	0.06	0.02	
Diseased	0.14	0.13	0.13	0.13	0.04	0.09	0.06	0.16	0.02	

[1]8, 12-iso-$iPF_{2\alpha}$-VI=8, 12-iso-Isoprostane-$F_{2\alpha}$-VI; 5-$iPF_{2\alpha}$-VI=5-iso Prostaglandin $F_{2\alpha}$-VI.

DISCUSSION

Differences in oxylipid profiles between groups of the present study were detected weeks prior to the development of clinical disease and implies that oxylipids measured during early mammary involution may be useful in assessing risk of postpartum diseases. Currently, periparturient disease risk assessment uses biomarkers such as NEFA and BHB. These biomarkers are generally measured within 2 wk prior to or after calving (Ospina et al., 2010). Assessing disease risk near the time of calving often does not leave sufficient time for successful interventions because disease processes may be too advanced at that stage (Wisnieski et al., 2019). More recent work suggests that biomarkers of other contributors to disease risk, such as inflammation, strengthen the ability to predict disease around the time of calving. Measuring these biomarkers at cessation of lactation could effectively predict disease risk, potentially allowing more time to provide interventions to mitigate disease (Wisnieski et al., 2019). As oxylipids are intimately associated with dysregulated inflammation, it is reasonable to consider them for biomarker use to assess disease risk (Sordillo and Mavangira, 2014).

Recent studies identified specific oxylipids with potential as biomarkers for assessing disease risk. Ryman et al. (2015) reported that cows with *Streptococcus uberis* mastitis had increased concentrations of $PGF_{2\alpha}$ and 9-HODE in mammary tissue relative to healthy controls. In our study, the same oxylipids were increased in plasma of CD cows at most sampling points. Thus, $PGF_{2\alpha}$ and 9-HODE may be especially promising candidates for biomarker use as they are detected in several biological fluids and are associated with disease. Furthermore, $PGF_{2\alpha}$ and 9-HODE may be influencing inflammatory outcomes via their biological actions. Well-described inflammatory roles of $PGF_{2\alpha}$ exist, such as stimulating COX-2 expression (Leimert et al., 2019). Expression of COX-2 is involved in inflammatory regulation and it has been demonstrated that

COX-2 is more active in milk leukocytes from bovine mammary quarters with mastitis compared to uninfected quarters (De and Mukherjee, 2014). However, the function of HODE is less clear (Leimert et al., 2019; Pecorelli et al., 2019). For instance, 9-HODE induced chemotaxis in bovine polymorphonuclear leukocytes in vitro but has also demonstrated decreased platelet adhesion in the vasculature (Henricks et al., 1991; Rolin and Maghazachi, 2014). Given the importance of $PGF_{2\alpha}$ and 9-HODE to leukocyte function during inflammation, future work should focus on the impact of these oxylipids in responses to environmental and contagious mastitis pathogens.

Amongst the oxylipids, IsoP may have the greatest potential as a biomarker. A specific isomer, 15-F_{2t}-IsoP, is currently considered the gold standard biomarker of in vivo oxidative stress in humans because it is highly specific for lipid peroxidation (Milne et al, 2015). Furthermore, 15-F_{2t}-IsoP has been established as a biomarker of several diseases in various species, including coliform mastitis in dairy cattle (Mavangira et al., 2016). Although we did not detect 15-F_{2t}-IsoP presently, we have provided evidence that other IsoP may be relevant as potential biomarkers of disease risk. One promising biomarker candidate may be 8-isoPGA_2, which is a stable metabolite of 8-iso-PGE_2. In environments replete of cellular reducing agents such as glutathione or α-tocopherol, 8-isoPGA_2 is made more readily than 15-F_{2t}-IsoP (Milne et al., 2011). Recent research demonstrated that α-tocopherol concentrations are decreased in dairy cattle around the time of calving relative to the day of dry-off, and therefore provides a plausible explanation for the increasing concentrations of 8-isoPGA_2 as calving approached but undetectable 15-F_{2t}-IsoP (Strickland et al, 2021). Another possible explanation is the use of updated analytical methods from previous studies in dairy cattle where antioxidant reducing agent was not added to the samples immediately after collection to prevent ex vivo peroxidation. As with other oxylipids,

IsoP biosynthesis is complex and future studies are necessary to determine the implications of their presence or absence at varying times in the lactation cycle. Indeed, it would be beneficial to establish threshold concentrations of oxylipids that may indicate disease risk and determine when measurement should occur during the lactation cycle for best production outcomes.

Given that each oxylipid holds a unique function during inflammation, determining the relative abundance of several oxylipids rather than just measuring a single molecule may be best for assessing disease risk. As an example, downstream metabolites of oxylipids often have differing potencies and actions than the parent compound they are derived from. While 9-HODE is a potent natural ligand for receptors such as peroxisome proliferator-activated receptor gamma, its metabolite 9-oxoODE is less potent and exerts an anti-inflammatory effect (Patwardhan et al., 2009; Vangaveti et al., 2010). In contrast, the metabolites of EpOME (DiHOME) are far more potent than their parent oxylipid (Powell et al., 1993; Moghaddam et al., 1997). The differences of timing and abundance of secondary oxylipid production between the groups of cows in this study may explain why AH cows did not develop disease but the CD group did. For example, DiHOME are produced during oxidative burst in inflammatory cells, which is a crucial component of the innate immune defense against pathogens (Powell et al., 1994; Thompson and Hammock, 2007; Mosca et al., 2020). Deficits in neutrophil oxidative burst are associated with retained placenta, metritis, and mastitis in dairy cattle, all of which were diseases noted in the present study (Cai et al, 1994). Hence, elevated concentrations of 12, 13-DiHOME at CU and C +7 in the AH group may suggest these cows have stronger oxidative burst towards pathogens at these times (Powell and Rokach, 2015). In fact, the combination of increased concentrations of 9-oxoODE and 12, 13-DiHOME after calving may suggest that the oxylipid profile of AH cows in this study supported more favorable inflammatory outcomes. Thus, it may be more beneficial

to measure a collective profile of oxylipids compared to measuring a single molecule for biomarker use. However, additional studies are required to identify the ideal composite of oxylipids to optimize inflammation.

The present study is an initial characterization of the oxylipid profile in dairy cattle during the dry and periparturient periods and therefore included a limited number of animals with diverse postpartum diseases. The variety of disease conditions coupled with diagnosis at a wide range of DIM represents a heterogeneous array of inflammatory processes. Furthermore, the observational nature of this study precludes the ability to establish causal relationships. As such, future studies should be conducted with a larger population from different geographic regions and dairying styles to validate oxylipids as biomarkers of disease risk. It would also be beneficial to perform studies focusing on specific postpartum diseases.

CONCLUSIONS

This study documents changes in the oxylipid profile of dairy cattle from the start of mammary gland involution through the first 7 d of the subsequent lactation. The data presented herein supports those differences in oxylipid concentrations between cows that developed disease after calving and those that remained apparently healthy can be detected during early mammary involution. This work has important implications for the dairy industry, as it suggests that factors contributing to disease after calving may begin as soon as the early dry period. Moreover, a collective measurement of the oxylipid pool during early mammary involution may represent a valuable diagnostic biomarker for postpartum diseases. This pilot study provides an initial characterization of the oxylipid profile of the dry and periparturient periods of 1 herd with a heterogeneous array of postpartum diseases. Thus, larger-scale studies should be performed to include cows from multiple dairies from differing geographical regions and dairying styles.

Further elaboration of associations between oxylipid concentrations and specific postpartum diseases is warranted. Understanding if and how the oxylipids detected in this study participate in inflammatory processes relevant to dairy cows would also be prudent. Longer-term, it would be beneficial to determine if implementing interventions (e.g., dietary supplementation) at early mammary gland involution would mitigate the development of disease after calving via the alteration of oxylipid profiles.

CHAPTER 5

Published in Frontiers in Veterinary Science: Putman, A.K., L.M Sordillo, and G.A. Contreras. 2022. The Link between 15-F_{2t}-Isoprostane Activity and Acute Bovine Endothelial Inflammation Remains Elusive. Front Vet Sci. 9:873544. doi: 10.3389/fvets.2022.873544.

INTRODUCTION

Modern dairy cows are subject to increased incidence and severity of mastitis during major physiological transitions of the lactation cycle. Principal underlying components of mastitis pathophysiology include dysregulated inflammation and oxidative stress resulting from the perturbations in immune system function and redox balance during these transitions (Sordillo, 2013; Mavangira and Sordillo, 2018). For instance, increased energy demands to support copious milk production after calving necessitate greater RONS production from the mitochondria. At the same time, decreased feed intake leads to insufficient consumption of antioxidants that defend against RONS (Mavangira and Sordillo, 2018). Such disruptions to redox balance can lead to oxidative stress, which occurs when proteins, nucleic acids, and lipids are damaged as a result of RONS overwhelming host antioxidant defenses (Luschak, 2014). Severe cellular damage from increased RONS during oxidative stress can lead to numerous consequences, including endothelial dysfunction.

A functional endothelium is crucial for appropriate inflammatory responses. Endothelial cells form a single cell layer between blood and tissue and thus, are responsible for activities such as maintaining vascular barrier integrity (Dalal et al., 2020). Dysfunctional EC allow for sustained dysregulated inflammation, leading to impaired immunity and increased disease susceptibility. For instance, apoptosis and necrosis are common features of dysfunctional EC (Yeh et al, 2020). Decreased barrier integrity permits increased flux of activated leukocytes and fluid into tissues,

perpetuating inflammation (Majolee et al., 2019). Certain lipid mediators formed during inflammation, known as oxylipids, can induce EC dysfunction. For example, 13-HPODE is associated with apoptosis and subsequent necrosis of bovine mammary EC along with decreased barrier integrity (Ryman et al., 2016). In fact, dysregulated inflammation and the associated altered barrier integrity is a key pathological finding in coliform mastitis (Mavangira et al., 2020). As EC are particularly susceptible to RONS attack, they will form specialized oxylipids known as isoprostanes (IsoP) during acute inflammation (Morrow et al., 1990; van Golen et al., 2014).

Isoprostanes are generated nonenzymatically when RONS react with polyunsaturated fatty acids in lipid membranes (Morrow et al., 1990). Although numerous biomarkers of oxidative stress exist, IsoP are currently considered superior due to their highly sensitive and specific nature in detecting lipid peroxidation (Czerska et al., 2015). At present, the omega-6-derived 15-F_{2t}-IsoP is the most commonly referenced IsoP in the literature (Galano et al. 2017). Indeed, growing evidence supports IsoP as a biomarker of oxidative stress in dairy cattle, including for diseases such as coliform mastitis (Mavangira et al., 2016; Kuhn et al., 2018; Putman et al., 2018). Isoprostanes may have a role beyond being biomarkers as several studies have established that IsoP have bioactivity on the vasculature, primarily by constricting or dilating blood vessels (Gonzalez-Luis et al., 2010; van der Sterren and Villamor, 2011). Furthermore, IsoP demonstrate an ability to alter inflammatory gene regulation, affecting cytokine production and macrophage adhesion to the vasculature (Scholz et al., 2003; Kumar et al, 2005; Bosviel et al., 2017). However, the physiological role of IsoP in the context of acute inflammation in dairy cattle remains poorly characterized. Thus, this study aimed to determine how IsoP alter oxidative stress outcomes in bovine EC under inflammatory challenge.

MATERIALS AND METHODS

Reagents

Fetal bovine serum was provided by Hyclone Laboratories, Inc. (Logan, UT). HAM's F-12K and HEPES buffer were from Corning Inc. (Corning, NY). Sodium selenite, insulin, heparin, and transferrin were from Sigma-Aldrich (St. Louis, MO). Antibiotics/antimycotics, glutamine, trypsin-EDTA, and bovine collagen were purchased from Life Technologies (Carlsbad, CA). Indomethacin, 15-F_{2t}-IsoP (formerly 8-isoP$GF_{2\alpha}$), and AAPH were purchased from Cayman Chemical (Ann Arbor, MI). Lipopolysaccharide (**LPS**) purified from E. coli 0111:B4 was purchased from Invivogen (San Diego, CA).

Cell Culture

Primary BAEC were used to model systemic vascular acute inflammation. A full description of the methods used to isolate BAEC have been previously described by our group (Mavangira et al., 2020). Isolated EC were distinguished from other cell types with von Willebrand factor staining and morphological analysis. Cells were stored in liquid nitrogen at pass 4 until being thawed out for experiments. Upon thawing cells, BAEC were grown to 75-80% confluency in flasks (Corning Inc., Corning, NY) incubated at 5% CO_2 and 37 ºC, and were used from passages 6-9. Cells were cultured in BAEC media containing HAM's F-12K, 20 mM HEPES, 10% fetal bovine serum, 100 U/mL antibiotic/antimycotic consisting of penicillin, streptomycin, and amphotericin B, 300 mg/mL L-glutamine, 10 ng/mL sodium selenite, 10 µg/mL insulin, 100 µg/mL heparin, and 5 µg/mL transferrin.

Experimental design

Conditions of increased ROS generation and acute inflammation were generated using AAPH or LPS. Treatments were as follows: untreated media control, vehicle control with 0.05% ethanol

by volume, positive control of either 5 mM AAPH or LPS (15 or 25 ng/mL) as an agonist, 10 nM 15-F_{2t}-IsoP, and co-culture of either 5 mM AAPH or LPS with 10 nM 15-F_{2t}-IsoP. Incubation times varied by assay, ranging from 1-24 hr. All BAEC treatments were delivered in F-12K media with either 10% or 0% FBS. A graphical summary of the experimental design is in Figure 5.1.

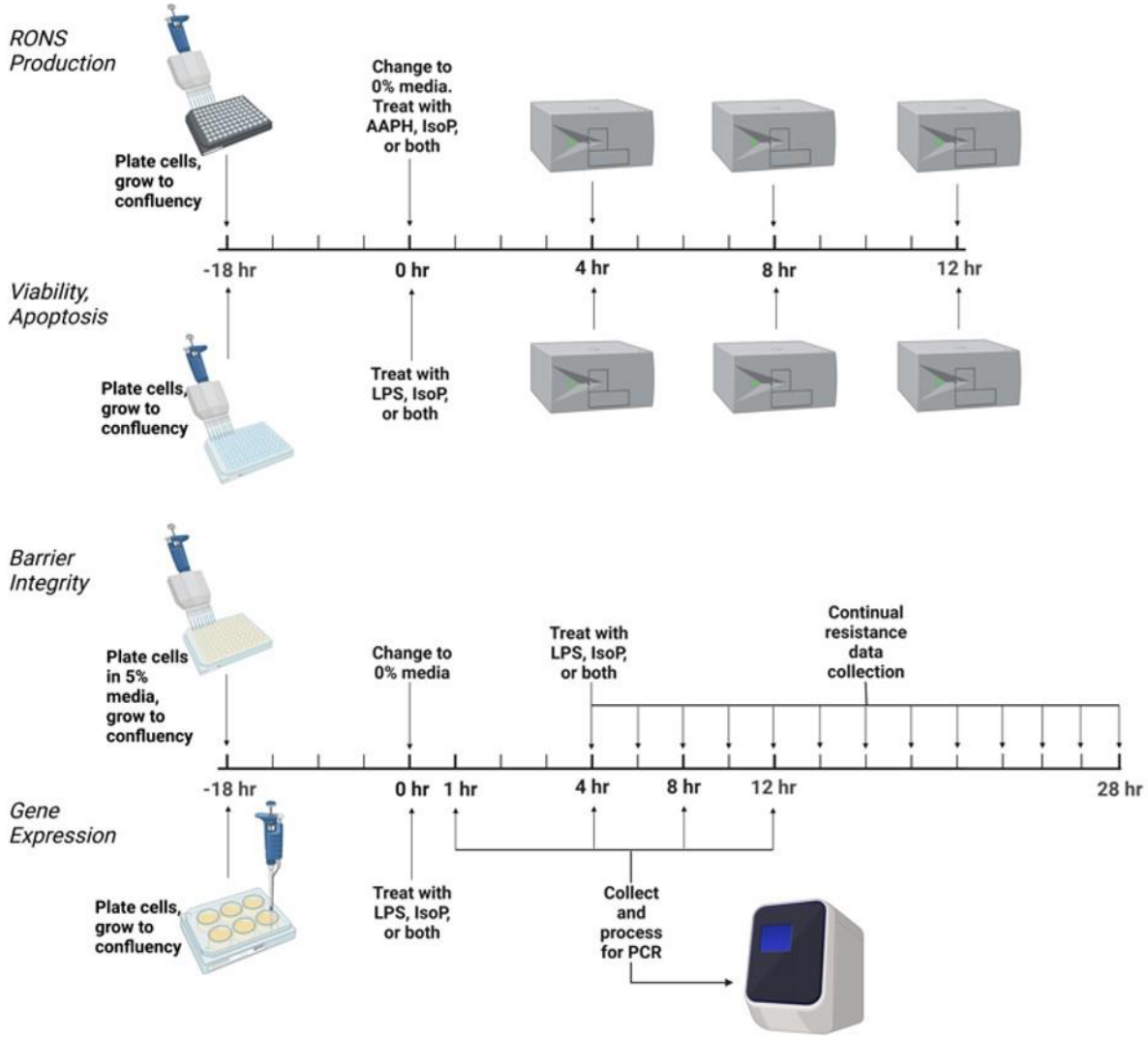

Figure 5.1. Experimental design to test the effect of isoprostane (15-F_{2t}-IsoP) on bovine aortic endothelial cells (n=4). AAPH=2,2'-azobis (2-amidinopropane) dihydrochloride; LPS=lipopolysaccharide. Figure created with biorender.com.

Cellular Viability

Cellular viability was assessed with Promega CellTiter-Glo Luminescent Cell Viability Assay (Madison, WI). This assay produces a luminescent signal proportional to the amount of ATP generated from metabolically active cells present in a well. Cells were plated in white flat-bottom 96-well plates at a density of 4.0×10^4 cells/well. The assay was then performed according to manufacturer's instructions. Luminescence was read on a Tecan Infinite 200 Pro (Männedorf, Switzerland).

Apoptosis

To determine if IsoP were influencing apoptosis in BAEC, a Promega Caspase-Glo 3/7 kit was employed. Briefly, caspase activation of the substrate releases aminoluciferin. Subsequent interaction of the free aminoluciferin with luciferase results in a luminescent signal proportional to caspase 3/7 activity. Similar to the viability assay, cells were plated in a white flat-bottom 96-well plate at a density of 4.0×10^4 cells/well. Manufacturer's instructions were followed to carry out the assay. Luminescence was read on a Tecan Infinite 200 Pro.

RONS Production

Total intracellular RONS production was assessed with Cell Biolabs OxiSelect Intracellular RONS kit (San Diego, CA). All reactive species of the sample were measured utilizing a dichlorodihydrofluorescin DiOxyQ (DCFH-DiOxyQ) probe. In brief, RONS will interact with the highly reactive DCFH, which rapidly oxidizes to 2,7'-dichlorodihydrofluorescein, producing a fluorescent signal. Therefore, fluorescence is directly proportional to the amount of reactive species in a sample. Cells were plated at 4.0×10^4 cells/well in black clear-bottom 96-well plates. After 18 hr, 10% FBS media was removed and replaced with 0% treatment media. The assay was

then performed according to manufacturer's instructions. A Tecan Infinite 200 Pro was employed to read fluorescence at 480 nm excitation and 530 nm emission.

Cell Barrier Integrity

Endothelial cell barrier integrity was assessed utilizing an electric cell-substrate impedance sensing (**ECIS**) ZTheta system (Applied Biophysics, Troy, NY). Cells were seeded (density = 1.0×10^5) on a 96-well array (96W10idf, Applied Biophysics) in 5% FBS F-12K media and allowed to grow for approximately 18 hours until resistances stabilized, suggesting a confluent monolayer of EC. Once confluency was reached, media was changed to 0% FBS and the resistances were allowed to equilibrate for approximately 4 hours. Treatments as listed above in the experimental design section were added. The ECIS system took measurements every 180 s at multiple frequencies for 24 hours. The resistance measurements taken at 4000 Hz after treatment were utilized for analysis.

Gene Expression via qRT-PCR

Cells were cultured in 6-well plates for RNA extraction. Wells were seeded at 1.0×10^6 cells and grown to 75-80% confluency. Each well was washed twice with HBSS and then 300 µL Buffer RLT (Qiagen, Hilden, Germany) was added to lyse the cells. The buffer was collected from each tube and then added to a 1.5 mL microcentrifuge tube and cell lysate was stored at -20ºC pending RNA extraction within 1 mo of collection.

Extraction of RNA occurred utilizing a Promega Maxwell RSC Instrument following the manufacturer's protocol. Quantification and the quality of RNA was assessed with a Nanodrop ND-1000 spectrophotometer (ThermoFisher, Waltham, MA) and then stored at -20ºC until cDNA was generated. Prior to cDNA generation, all samples were standardized with nuclease-free water to 100 ng/µL. An equal volume of master mix containing 10× reverse-transcription

buffer, 25× dNTP, 10× random primers, Multiscribe reverse transcriptase, RNase inhibitor, and RNase nuclease-free water from a high-capacity cDNA reverse-transcription kit with RNase inhibitor (Applied Biosystems High Capacity cDNA Archive Kit, Waltham, MA) was added to each standardized RNA sample. Samples were placed in a MiniAmp Plus Thermal Cycler (Applied Biosystems, Waltham, MA) programmed with the following settings: 25ºC for 10 min, followed by 37ºC for 2 hr, then 85ºC for 5 min, finishing with 4ºC hold until samples are removed. Samples were then stored at -20ºC until qRT-PCR was completed.

Real-time PCR was carried out with predesigned TaqMan primers and FAM-MGB probes (Applied Biosystems). Samples were assessed for nitric oxide synthase 2 (*NOS2*, Bt03249586_m1), peroxisome proliferator activated receptor alpha (*PPARA*, Bt03220821_m1), peroxisome proliferator activated receptor gamma (*PPARG*, Bt03217547_m1), nuclear factor kappa B subunit 1 (*NFKB1*, Bt03243457_m1), thromboxane A2 receptor (*TBXA2R*, Bt04301659_m1), and beta-2-microglobulin (*B2M*, endogenous control, Bt03251630_g1). Genes were evaluated in triplicate with 2× TaqMan Gene Expression Master Mix (Applied Biosystems), 20× TaqMan Gene Expression Assay Mix (Applied Biosystems), sample cDNA (50 ng/well), and nuclease-free water for a total of 10 μL per reaction well. Thermal cycling conditions for the Fast 2-step PCR system were as follows: stage 1, 95°C for 20 s; stage 2, 95°C for 3 s; stage 3, 60°C for 30 s, with 40 cycles of stages 2 and 3. Data were recorded and compiled using ThermoFisher ExpressionSuite Software version 1.3.

Statistical Analysis

Results for all analyses except for PCR are presented as the ratio of least squares means in treated cells to the untreated control + SEM. The results for PCR were analyzed with a modified ΔΔCt method and are graphically represented as $2^{-\Delta\Delta Ct}$ (Hellemans et al., 2007). Sample size was

calculated a priori based on unpublished preliminary apoptosis data. The PROC POWER statement was used in SAS 9.4 (Cary, North Carolina) with the following syntax: procpower; onewayanova; groupmeans = 1 (untreated media control), 1.11 (ethanol vehicle control), 1 (10 nM 15-F_{2t}-IsoP), 18.6 (25 ng/mL LPS), 15.2 (25 ng/mL LPS + 10 nM 15-F_{2t}-IsoP); stddev = 1.15; alpha = 0.05; npergroup = .; power = 0.9. The calculation suggested a sample size of at least 3 was sufficient to detect a difference of 1-fold change in apoptotic response. Data were analyzed for normality by visualizing Q-Q plots and confirmed with Shapiro-Wilk normality test. For commercial assays and PCR, a one-way ANOVA with Tukey's HSD posthoc test was performed. For analysis of EC barrier resistance, a two-way ANOVA was performed with the factors being time and treatment. Two-way ANOVA was followed by Tukey's HSD posthoc test. All statistical analyses were carried out with SAS 9.4.

RESULTS

15-F_{2t}-IsoP does not affect BAEC Viability during LPS Challenge

Viability results at 4, 8, and 12 hr were all similar and therefore, only 12 hr data are presented here. The viability of cells treated only with 10-500 nM 15-F_{2t}-IsoP was not different from untreated cells ($P = 0.64$), suggesting that IsoP do not have a detrimental effect on BAEC viability (Figure 5.2a). In BAEC treated with LPS, viability was 85% of that seen in untreated cells ($P < 0.0001$). Furthermore, up to 500 nM 15-F_{2t}-IsoP doses did not increase cell viability relative to LPS ($P = 0.85$; Figure 5.2b). Therefore, while 15-F_{2t}-IsoP does not affect viability on its own, it also does not appear to reduce cell death during LPS challenge.

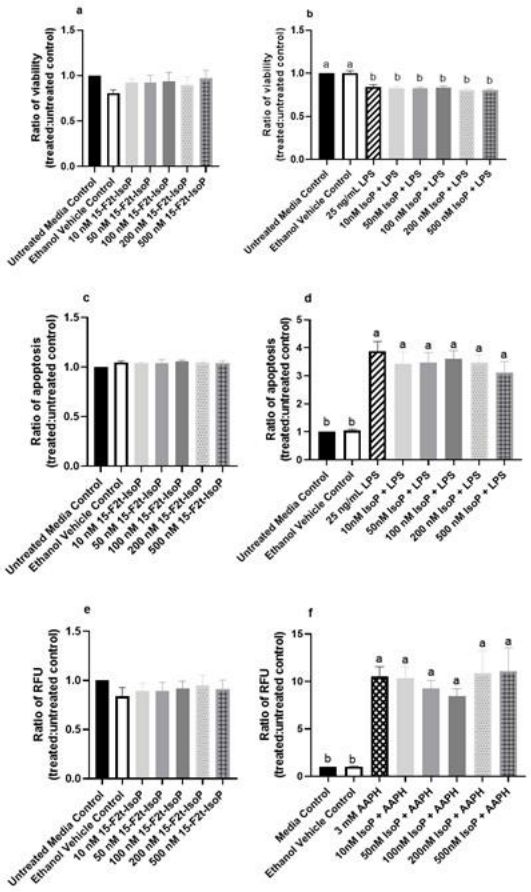

Figure 5.2. 15-F_{2t}-IsoP does not alter bovine aortic endothelial cell (n=4) viability, apoptosis, or RONS production in either unstimulated (a, c, e, respectively) or lipopolysaccharide-stimulated cells after 12 hours of incubation (b, d, f, respectively). RFU=Relative fluorescence units. Different superscripts are different ($P < 0.05$).

15-F_{2t}-IsoP does not Alter Apoptosis in BAEC under LPS Challenge

As above, 12 hr data were chosen to represent the effect of IsoP on apoptosis at all timepoints. Complimentary to our viability data, apoptosis in BAEC treated with only 15-F_{2t}-IsoP was not altered from untreated controls ($P = 0.64$; Figure 5.2c). When cells were treated with LPS, apoptosis increased 389% after 12 hr compared to untreated cells ($P < 0.0001$). However, treating BAEC with LPS and 10-500 nM 15-F_{2t}-IsoP did not decrease apoptosis relative to LPS only ($P = 0.65$; Figure 5.2d). Thus, 15-F_{2t}-IsoP does not have an effect on BAEC apoptosis alone nor in the presence of LPS.

15-F_{2t}-IsoP does not Change RONS Production in BAEC under Oxidant Challenge

As with viability and apoptosis, only the 12 hr data are presented given 4, 8, and 12 hr results were similar. Compared to untreated controls, 15-F_{2t}-IsoP did not alter RONS production on its own in BAEC ($P = 0.87$; Figure 5.2e). When challenged with the free radical generator AAPH, a 10-fold increase in BAEC RONS production was seen compared to media controls ($P = 0.0015$). When treated with 15-F_{2t}-IsoP in addition to AAPH, RONS production was not different from AAPH alone ($P = 0.99$). However, RONS production was only 9-fold (P=0.007) and 8.5-fold ($P = 0.02$) higher than untreated cells at 50 and 100 nM doses of IsoP, respectively. These data therefore demonstrate a relative decrease of RONS production at intermediate doses (Figure 5.2f).

15-F_{2t}-IsoP does not affect BAEC Barrier Integrity during LPS Challenge

As maintaining EC barrier integrity is a critical component of appropriate inflammatory responses, we were interested in assessing if IsoP could improve the resistance across a BAEC monolayer under LPS challenge. A significant time-treatment interaction was detected ($P < 0.0001$; Figure 5.3). Between 8 and 24 hr, barrier integrity was significantly decreased in LPS-treated cells compared to the untreated media control ($P < 0.0001$). A relative increase of barrier integrity was noted in LPS + 15-F_{2t}-IsoP-treated BAEC compared to LPS only between 8 and 24 hr ($P = 0.06$).

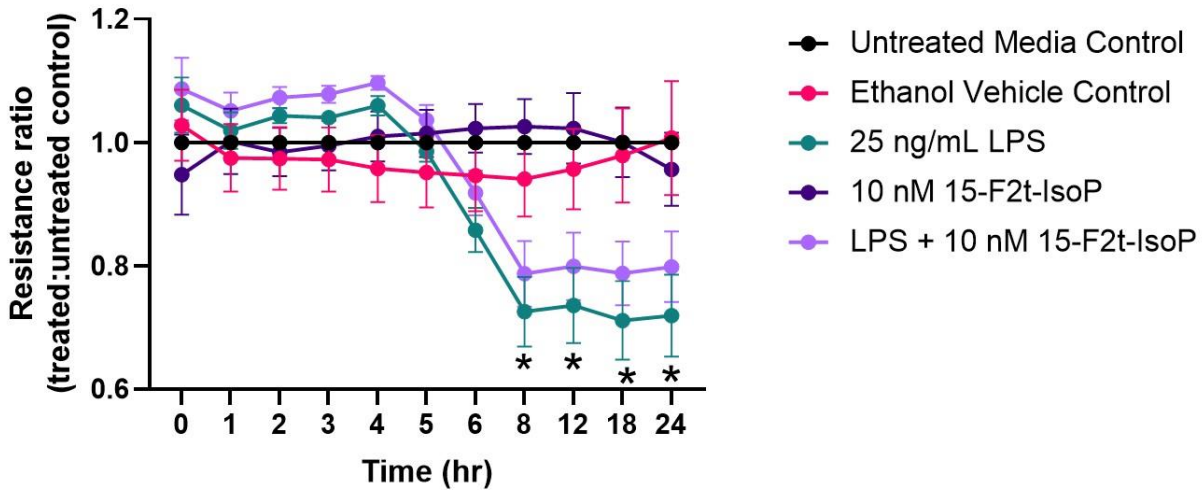

Figure 5.3. Bovine aortic endothelial cell (n=4) barrier integrity is not significantly improved by 15-F_{2t}-IsoP during lipopolysaccharide (LPS) challenge. *Significant time x treatment interaction ($P < 0.05$).

Inflammatory Gene Expression is not Altered by 15-F_{2t}-IsoP

One possible mechanism involved with the relative increase in barrier integrity described above could be due to alterations in inflammatory gene regulation. In relevant inflammatory genes, IsoP did not have an appreciable effect on the gene expression of BAEC challenged with LPS. As the data were similar across genes and timepoints, *TBXA2R*, *NFKB1*, and *NOS2* at 4 hr were selected as representatives to be reported herein (Figure 5.4a, b, and c, respectively). Table 5.1 shows the *P* values for all genes and timepoints assessed. There was a higher expression of *NFKB1* and *NOS2* in LPS-treated cells compared to those without the agonist ($P = 0.001$ and 0.002, respectively). However, no differences were noted between LPS and LPS + 15-F_{2t}-IsoP groups ($P > 0.05$). Therefore, IsoP did not influence inflammatory gene expression in the face of LPS challenge.

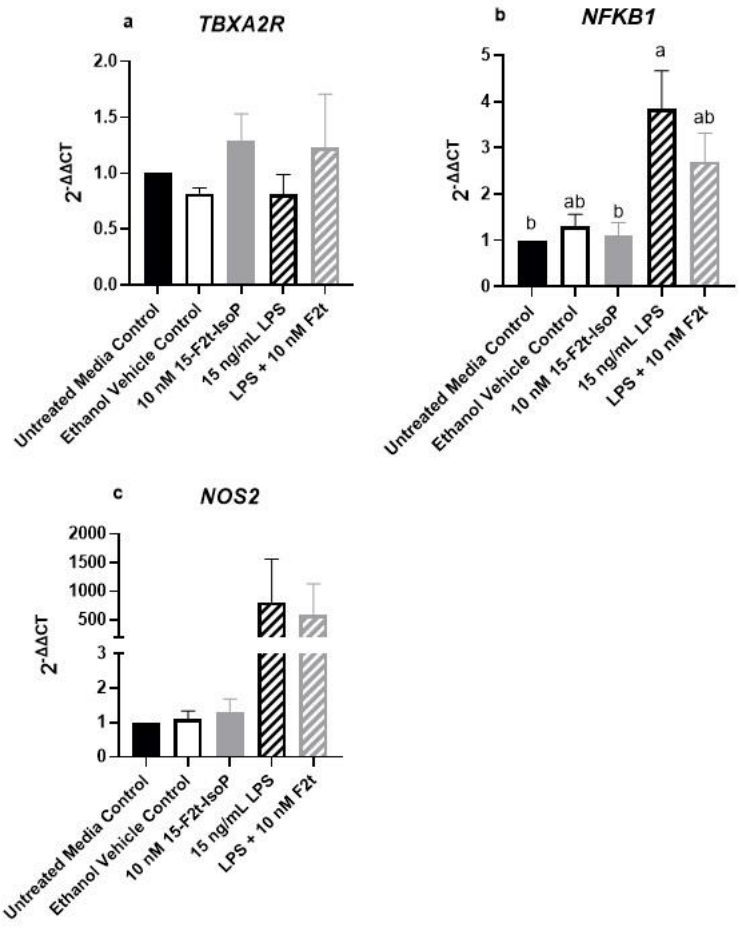

Figure 5.4. Gene expression of relevant inflammatory genes in bovine aortic endothelial cells (n=4) treated with lipopolysaccharide (LPS), 15-F_{2t}-IsoP, or both for 4 hours. a. Thromboxane A2 receptor (*TBXA2R*). b. Nuclear factor kappa B subunit 1 (*NFKB1*). c. Nitric oxide synthase 2 (*NOS2*). Different superscripts are different ($P < 0.05$).

Table 5.1. *P* values for each inflammatory gene assessed at 4-, 8-, and 12-hour treatment incubations. *Overall ANOVA value was significant, but no differences were detected between treatment groups after adjusting for multiple comparisons.

	4 hours	8 hours	12 hours
Thromboxane A2 receptor (*TBXA2R*)	0.9	0.97	0.92
Nuclear factor kappa B subunit 1 (*NFKB1*)	0.001	0.0001	0.0001
Peroxisome proliferator activated receptor alpha (*PPARA*)	0.2	0.45	0.95
Peroxisome proliferator activated receptor gamma (*PPARG*)	0.29	0.86	0.18
Nitric oxide synthase 2 (*NOS2*)	0.002*	0.002	0.0001

To ensure the lack of change in inflammatory gene expression was not due to prolonged time in cell culture or low dosing of IsoP, we also evaluated *TBXA2R*, *NFKB1*, and *NOS2* expression at 1 hr with 10 and 100 nM IsoP concentrations. Similar to the 4, 8, and 12 hr timepoints, no differences were noted between any treatment group for any of the genes ($P > 0.14$). However, numerical decreases in *NFKB1* (Figure 5.5a) and *NOS2* (Figure 5.5b) expression were demonstrated in LPS and 15-F_{2t}-IsoP compared to LPS treatments ($P = 0.64$ and 0.52, respectively). Moreover, although a relative increase of *NOS2* expression was seen in ethanol-treated cells compared to untreated controls at 1 hr, the IsoP treatments that were delivered with the vehicle did not appear to be affected to a similar degree ($P = 0.63$).

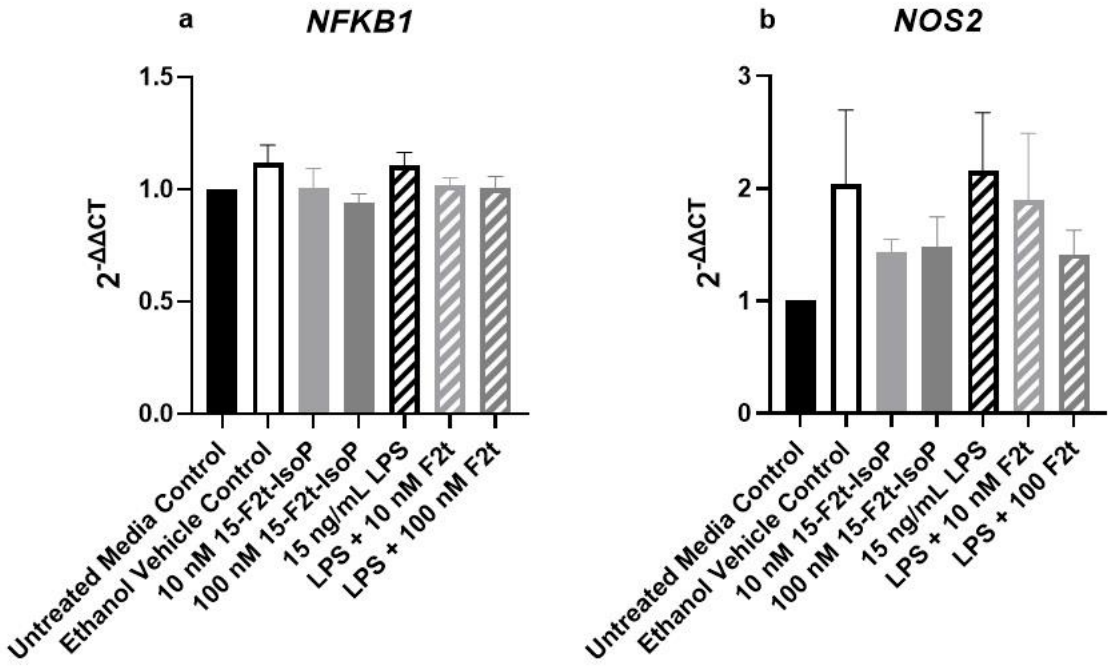

Figure 5.5. Gene expression of nuclear factor kappa B subunit 1 (*NFKB1*; 5.5a) and nitric oxide synthase 2 (*NOS2*; 5.5b) in bovine aortic endothelial cells (n=4) treated with lipopolysaccharide (LPS), 15-F_{2t}-IsoP, or both for 1 hour.

DISCUSSION

The data presented herein demonstrate that 15-F_{2t}-IsoP does not alter viability, apoptosis, barrier integrity, or gene transcription networks of acute inflammation and EC dysfunction in our BAEC inflammation model. However, there was evidence of cytoprotection during the agonist challenge. This study is important for bovine medicine and dairy science because it clarifies effects IsoP do not have during acute EC inflammation characteristic of bovine mastitis.

As oxylipids are potent inflammatory mediators, it stands to reason that IsoP are capable of participating in mastitis pathophysiology. Decreased EC viability and increased apoptosis are common outcomes resulting from dysregulated inflammation and oxidative stress (Ryman et al., 2015). Past evidence suggested that IsoP affect viability in EC. For example, Yura et al., (1999)

detailed that 15-F_{2t}-IsoP increased viability in BAEC at concentrations similar to those used at present. Conversely, Brault and colleagues (2003) established that 15-F_{2t}-IsoP decreased brain microvascular EC viability and did not affect viability of human umbilical vein EC. Evidence of IsoP altering apoptosis is scarce in the literature. In our model, however, IsoP did not affect viability or apoptosis. One plausible explanation for the differences between our results and those reported previously may be due to differences in methodology. Brault et al. (2003), for example, measured viability with MTT assays as opposed to the ATP-based assay we used. Furthermore, ample evidence suggests that the action of IsoP depends on the vascular bed being studied (Putman et al., 2021). Therefore, BAEC viability and apoptosis may not be affected while EC from other locations (e.g., mammary EC) might.

Increased RONS production can also participate in mastitis pathophysiology. Unopposed excessive RONS directly contribute to oxidative stress by causing damage to host DNA, proteins, and lipids. Once macromolecules are damaged, normal cellular function is impaired (Mavangira and Sordillo, 2018). For instance, stimulating bovine mammary epithelial cells with hydrogen peroxide resulted in substantial lipid peroxidation, altered cell morphology, decreased cell proliferation, decreased antioxidant activity, and decreased viability (Ma et al., 2018). Furthermore, the lipid peroxidation products formed during oxidative stress can further perpetuate macromolecule damage (Gaschler and Stockwell, 2017; Musiek et al., 2007). Thus, we were interested in determining if IsoP could affect RONS production given their mechanism of formation. While RONS production was not similar to amounts seen in untreated controls presently, 50 and 100 nM 15-F_{2t}-IsoP combined with AAPH showed a numerical decrease from cells treated only with AAPH. In contrast to our data, electrophilic arachidonic acid-derived IsoP (e.g., 15-A_2/J_2-IsoP) can increase ROS production via depletion of the antioxidant glutathione in

neurons (Musiek et al., 2007). However, 15-F_{2t}-IsoP lacks the cyclopentenone moiety that is attributed to electrophilic IsoP reactivity. Therefore, how 15-F_{2t}-IsoP might cause an absolute decrease in RONS production in a mastitis model remains unclear but warrants further investigation.

Classical signs of clinical mastitis, such as heat and swelling of the mammary gland, can be attributed to decreased EC barrier integrity (Mavangira et al., 2020). We observed a relative increase in barrier integrity of BAEC treated with LPS and 15-F_{2t}-IsoP compared to LPS alone. This cytoprotective effect was interesting considering omega-6-derived oxylipids are commonly associated with negative impacts on barrier integrity. In fact, enzymatically-derived 13-HPODE and 20-HETE decreased barrier integrity in bovine EC (Ryman et al., 2016; Mavangira et al., 2020). Furthermore, Hart and colleagues (1998) found 500 nM 15-F_{2t}-IsoP decreased barrier integrity in pulmonary artery EC. Some oxidized phospholipid products may be beneficial to the EC barrier, however. Birukov et al. (2004) detailed a barrier-protective effect of the epoxyisoprostane-containing phospholipid, 1-palmitoyl-2-(epoxyisoprostane E_2)-sn-glycero-3-phosphocholine. Thus, certain IsoP may be capable of maintaining EC barrier integrity. Future studies should investigate how various IsoP isomers impact monolayer barrier integrity to determine which would be most beneficial to dairy cattle during mastitis.

Many inflammatory gene networks are altered during mastitis. For example, cells stimulated by LPS, as would be the case during coliform mastitis, show increased *NOS2* and *NFKB1* expression (Lebda et al, 2022; Kan et al., 2021). Activation of *NFKB1* suppresses the activity of *PPARA* and *PPARG* (Wang et al., 2019; Bougarne et al., 2018). An additional gene important for EC inflammatory responses is *TBXA2R*, of which IsoP serve as a ligand (Capra et al., 2014). Previous studies have demonstrated that various IsoP can modify the aforementioned genes.

Brooks and colleagues (2011) found that the omega-3-derived 15-A_{3t}-IsoP inhibited *NFKB1* in macrophages. Moreover, Bosviel et al. (2017) showed activation of *PPARG* in macrophages treated with omega-3-derived IsoP. Although previous studies have shown an effect, we did not observe a change in the gene expression as a result of IsoP treatment. However, it was intriguing to see a more pronounced, albeit nonsignificant, alteration in gene expression when cells were treated for 1 hr compared to 4, 8, or 12 hr. Given their short half-life, these results support that IsoP may not be stable in cell culture for extended periods of time (Basu, 1998). Further characterization of optimal dosing and treatment timing should serve as the basis for future studies.

CONCLUSIONS

In our BAEC inflammatory model, IsoP do not alter viability, apoptosis, reactive metabolite production, barrier integrity, or gene transcription networks. However, time of exposure and doses may be important factors that can be regulated by the tissue environment and therefore are complex to model in vitro. Advanced modeling including cellular bioenergetics may be necessary to realize a significant cytoprotective effect of IsoP in bovine cells and should be the goal of future studies.

CHAPTER 6

Published in Antioxidants: Putman, A.K., and G.A. Contreras. 2022. 15-F_{2t}-isoprostane favors an anti-inflammatory phenotype in RAW 264.7 macrophages during endotoxin challenge. Antioxidants (Basel) 11(3):586. doi: 10.3390/antiox11030586.

INTRODUCTION

Oxidative stress is a recognized underlying component of numerous pathologies, including cardiovascular disease, neurodegenerative disorders, and diabetes (Malko and Jiang, 2020). Oxidative stress occurs when chemically reactive oxygen and nitrogen species (**ROS** and **RNS**, respectively) overwhelm antioxidant defenses, leading to damage of host DNA, proteins, and lipids (Lushchak, 2014). At amounts that are well-balanced by antioxidant mechanisms, reactive metabolites participate in many homeostatic immune functions, such as phagocytosis and inflammatory signaling pathways (Sordillo, 2013). However, increased reactive metabolites during times of oxidative stress contribute to sustained dysregulated inflammation. For example, ROS damage to lipid membranes causes a loss of cellular function leading to impaired immunity, which ultimately predisposes individuals to increased disease susceptibility (Sordillo, 2013; Golia et al., 2014). Macrophages are critical effector cells in immune responses, which can contribute to or be influenced by oxidative stress and dysregulated inflammatory responses. Macrophages are active participants in promoting and resolving inflammation. Upon stimulation with bacterial components, such as lipopolysaccharide (**LPS**), macrophages are activated to a proinflammatory phenotype (Viola et al., 2019). Initiating this reaction during endotoxin challenge is necessary to neutralize the inciting cause. As inflammation progresses, an anti-inflammatory phenotype must be acquired to promote resolution and tissue healing (Sordillo, 2018). Traditionally, the proinflammatory phenotype is associated with expression of nitric oxide

synthase 2 (***Nos2***) and cytokines such as interleukin (**IL**) 1β and IL6 (Viola et al., 2019). It is also well-established that macrophages stimulated with LPS undergo a metabolic switch from oxidative phosphorylation to aerobic glycolysis (O'Neill and Pearce, 2016). By converting to glycolysis, these cells are primed for the rapid ATP, ROS, and cytokine production necessary for host defense (Infantino et al., 2013; Kelly and O'Neill, 2015). On the other hand, macrophages polarized to the alternatively-activated phenotype are generally associated with anti-inflammatory effects. Expression of markers such as *Il10* and arginase 1 (***Arg1***), along with energy production via oxidative phosphorylation, characterize this subtype of macrophage (Viola et al., 2019). It is suggested that these changes may be beneficial in promoting cell survival and tissue repair rather than being optimized for pathogen killing like glycolysis-utilizing cells (O'Neill and Peace, 2016). Regardless of phenotype, macrophages are primary producers of ROS. For instance, ROS are produced by macrophages as a part of the oxidative burst during phagocytosis or from the mitochondria during innate immune responses (Canton et al., 2021). The close proximity of generated ROS and cellular lipid membranes puts macrophages in optimal position to generate a certain byproduct of oxidative damage known as IsoP. Isoprostanes are produced via a nonenzymatic mechanism when reactive metabolites interact with polyunsaturated fatty acids in lipid membranes (Morrow et al., 1990). Due to this mechanism of formation, IsoP are currently considered highly sensitive and specific biomarkers of oxidative stress in vivo (Biomarker Working Group, 2016). Amongst the hundreds of isomers that can theoretically be generated, the arachidonic acid-derived 15-F_{2t}-IsoP is abundant in mammals and is particularly well-cited in the literature (Milne et al., 2015; Galano et al., 2017). In addition to their role as excellent biomarkers, past studies support that IsoP can influence macrophages during inflammation. For instance, Kumar et al. (2005) found that 15-F_{2t}-IsoP

decreased monocyte adhesion to human dermal endothelial cells challenged with tumor necrosis factor alpha (**TNFα**). Alterations in macrophage cytokine expression are also possible. Scholz and colleagues (2003) demonstrated increased IL8 expression in cells treated with 15-F_{2t}-IsoP. Since IsoP synthesis is enhanced as the inflammatory process evolves, these lipid mediators may play a key role in modulating later stages of inflammation However, the ability of IsoP to alter macrophages towards a pro- or anti-inflammatory phenotype remains poorly characterized. Thus, the objective of this study was to define the effect of 15-F_{2t}-IsoP on macrophage polarization during endotoxin challenge.

MATERIALS AND METHODS

Reagents

Fetal bovine serum (**FBS**) was provided by Hyclone Laboratories, Inc. (Logan, UT). The antibiotics/antimycotic solution and L-glutamine were obtained from Life Technologies (Carlsbad, CA). Sodium selenite and the known inducer of apoptosis in RAW cells, staurosporine, were purchased from Sigma-Aldrich (St. Louis, MO). RPMI 1640 media was bought from Cellgro (Manassas, VA). Lipopolysaccharide purified from E. coli 0111:B4 was purchased from Invivogen (San Diego, CA). The arachidonic acid-derived IsoP, 15-F_{2t}-IsoP (formerly 8-iso-$PGF_{2\alpha}$), was bought from Cayman Chemical (Ann Arbor, MI).

Cell Culture

RAW 264.7 macrophages were obtained from the American Type Culture Collection (TIB-71; American Type Culture Collection, Manassas, VA). Cells between passages 9 and 45 were grown to 75-80% confluency in flasks incubated at 5% CO_2 and 37 ºC. Media for the RAW 264.7 cells consisted of RPMI 1640 (Cellgro, Manassas, VA) containing 5% FBS, 100 U/mL antibiotics and antimycotics, 300 mg/mL L-glutamine, and 0.1 μM sodium selenite.

Experimental Design

Conditions of acute inflammation were generated with LPS. Following plating, cells were allowed to grow to confluency for 18 hr. In general, treatments consisted of the following: untreated media control, vehicle control with 0.05% by volume ethanol, 5 ng/mL LPS, 500 nM 15-F_{2t}-IsoP, and 5 ng/mL LPS + 500 nM 15-F_{2t}-IsoP. For assessment of apoptosis, an additional treatment of 1000 nM staurosporine was included as a positive control. For all assays except for apoptosis, LPS was added to cell culture media and incubated for 8 h, followed by the addition of IsoP for 1 h. For the apoptosis assay, cells were incubated for 5 h after the addition of LPS or staurosporine before the addition of IsoP for 1 h. A graphical summary of the experimental design is in Figure 6.1.

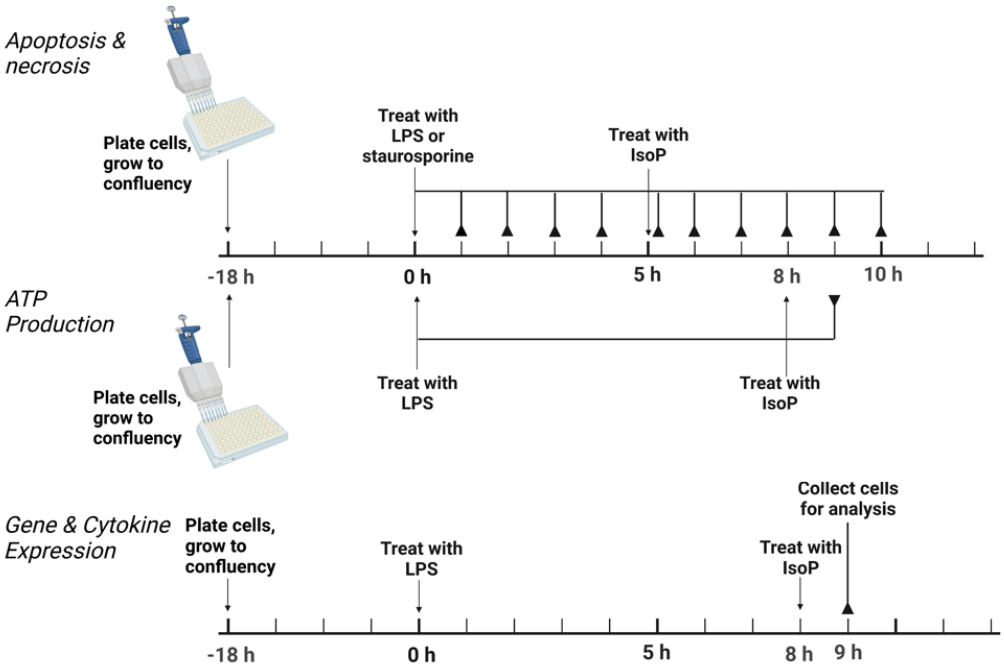

Figure 6.1. Experimental design to test the effect of 15-F_{2t}-isoprostane on RAW 264.7 macrophage polarization. For apoptosis, necrosis, and ATP production, the solid lines ending inreverse arrow heads represent timepoints when plates were read on a Tecan Infinite 200 Pro. For gene and cytokine expression, the solid line ending in a reverse arrow head represents the point at which cells were collected for further analysis. LPS=lipopolysaccharide; IsoP=isoprostane; h=hour.

Apoptosis and Necrosis

To ensure that both the dose of LPS and IsoP used in the present study were not causing apoptosis and subsequent necrosis in the RAW 264.7 cells, a Promega RealTime-Glo Annexin V Apoptosis and Necrosis Assay (Madison, WI) was employed. Briefly, this assay measures the amount of phosphatidylserine present on the outer leaflet of cell membranes. An increase in luminescence is detected when a greater amount of phosphatidylserine is exposed on the outer leaflet, which occurs during early apoptosis. As membrane integrity decreases with the progression of apoptosis to necrosis, a DNA-binding dye generates a fluorescent signal. Cells were seeded in white flat-bottom 96-well plates at a density of 4.0×10^4/well and then the protocol was carried out following the instructions provided in the kit. Using a Tecan Infinite 200 Pro (Männedorf, Switzerland), luminescence was read along with fluorescence at 485 nm excitation and 525 nm emission.

ATP Production

The production of ATP was assessed with Promega CellTiter-Glo Luminescent Cell Viability Assay. This assay produces a luminescent signal proportional to the amount of ATP present in a well. Cells were plated in Costar white flat-bottom 96-well plates at a density of 4.0×10^4/well. The assay was performed according to manufacturer's instructions. Luminescence was read on a Tecan Infinite 200 Pro. Doses of 10-500 nM IsoP were used to establish the optimal concentration to produce a maximal alteration of ATP production in macrophages relative to LPS treatment.

Gene Expression

RAW 264.7 cells were cultured in 6-well plates for RNA extraction. Wells were seeded at 1.0×10^6 cells and grown to 75-80% confluency. After incubation following the treatments

described above, each well was washed twice with HBSS followed by 300 µL Buffer RLT (Qiagen, Hilden, Germany) to lyse the cells. The buffer was collected from each well and then added to a 1.5 mL microcentrifuge tube. Cell lysate was stored at -20ºC pending RNA extraction within 1 mo of collection.

Extraction of RNA occurred utilizing a Promega Maxwell RSC Instrument following the manufacturer's protocol. Quantification and the quality of RNA was assessed with the Nucleid Acid Quantification program (i-control 1.11, Tecan, Männedorf, Switzerland) using a NanoQuant plate read on a Tecan Infinite 200 Pro. RNA was then stored at -20ºC until cDNA was generated.

Prior to cDNA generation, all samples were standardized with nuclease-free water to 100 ng/µL. An equal volume of master mix containing 10× reverse-transcription buffer, 25× dNTP, 10× random primers, Multiscribe reverse transcriptase, RNase inhibitor, and RNase nuclease-free water from a high-capacity cDNA reverse-transcription kit with RNase inhibitor (Applied Biosystems High Capacity cDNA Archive Kit, Waltham, MA) was added to each standardized RNA sample. Samples were placed in a MiniAmp Plus Thermal Cycler (Applied Biosystems, Waltham, MA) programmed with the following settings: 25ºC for 10 min, followed by 37ºC for 2 h, then 85ºC for 5 min, finishing with 4ºC hold until samples are removed. Samples were then stored at -20ºC until qRT-PCR was completed.

Real-time PCR was carried out with predesigned TaqMan primers and FAM-MGB probes (Applied Biosystems). Samples were assessed for *Nos2* (Mm00440502_m1), *Il1β* (Mm00434228_m1), *Il10* (Mm01288386_m1), *Arg1* (Mm00475988_m1), actin B (*Actb*, endogenous control, Mm02619580_g1), and glyceraldehyde-3-phosphate dehydrogenase (*Gapdh*, endogenous control, Mm99999915_g1). Genes were evaluated in triplicate with 2×

TaqMan Gene Expression Master Mix (Applied Biosystems), 20× TaqMan Gene Expression Assay Mix (Applied Biosystems), sample cDNA (50 ng/well), and nuclease-free water for a total of 10 μL per reaction well. Thermal cycling conditions for the Fast 2-step PCR system were as follows: stage 1, 95°C for 20 s; stage 2, 95°C for 3 s; stage 3, 60°C for 30 s, with 40 cycles of stages 2 and 3. Data were recorded and compiled using ExpressionSuite Software version 1.3.

Cytokine and Chemokine Production

Cytokines and chemokines commonly associated with inflammation were evaluated with a Milliplex Mouse Cytokine/Chemokine Magnetic Bead Panel - Premixed 25 Plex - Immunology Multiplex Assay (Millipore Sigma, Burlington, MA). The cytokines and chemokines in this panel included the following: granulocyte colony-stimulating factor (**G-CSF**); granulocyte-macrophage colony-stimulating factor (**GM-CSF**); interferon gamma (**INFγ**); IL1α; IL1β; IL2; IL4; IL5; IL6; IL7; IL9; IL10; IL12p40; IL12p70; IL13; IL15; IL17; interferon gamma-induced protein 10 (**IP10**); chemokine ligand 1 (alternatively, keratinocyte-derived chemokine; **mKC**); monocyte chemoattractant protein-1 (**MCP-1**); macrophage inflammatory protein-1 alpha (**MIP-1α**); MIP-1β; MIP-2; regulated on activation, normal T cell expressed and secreted (**RANTES**); and TNFα. The assay was performed according to manufacturer's instructions. Untreated media control, ethanol vehicle control, and 500 nM 15-F_{2t}-IsoP samples were not diluted for the assay. However, 5 ng/mL LPS and 5 ng/mL LPS + 500 nM 15-F_{2t}-IsoP samples were diluted 1:10 to ensure the concentrations would fall within the dynamic range of the assay. The plate was read with a Luminex 200 System (Austin, TX). The data was analyzed with xPONENT software version 3.1.

Statistical Analysis

Results for apoptosis, necrosis, and cytokine production are presented as the least squares means + standard error of the mean. Production of ATP is represented as a ratio of the least squares means + standard error of the mean in treated cells to the untreated media control. The results for PCR were analyzed with the ΔΔCt method and are graphically represented as $2^{-\Delta\Delta Ct}$ (Schmittengen and Livak, 2008). Sample size was calculated a priori based on unpublished preliminary ATP production data. The PROC POWER function of SAS 9.4 (Cary, NC) was utilized with the following syntax: proc power; onewayanova; groupmeans = 1 (untreated media control), 0.84 (ethanol vehicle control), 0.68 (5 ng/mL LPS), 0.82 (5 ng/mL LPS + 500 nM 15-F_{2t}-IsoP); stddev = 0.1; alpha = 0.05; npergroup = .; power = 0.9. Power analysis revealed that a sample size of 4 was sufficient to detect a 1-fold difference in ATP production between treatments. Normality was visually assessed and confirmed with a Shapiro-Wilk test. A linear mixed effects model (variables = time and treatment) and Tukey's HSD posthoc test were used for apoptosis and necrosis results. ATP production, PCR, and cytokine expression were analyzed with one-way ANOVA and Tukey's posthoc test. For cytokine production, cytokines with R^2 < 90% were excluded from analyses (GM-CSF, IL9, IL15, and MIP-2). To account for family-wise error rate when analyzing the cytokine production data, Bonferroni's correction was used. Therefore, differences in concentrations between treatments were considered if the ANOVA *P* value was less than 0.002 (0.05/25). All statistical analyses were carried out in SAS 9.4.

RESULTS

15-F_{2t}-IsoP is not Cytotoxic to RAW 264.7 Cells

Figure 6.2 represents apoptosis and necrosis in untreated and treated RAW cells. Staurosporine-treated cells exhibited increased apoptosis relative to all other treatments between 4 and 9 hr (*P* <

0.01). Neither LPS nor 15-F_{2t}-IsoP changed apoptosis relative to untreated controls at any time point (P = 0.27 and 0.56, respectively; Figure 6.2a). Although there was an effect of time (P < 0.0001) and time x treatment interaction (P = 0.006) for necrosis, differences were not detected after correcting for multiple comparisons (Figure 6.2b). Thus, LPS and 15-F_{2t}-IsoP did not cause cell death or secondary necrosis in RAW cells at the doses and incubation times utilized in the present study.

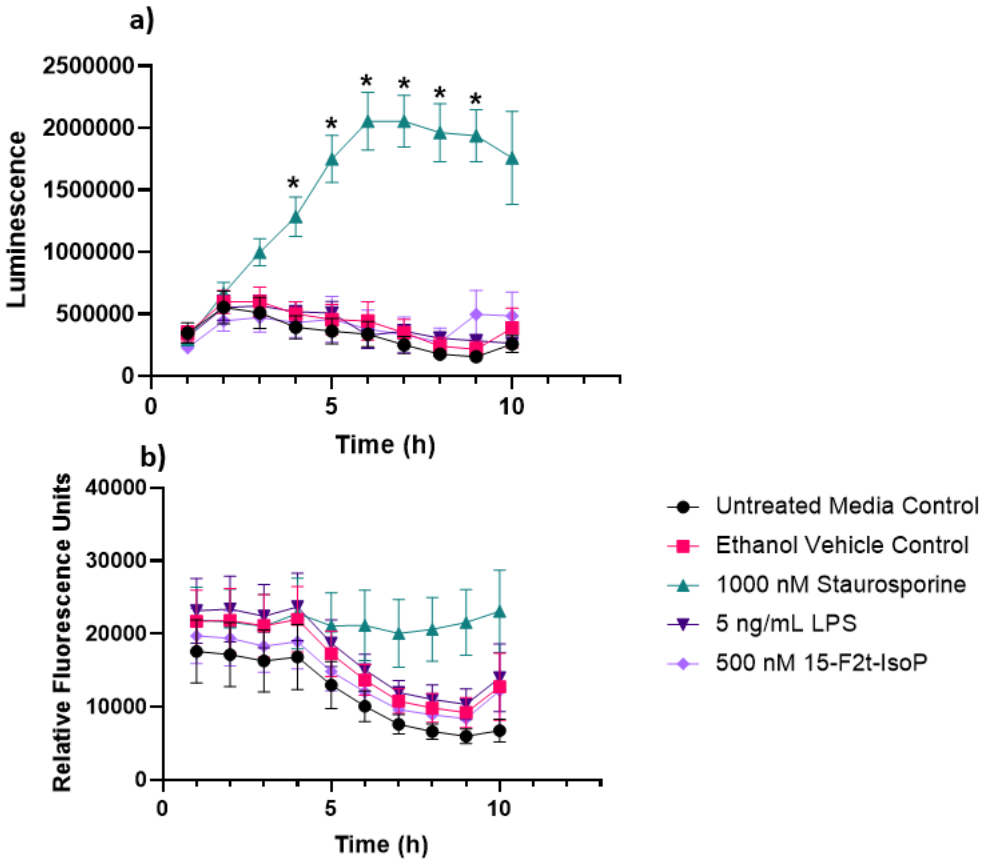

Figure 6.2. Endotoxin and 15-F_{2t}-Isoprostane do not cause apoptosis or necrosis in RAW 264.7 macrophages (n=7). (a) Mean luminescence, representative of apoptosis; *increased luminescence in the staurosporine treatment group at a given time point (P < 0.05) (b) Mean fluorescence, resulting from necrosis secondary to apoptosis; Statistical analyses included a linear mixed effects model with Tukey's HSD posthoc test. LPS=lipopolysaccharide; IsoP=isoprostane; h=hour.

15-F_{2t}-IsoP Increases ATP Production during Endotoxin Challenge

During LPS challenge, ATP production was decreased to 73% of that seen in untreated controls (Figure 6.3; $P = 0.002$). Every treatment that included 10-200 nM 15-F_{2t}-IsoP in addition to LPS was not different from LPS only ($P > 0.26$) or untreated controls ($P > 0.07$). Cells treated with LPS + 500 nM 15-F_{2t}-IsoP had greater ATP production than cells treated only with LPS ($P = 0.002$). In fact, the LPS + 500 nM 15-F_{2t}-IsoP treatment had similar ATP production to untreated controls ($P > 0.99$). As 500 nM IsoP altered ATP production the most compared to LPS alone, it was the concentration utilized for subsequent assays.

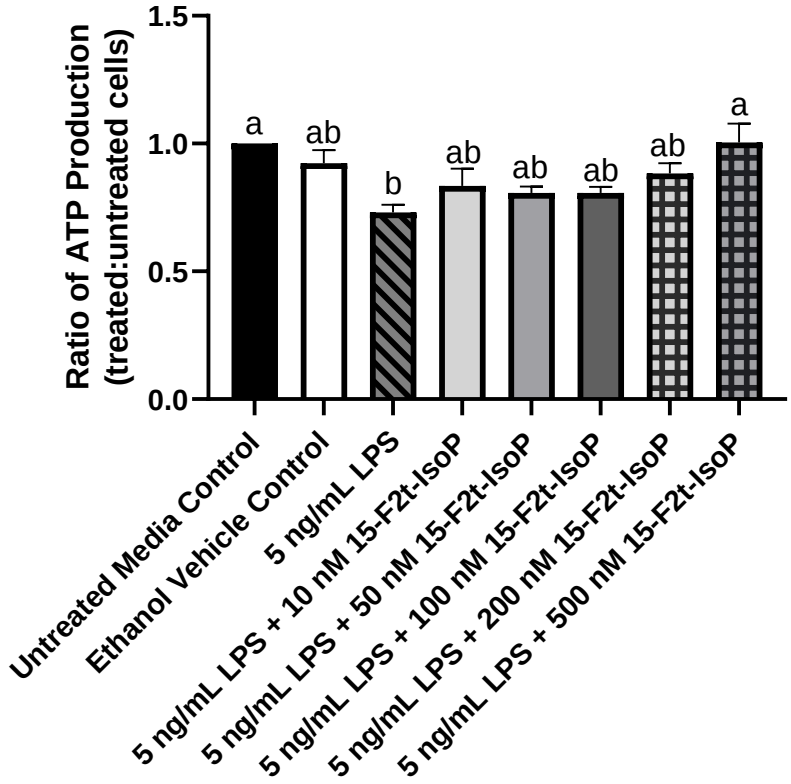

Figure 6.3. ATP production in RAW 264.7 macrophages (n=7) is altered by 15-F_{2t}-isoprostane during endotoxin challenge. Statistical analyses included a one-way ANOVA with Tukey's HSD posthoc test. [a,b]Different superscripts are different ($P < 0.05$). LPS=lipopolysaccharide; IsoP=isoprostane.

15-F_{2t}-IsoP Shifts Inflammatory Gene Expression towards an Anti-inflammatory Phenotype

Macrophage phenotype is commonly determined by the relative expression of specific genes. Relative to untreated controls, RAW 264.7 treated with LPS showed increased expression of *Nos2* ($2^{-\Delta\Delta Ct}$ = 8.57; P = 0.004; Figure 6.4a) and *Il1β* ($2^{-\Delta\Delta Ct}$ = 190; P = 0.02; Figure 6.4b) while relative expression of *Arg1* was decreased to 0.78 (P < 0.03; Figure 6.4c). There was a tendency towards increased *Il10* expression in the LPS-treated cells compared to untreated controls (P = 0.08; Figure 6.4d). When 15-F_{2t}-IsoP was added to LPS-treated cells, *Nos2* expression ($2^{-\Delta\Delta Ct}$ = 6.34) was not different from untreated controls (P = 0.07) or LPS-only treated cells (P = 0.78; Figure 6.4a). Expression of *Il1β* was similarly affected in the LPS and 15-F_{2t}-IsoP combination treatment ($2^{-\Delta\Delta Ct}$ = 152) compared to untreated and LPS-treated cells. Indeed, LPS + 15-F_{2t}-IsoP treatments did not differ from either untreated controls (P = 0.1) or LPS treatments (P = 0.96; Figure 6.4b). We did not observe an increase of *Arg1* expression in LPS + 15-F_{2t}-IsoP-treated cells relative to the LPS-treated cells (P = 0.37; Figure 6.4c). Finally, the greatest relative expression of *Il10* was observed in cells treated with both LPS and 15-F_{2t}-IsoP ($2^{-\Delta\Delta Ct}$ = 13.3; Figure 6.4d). This is compared to relative expression values of 7.5 in LPS-treated RAW cells (P = 0.17) and 1 in untreated controls (P < 0.0001).

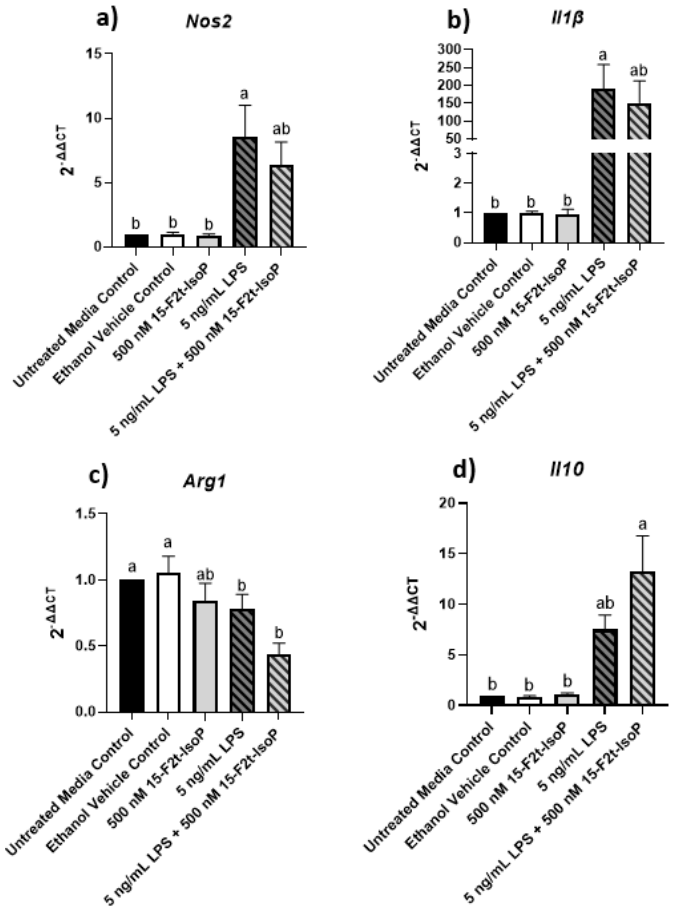

Figure 6.4. Relative gene expression of common macrophage phenotype markers is shifted in RAW 264.7 cells (n=7) treated with endotoxin and 15-F_{2t}-isoprostane (a) nitric oxide synthase 2 (*Nos2*) (b) interleukin (*Il*) *1β* (c) arginase 1 (*Arg1*) (d) *Il10*; Statistical analyses included a one-way ANOVA with Tukey's HSD posthoc test. [a,b]Different superscripts are different ($P < 0.05$); LPS=lipopolysaccharide; IsoP=isoprostane.

15-F_{2t}-IsoP Alters Cytokine Production Consistent with an Anti-inflammatory Phenotype

Similar to inflammatory gene expression, production of certain cytokines can indicate macrophage phenotype. The presence of IL4 and IL7 was not detected in any treatment group, while concentrations of MIP-1β were consistently outside of the assay's limit of detection. Several outliers were detected for IL2, and therefore it was excluded from the study. Table 6.1 includes the mean concentrations of each remaining cytokine.

Table 6.1. Mean concentrations (pg/mL) of cytokines produced by RAW 264.7 cells (n=7) treated with endotoxin and 15-F_{2t}-isoprostane. Statistical analyses included a one-way ANOVA with Tukey's HSD posthoc test unless indicated otherwise. Bonferroni's correction was used to account for familywise error ($P < 0.002$). [a-c]Means within a row with different superscripts are different ($P < 0.05$). LPS=lipopolysaccharide; G-CSF=granulocyte colony-stimulating factor; INF=interferon; IL=interleukin; IP=interferon gamma-induced protein; mKC=chemokine ligand 1; MCP=monocyte chemoattractant protein; MIP=macrophage inflammatory protein; RANTES= regulated on activation, normal T cell expressed and secreted; SD=standard deviation *The Kruskal-Wallis analysis ($P < 0.05$), but no significant differences after correcting for multiple comparisons with Dunn's test.

	Untreated media control	Ethanol vehicle control	500 nM 15-F_{2t}-IsoP	5 ng/mL LPS	LPS + 15-F_{2t}-IsoP	Pooled SD	*P*
G-CSF	149^{c}	642^{c}	320^{c}	216025^{b}	297845^{a}	45800	<0.0001
INFγ	2.42^{b}	5.41^{b}	3^{b}	94.1^{a}	97^{a}	22.1	<0.0001
IL1α	19.2^{c}	29^{c}	30.8^{c}	575^{b}	993^{a}	190	<0.0001
IL1β	3	3	3	3	8.35	4.41	0.38
IL5	12.3^{b}	14.1^{b}	13.1^{b}	91.1^{a}	92.1^{a}	9.89	<0.0001
IL6	112^{bc}	161^{c}	97^{c}	42369^{a}	37268^{ab}	21400	0.001
IL10	4.82^{b}	6.22^{b}	6.59^{b}	65.5^{a}	74^{a}	10.8	<0.0001
IL12p40*	4.49	12.4	7.19	21.9	3	20.4	0.14
IL12p70	3^{b}	3^{b}	58.8^{a}	3^{b}	38.6^{a}	17.5	< 0.0001
IL13	38.3^{b}	21.1^{b}	20.6^{b}	958^{a}	894^{a}	257	<0.0001
IL17	41.5^{c}	42.9^{c}	40^{c}	418^{b}	446^{a}	13.2	<0.0001
IP10	8.42	7.43	10.8	63.1	94.3	75.3	0.22
mKC	3^{b}	3^{b}	2.66^{b}	59.8^{a}	50.1^{a}	15.8	< 0.0001
MCP-1	6113^{c}	10066^{c}	9840^{bc}	17655^{ab}	30013^{a}	9740	0.002
MIP-1α	3109^{b}	4413^{b}	4652^{b}	133077^{a}	155781^{a}	35900	< 0.0001
RANTES	4.3^{b}	4.41^{b}	4.58^{b}	98.8^{a}	146^{a}	57.6	0.0001
TNFα*	240	209	222	66800	10001	34900	0.005

The greatest production of G-CSF (297845 pg/mL) was seen in 5 ng/mL LPS + 500 nM 15-F_{2t}-IsoP-treated cells, which was greater than all other treatments ($P < 0.03$; Figure 6.5a). Similarly, the LPS and IsoP combination treatment had greatest concentrations of IL1α compared to all other treatment groups (993 pg/mL; $P < 0.03$; Figure 6.5b). Concentrations of IL6 were 42369 pg/mL in LPS-treated cells, which was more production than every treatment ($P < 0.02$) except LPS + 15-F_{2t}-IsoP (37268 pg/mL; $P = 0.99$). Although IL6 concentrations of LPS + 15-F_{2t}-IsoP were not different from LPS-only treated cells, they were also not different from untreated media controls ($P = 0.06$; Figure 6.5c). Production of IL10 (74 pg/mL) was greatest in RAW 264.7 cells treated with both LPS and 15-F_{2t}-IsoP. These concentrations were greater than untreated media controls (4.82 pg/mL; $P < 0.0001$) and numerically greater than 5 ng/mL LPS concentrations (66 pg/mL; $P = 0.65$; Figure 6.5d). Similarly, the 5 ng/mL LPS + 500 nM 15-F_{2t}-IsoP treatment had greatest mean IL17 concentrations of 446 pg/mL. The mean concentration of IL17 in cells treated with only LPS was less (418 pg/mL; $P = 0.008$) while the mean concentration in untreated media controls was even less still (41 pg/mL; $P < 0.0001$; Figure 6.5e). Concentrations of MCP-1 were 30013 pg/mL in the LPS and IsoP combination treatment, which were greater than every other treatment except LPS only (17655 pg/mL; $P = 0.21$; Figure 6.5f). The production of these cytokines across treatments have been highlighted in Figure 6.5.

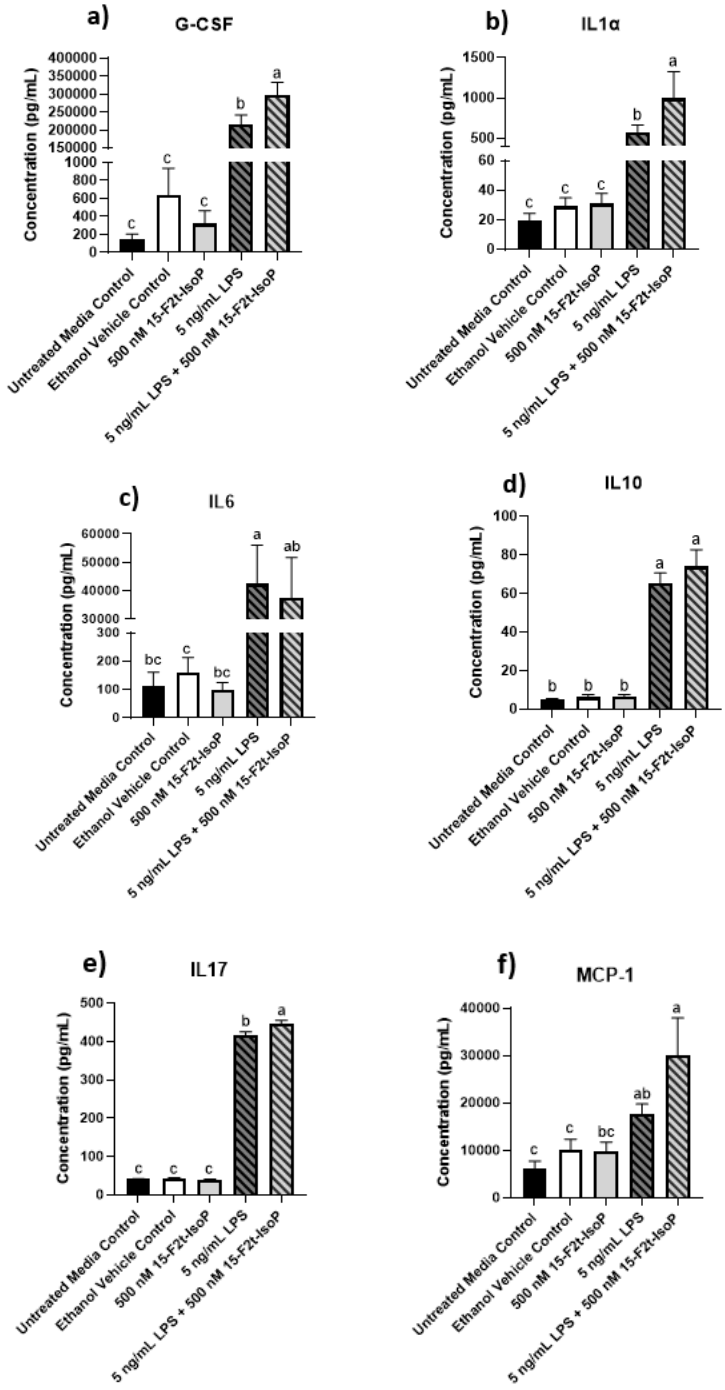

Figure 6.5. Mean cytokine concentrations in RAW 264.7 cells (n=7) challenged with endotoxin and 15-F_{2t}-isoprostane. (a) granulocyte colony-stimulating factor (G-CSF) (b) interleukin (IL) 1α (c) IL6 (d) IL10 (e) IL17 (f) monocyte chemoattractant protein-1 (MCP-1); Statistical analyses included a one-way ANOVA with Tukey's HSD posthoc test. $^{a\text{-}c}$Different superscripts are different ($P < 0.05$); LPS=lipopolysaccharide; IsoP=isoprostane.

For the following cytokines, concentrations were increased in cells treated with 5 ng/mL LPS compared to untreated media controls: INFγ, IL5, IL12p70, IL13, mKC, MIP-1α, and RANTES ($P < 0.05$; Table 6.1). Concentrations of the aforementioned cytokines were also increased in LPS + 15-F_{2t}-IsoP treatments compared to untreated cells ($P < 0.05$); however, concentrations were not less than LPS-treated cells ($P > 0.5$).

DISCUSSION

This study provides evidence that 15-F_{2t}-IsoP shift RAW 264.7 macrophages towards an anti-inflammatory phenotype during LPS challenge. Altering macrophage subtype as inflammation proceeds represents a link between increased IsoP formation during oxidative stress and inflammatory outcomes.

Metabolic parameters, such as ATP production, can be used to help distinguish macrophage phenotypes (Chen et al., 2018). It is well-established that LPS shifts macrophage metabolism from oxidative phosphorylation to aerobic glycolysis, thus preparing proinflammatory cells for host defense. However, while glycolysis produces ATP rapidly, it does so inefficiently (O'Neill and Pearce, 2016). Therefore, LPS-stimulated, proinflammatory macrophages generate less ATP compared to the anti-inflammatory subtype (Chen et al., 2018). Thus, our findings that LPS decreases ATP production without a concurrent increase in cell death agree with several other studies (Mills et al., 2016; Wang et al., 2018; Park et al., 2019). Furthermore, the finding that adding 15-F_{2t}-IsoP to LPS-treated cells returns ATP production to amounts similar to unstimulated macrophages supports that the lipid mediator may promote a metabolic switch back to oxidative phosphorylation. As cells performing oxidative phosphorylation are well-positioned for inflammatory resolution, IsoP may be fostering anti-inflammatory responses during endotoxin challenge (Viola et al., 2019).

The metabolic switch that occurs in macrophages is also associated with altered gene transcription. In particular, *Nos2* and *Il1β* are commonly reported for proinflammatory macrophages while *Il10* and *Arg1* are considered landmark genes for the anti-inflammatory subtype (Oyarce et al., 2021). Indeed, increased *Nos2* expression is paramount in the phenotypic switch towards a proinflammatory state partially because of the subsequent changes in mitochondrial respiration and ROS production (Bailey et al., 2019). In our study, RAW 264.7 cells treated with both LPS and IsoP showed a numerical decrease in *Nos2* expression relative to the LPS treatment. Therefore, by decreasing *Nos2* (and theoretically ROS production), 15-F_{2t}-IsoP may be capable of antioxidant activity.

In addition to the alterations in *Nos2*, the transcriptional signature of cells treated with 15-F_{2t}-IsoP and LPS were suggestive of an anti-inflammatory macrophage phenotype. For instance, there was a relative decrease in *Il1β* with a concurrent relative increase in *Il10* compared to the cells challenged with only LPS. Transcription of *Il1β* is associated with increased inflammation while *Il10* is able to decrease glycolysis, effectively inhibiting proinflammatory macrophage function (Ip et al., 2017; Park et al., 2020). Hence, IsoP may be supporting the anti-inflammatory macrophage subtype by decreasing expression of these genes. We also observed an expected decrease in *Arg1* expression from LPS-treated RAW cells. Interestingly, however, the downregulation was even more pronounced in the LPS and IsoP combination treatment. This is in contrast to previous work demonstrating an increase in *Arg1* expression in alternatively-activated cells (Ji et al., 2016; Gong et al., 2017; Viola et al., 2019). However, macrophage gene expression can be complex, falling outside the traditional polarization dichotomy (Mantovani et al., 2004; Menzies et al., 2010). Thus, similar to conditions found in tissues under oxidative stress, it is likely that the polarization of macrophages in our model is along a spectrum rather

than at either extreme. Further functional and mechanistic characterization of macrophages treated with IsoP are necessary to determine the implications of the gene expression signatures noted herein.

In the face of endotoxin challenge, altered gene regulation leads to the production of cytokines and chemokines meant to appropriately progress and resolve inflammation. Proinflammatory macrophages will secrete proteins that are designed to trigger Th1 responses (e.g., IL6) with the goal of killing pathogens (Mantovani et al., 2004). On the other hand, anti-inflammatory cells will generate cytokines like IL10 that invoke tissue repair and downregulation of inflammatory responses (Proto et al., 2018). Several cytokines associated with pro-resolving functions were upregulated in RAW cells treated with both LPS and 15-F_{2t}-IsoP presently. These included G-CSF, IL10, and IL17. Furthermore, there were numerical decreases in the proinflammatory IL6 compared to LPS-treated cells. Taken together, these data support an anti-inflammatory phenotype predominated when IsoP was added to LPS-treated cells. Indeed, G-CSF is a well-established inducer of alternatively-activated macrophages and IL17 has many protective effects during inflammation, such as initiating a negative feedback loop to downregulate nuclear factor kappa b activity (Joshi et al., 2014; McGeachy et al., 2019). Additionally, IL1α and MCP-1 were also upregulated in LPS + IsoP-treated cells. Although IL1α is commonly associated with proinflammatory effects, it is unclear at this time how the increased concentrations seen with LPS + IsoP treatment may influence inflammatory outcomes (Malik and Kanneganti, 2018). Several studies indicate that MCP-1 potently promotes Th2 responses and can therefore be associated with anti-inflammatory functions (Deshmane et al., 2009). Furthermore, F2-IsoP were positively correlated with MCP-1 expression in chronic obstructive pulmonary disease (Di Stefano et al., 2018). Thus, there may be a mechanism in which elevated IsoP contribute to

increased MCP-1 expression to mitigate oxidative stress and inflammation as the processes progress.

CONCLUSIONS

This study demonstrates a novel physiological role of 15-F_{2t}-IsoP, where this lipid mediator may participate in healing pathways during late-stage inflammation when they are elevated. Thus, this study supports that 15-F_{2t}-IsoP serve as a link between oxidative stress and inflammation. Future studies should be directed towards determining specific mechanisms in which this isomer influences macrophages, such as the receptor they are acting through and downstream signaling pathways. It would also be beneficial to investigate functional consequences of the IsoP-mediated switch to an anti-inflammatory phenotype.

CONCLUSIONS

This dissertation describes a link between IsoP, oxidative stress, inflammation, and dairy cattle health and wellbeing. We demonstrated for the first time that the grossly understudied period of early mammary involution in dairy cattle is accompanied by numerous changes in biomarkers of nutrient metabolism, inflammation, and oxidative stress. Amongst those biomarkers, certain oxylipids may allow early prediction of cows at-risk of developing postpartum diseases in the subsequent lactation. Of particular interest were the IsoP because they were detected at varying magnitudes and times throughout the study period. This may suggest that various isomers hold differential physiological roles during inflammation. We provide evidence that 15-F_{2t}-IsoP does not alter EC viability, apoptosis, RONS production, barrier integrity, or inflammatory gene networks in a model of bovine vascular inflammation. However, this isomer promotes an anti-inflammatory macrophage phenotype during endotoxin challenge.

The in vitro models described herein can help others better understand different stages of inflammation in dairy cows, including those typical of early mammary involution, by defining how 15-F_{2t}-IsoP influences cells critical to orchestrating inflammatory responses. By switching macrophages from the proinflammatory phenotype necessary to combat pathogens to a pro-resolving subtype, IsoP may promote healing in late-stage inflammation when they are elevated. Considering both the in vivo and in vitro data, IsoP may play a role in restoring mammary tissue homeostasis during times of inflammation, such as early mammary involution and coliform mastitis.

Our findings defined new gaps in our knowledge of the role of IsoP on inflammatory processes. First, there is a need to further characterize how IsoP serve as a nexus between oxidative stress, inflammation, and dairy cow health and wellbeing. For instance, can oxylipids measured at early

dry-off predict specific postpartum diseases? Enrolling more animals from varying geographic regions and dairying styles would be necessary to answer this question. If 15-F_{2t}-IsoP did not alter EC viability, apoptosis, RONS production, barrier integrity, or inflammatory gene expression, how does this isomer influence these cells? Advanced modeling may unveil novel effects in bovine EC. Furthermore, to fully understand their role during inflammation, the mechanisms by which IsoP are involved in altering macrophage phenotype must be elucidated. Thus, future work should focus on defining receptor interactions, downstream signaling pathways, and functional consequences of phenotypic switch in these cells.

REFERENCES

Abdelli, A., D. Raboisson, R. Kaidi, B. Ibrahim, A. Kalem, and M. Iguer-Ouada. 2017. Elevated non-esterified fatty acid and beta-hydroxybutyrate in transition dairy cows and their association with reproductive performance and disorders: A meta-analysis. Theriogenology 93:99–104. doi: 10.1016/j.theriogenology.2017.01.030.

Abuelo, A., J. Hernández, J. L. Benedito, and C. Castillo. 2013. Oxidative stress index (OSi) as a new tool to assess redox status in dairy cattle during the transition period. Animal 7:1374–1378. doi: 10.1017/S1751731113000396.

Abuelo, A., J. Hernández, J. L. Benedito, and C. Castillo. 2014. The importance of the oxidative status of dairy cattle in the periparturient period: Revisiting antioxidant supplementation. J. Anim. Physiol. Anim. Nutr. 99:1003–1016. doi: 10.1111/jpn.12273.

Akers, R. M., and S. C. Nickerson. 2011. Mastitis and its impact on structure and function in the ruminant mammary gland. J. Mam-mary Gland Biol. Neoplasia 16:275–289. doi: 10.1007/s10911-011-9231-3.

Altmann, R., M. Hausmann, T. Spöttl, M. Gruber, A. W. Bull, K. Menzel, D. Vogl, H. Herfarth, J. Schölmerich, W. Falk, and G. Rogler. 2007. 13-Oxo-ODE is an endogenous ligand for PPARγ in human colonic epithelial cells. Biochem. Pharmacol. 74:612–622. doi: 10.1016/j.bcp.2007.05.027.

Arslan, F., M. B. Smeets, B. Buttari, E. Profumo, R. Rigano, L. Akeroyd, E. Kara, L. Timmers, J. P. Sluijter, B. van Middelaar, K. den Ouden, G. Pasterkamp, S. K. Lim, and D. P. de Kleijn. 2013. Lack of haptoglobin results in unbalanced VEGFα/angiopoietin-1 expression, intramural hemorrhage and impaired wound healing after myocardial infarction. J. Mol. Cell. Cardiol. 56:116–128. doi: 10.1016/j.yjmcc.2012.12.012.

Aslam, M., and W. B. Tucker. 1998. Influence of intramammary infusion of calcium on the calcium status of periparturient lactating dairy cows. J. Dairy Sci. 81:1883–1888. doi: 10.3168/jds.S0022-0302(98)75759-5.

Aszyk, J., J. Kot, Y. Tkachenko, M. Woźniak, A. Bogucka-Kocka, and A. Kot-Wasik. 2017. Novel liquid chromatography method based on linear weighted regression for the fast determination of isoprostane isomers in plasma samples using sensitive tandem mass spectrometry detection. J. Chromatogr. B 1051:17–23. doi: 10.1016/j.jchromb.2017.02.021.

Atabai, K., D. Sheppard, and Z. Werb. 2007. Roles of the innate immune system in mammary gland remodeling during involution. J. Mammary Gland Biol. Neoplasia 12:37–45. doi: 10.1007/s10911-007-9036-6.

Audoly, L. P., B. Rocca, J. E. Fabre, B. H. Koller, D. Thomas, A. L. Loeb, T. M. Coffman, and G. A. Fitzgerald. 2000. Cardiovascular responses to the isoprostanes iPF(2alpha)-III and iPE(2)-

III are mediated via the thromboxane A(2) receptor in vivo. Circulation 101:2833–2840. doi: 10.1161/01.cir.101.24.2833.

Bailey, J. D., M. Diotallevi, T. Nicol, E. McNeill, A. Shaw, S. Chuaiphichai, A. Hale, A. Starr, M. Nandi, E. Stylianou, H. McShane, S. Davis, R. Fischer, B. M. Kessler, J. McCullagh, K. M. Channon, and M. J. Crabtree. 2019. Nitric Oxide Modulates Metabolic Remodeling in Inflammatory Macrophages through TCA Cycle Regulation and Itaconate Accumulation. Cell Rep. 28(1):218-230e7. doi: 10.1016/j.celrep.2019.06.018.

Barden, A., E. Mas, K. D. Croft, M. Phillips, and T. A. Mori. 2014. Minimizing artifactual elevation of lipid peroxidation products (F2-isoprostanes) in plasma during collection and storage. Anal. Biochem. 449:129–131. doi: 10.1016/j.ab.2013.12.030.

Basu, S., and J. Helmersson. 2005. Factors Regulating Isoprostane Formation In Vivo. Antioxid. Redox Signal. 7:221–235. doi: 10.1089/ars.2005.7.221.

Basu, S. Metabolism of 8-iso-prostaglandin F2alpha. 1998. FEBS Lett. 428(1-2):32-6. doi: 10.1016/s0014-5793(98)00481-5.

Bauer, J., A. Ripperger, S. Frantz, S. Ergün, E. Schwedhelm, and R. A. Benndorf. 2014. Pathophysiology of isoprostanes in the cardiovascular system: Implications of isoprostane-mediated thromboxane A2receptor activation. Br. J. Pharmacol. 171:3115–3131. doi: 10.1111/bph.12677.

Bell, A. W. 1995. Regulation of organic nutrient metabolism during transition from late pregnancy to early lactation. J. Anim. Sci. 73:2804–2819.

Benndorf, R. A., E. Schwedhelm, A. Gnann, R. Taheri, G. Kom, M. Didié, A. Steenpass, S. Ergün, and R. H. Böger. 2008. Isoprostanes inhibit vascular endothelial growth factor-induced endothelial cell migration, tube formation, and cardiac vessel sprouting in vitro, as well as angiogenesis in vivo via activation of the thromboxane A(2) receptor: A potential link between oxidative stress and impaired angiogenesis. Circ. Res. 103:1037–1046. doi: 10.1161/CIRCRESAHA.108.184036.

Biomarker Working Group, FDA-NIH. 2016. BEST (Biomarkers, EndpointS, and other Tools) Resource. Food and Drug Administration; National Institutes of Health.

Birukov, K. G., V. N. Bochkov, A. A. Birukova, K. Kawkitinarong, A. Rios, A. Leitner, A. D. Verin, G. M. Bokoch, N. Leitinger, and J. G. Garcia. 2004. Epoxycyclopentenone-containing oxidized phospholipids restore endothelial barrier function via Cdc42 and Rac. Circ Res. 95(9):892-901. doi: 10.1161/01.RES.0000147310.18962.06.

Bodiga, S., S. K. Gruenloh, Y. Gao, V. L. Manthati, N. Dubasi, J. R. Falck, M. Medhora, and E. R. Jacobs. 2010. 20-HETE-induced nitric oxide production in pulmonary artery endothelial cells is mediated by NADPH oxidase, H2O2, and PI3-kinase/Akt. Am. J. Physiol. Lung Cell. Mol. Physiol. 298:L564–L574. doi: 10.1152/ajplung.00298.2009.

Bosviel, R., L. Joumard-Cubizolles, G. Chinetti, D. Bayle, C. Copin, N. Hennuyer, I. Duplan, B. Staels, G. Zanoni, A. Porta, L. Balas, J. M. Galano, C. Oger, A. Mazur, T. Durand, and C. Gladine. 2017. DHA-derived oxylipins, neuroprostanes and protectins, differentially and dose-dependently modulate the inflammatory response in human macrophages: Putative mechanisms through PPAR activation. Free Radic. Biol. Med. 103:146–154. doi: 10.1016/j.freeradbiomed.2016.12.018.

Bougarne, N., B. Weyers, S. J. Desmet, J. Deckers, D. W. Ray, B. Staels B, and K. De Bosscher. 2018. Molecular Actions of PPARalpha in Lipid Metabolism and Inflammation. Endocr Rev. 39(5):760-802. doi: 10.1210/er.2018-00064.

Bradley, A. J., and M. J. Green. 2004. The importance of the nonlactating period in the epidemiology of intramammary infection and strategies for prevention. Vet. Clin. North Am. Food Anim. Pract. 20:547–568. doi: 10.1016/j.cvfa.2004.06.010.

Briskey, D. R., G. R. Wilson, R. G. Fassett, and J. S. Coombes. 2014. Optimized method for quantification of total F2-isoprostanes using gas chromatography–tandem mass spectrometry. J. Pharm. Biomed. Anal. 90:161–166. doi: 10.1016/j.jpba.2013.11.028.

Brault, S. A. K. Martinez-Bermudez, A. M. Marrache, F. Gobeil Jr., X. Hou, M. Beauchamp, C. Quiniou, G. Almazan, C. Lachance, J. Roberts 2nd, D. R. Varma, and S. Chemtob. 2003. Selective neuromicrovascular endothelial cell death by 8-Iso-prostaglandin F2alpha: possible role in ischemic brain injury. Stroke. 34(3):776-82. doi: 10.1161/01.STR.0000055763.76479.E6.

Brooks, J. D., E. S. Musiek, T. R. Koestner, J. N. Stankowski, J. R. Howard, E. M. Brunoldi, A. Porta, G. Zanoni, G. Vidari, J. D. Morrow, G. L. Milne, and B. McLaughlin. 2011. The fatty acid oxidation product 15-A3t-Isoprostane is a potent inhibitor of NFκB transcription and macrophage transformation. J. Neurochem. 119:604–616. doi: 10.1111/j.1471-4159.2011.07422.x.

Brscic, M., G. Cozzi, I. Lora, A. L. Stefani, B. Contiero, L. Ravarotto, and F. Gottardo. 2015. Short communication: Reference limits for blood analytes in Holstein late-pregnant heifers and dry cows: Effects of parity, days relative to calving, and season. J. Dairy Sci. 98:7886–7892. doi: 10.3168/jds.2015-9345.

Buczynski, M. W., D. S. Dumlao, and E. A. Dennis. 2009. Thematic Review Series: Proteomics. An integrated omics analysis of eicosanoid biology. J. Lipid Res. 50:1015–1038. doi: 10.1194/jlr .R900004 -JLR200.

Butterfield, D. A., J. Drake, C. Pocernich, and A. Castegna. 2001. Evidence of oxidative damage in Alzheimer's disease brain: central role for amyloid beta-peptide. Trends Mol. Med. 7: 548-554. doi: 10.1016/s1471-4914(01)02173-6.

Calder, P. C. 2009. Polyunsaturated fatty acids and inflammation: New twists in an old tale. Biochimie 91:791–795. doi: 10.1016/j.biochi.2009.01.008.

Canton, M., R. Sanchez-Rodriguez, I. Spera, F. C. Venegas, M. Favia, A. Viola, and A. Castegna. 2021. Reactive Oxygen Species in Macrophages: Sources and Targets. Front Immunol. 12: 734229. doi: 10.3389/fimmu.2021.734229.

Capra, V., M. Busnelli, A. Perenna, M. Ambrosio, M. R. Accomazzo, C. Galés, B. Chini, and G. E. Rovati. 2013. Full and Partial Agonists of Thromboxane Prostanoid Receptor Unveil Fine Tuning of Receptor Superactive Conformation and G Protein Activation. PLoS ONE 8, e60475. doi: 10.1371/journal.pone.0060475.

Capra V., M. Back, D. J. Angiolillo, M. Cattaneo, and K. S. Sakariassen. 2014. Impact of vascular thromboxane prostanoid receptor activation on hemostasis, thrombosis, oxidative stress, and inflammation. J Thromb Haemost. 12(2):126-37. doi: 10.1111/jth.12472.

Celi, P. 2010. Biomarkers of oxidative stress in ruminant medicine. Immunopharmacol. Immunotoxicol. 33:233–240. doi: 10.3109/08923973.2010.514917.

Chen, W., H. Sandoval, J. Z. Kubiak, X. C. Li, R. M. Ghobrial, and M. Kloc. 2018. The phenotype of peritoneal mouse macrophages depends on the mitochondria and ATP/ADP homeostasis. Cell Immunol. 324:1-7. doi: 10.1016/j.cellimm.2017.11.003.

Chen, H., Y. Avital, Y. Bruchim, I. Aroch, and G. Segev. 2019. Urinary heat shock protein-72: A novel marker of acute kidney injury and chronic kidney disease in cats. Veter- J. 243:77–81. doi: 10.1016/j.tvjl.2018.11.015.

Contreras, G. A., C. Strieder-Barboza, and W. Raphael. 2017. Adipose tissue lipolysis and remodeling during the transition period of dairy cows. J. Anim. Sci. Biotechnol. 8:1–12. doi: 10.1186/s40104-017-0174-4.

Courtois, A., G. Makrygiannis, J. P. Cheramy-Bien, A. Purnelle, B. Pirotte, J. M. Dogne, J. Hanson, J. O. Defraigne, P. Drion, and N. Sakalihasan. 2018. Therapeutic applications of prostaglandins and thromboxane A2 inhibitors in abdominal aortic aneurysms. Curr. Drug Targets. doi: 10 .2174/1389450119666171227224314.

Cranshaw, J. H., T. W. Evans, and J. A. Mitchell. 2001. Characterization of the effects of isoprostanes on platelet aggregation in human whole blood. Br. J. Pharmacol. 132:1699–1706. doi: 10.1038/sj.bjp.0704019.

Creamer, B. A., K. Sakamoto, J. W. Schmidt, A. A. Triplett, R. Moriggl, and K. U. Wagner. 2010. Stat5 promotes survival of mammary epithelial cells through transcriptional activation of a distinct promoter in Akt1. Mol. Cell. Biol. 30:2957–2970. doi: 10 .1128/MCB.00851-09.

Czerska, M., K. Mikolajewska, M. Zielinski, J. Gromadzinska, and W. Wasowicz. 2015. Today's oxidative stress markers. Med. Pr. 66(3):393-405. doi: 10.13075/mp.5893.00137.

Dahl, J. H., and R. B. van Breemen. 2010. Rapid quantitative analysis of 8-iso-prostaglandin-F(2alpha) using liquid chromatography-tandem mass spectrometry and comparison with an enzyme immunoassay method. Anal. Biochem. 404:211–610. doi: 10.1016/j.ab.2010.05.023.

Dalal, P. J., W. A. Muller, and D. P. Sullivan. 2020. Endothelial cell calcium signaling during barrier function and inflammation. Am. J. Pathology. 190(3):535-542. doi: 10.1016/j.ajpath.2019.11.004.

Dalle-Donne, I., R. Rossi, R. Colombo, D. Giustarini, and A. Milzani. 2006. Biomarkers of Oxidative Damage in Human Disease. Clin. Chem. 52:601–623. doi: 10.1373/clinchem.2005.061408.

Dennis, E. A., and P. C. Norris. 2015. Eicosanoid storm in infection and inflammation. Nat. Rev. Immunol. 15:511–523. doi: 10.1038/nri3859.

Deshmane, S. L., S. Kremlev, S. Amini, and B. E. Sawaya. 2009. Monocyte chemoattractant protein-1 (MCP-1): an overview. J Interferon Cytokine Res. 29(6):313-326. doi: 10.1089/jir.2008.0027.

Di Stefano, A., T. Coccini, E. Roda, C. Signorini, B. Balbi, G. Brunetti, P. Ceriana. 2018. Blood MCP-1 levels are increased in chronic obstructive pulmonary disease patients with prevalent emphysema. Int J Chron Obstruct Pulmon Dis. 13:1691-1700. doi: 10.2147/COPD.S159915.

Downey, L. A., T. Simpson, J. Timmer, K. Nolidin, K. Croft, K. A. Wesnes, A. Scholey, S. Deleuil, and C. Stough. 2018. Impaired verbal episodic memory in healthy older adults is marked by increased F 2 -Isoprostanes. Prostaglandins Leukot. Essent. Fat. Acids 129:32–37. doi: 10.1016/j.plefa.2018.02.001.

Duflot, T., T. Pereira, C. Roche, M. Iacob, P. Cardinael, N. E. Hamza, C. Thuillez, P. Compagnon, R. Joannides, F. Lamoureux, and J. Bellien. 2017. A sensitive LC-MS/MS method for the quantification of regioisomers of epoxyeicosatrienoic and dihydroxyeicosatrienoic acids in human plasma during endothelial stimulation. Anal. Bioanal. Chem. 409:1845–1855. doi: 10.1007/s00216-016-0129-1.

Eckersall, P. D., and R. Bell. 2010. Acute phase proteins: Biomarkers of infection and inflammation in veterinary medicine. Vet. J. 185:23–27. doi: 10.1016/j.tvjl.2010.04.009.

Else, P. L., and E. Kraffe. 2015. Docosahexaenoic and arachidonic acid peroxidation: It's a within molecule cascade. Biochim. Biophys. Acta 1848:417–421. doi: 10.1016/j.bbamem.2014.10.039.

Erdmann, S., E. Mohr, M. Derno, A. Tuchscherer, C. Schäff, S. Börner, U. Kautzsch, B. Kuhla, H. M. Hammon, and M. Röntgen. 2018. Indices of heart rate variability as potential early markers of metabolic stress and compromised regulatory capacity in dried-off high-yielding dairy cows. Animal 12:1451–1461. doi: 10.1017/S1751731117002725.

Esposito, G., P. C. Irons, E. C. Webb, and A. Chapwanya. 2014. Interactions between negative energy balance, metabolic diseases, uterine health and immune response in transition dairy cows. Anim. Reprod. Sci. 144:60–71. doi: 10.1016/j.anireprosci.2013.11.007.

Farahani, T. A., H. Amanlou, and M. Kazemi-Bonchenari. 2017. Effects of shortening the close-up period length coupled with increased supply of metabolizable protein on performance and metabolic status of multiparous Holstein cows. J. Dairy Sci. 100:6199– 6217. doi: 10.3168/jds.2016-12263.

Fenga, C., S. Gangemi, M. Teodoro, V. Rapisarda, K. Golokhvast, A. O. Docea, A. M. Tsatsakis, and C. Costa. 2017. 8-Hydroxydeoxyguanosine as a biomarker of oxidative DNA damage in workers exposed to low-dose benzene. Toxicol. Rep. 4:291–295. doi: 10.1016/j.toxrep.2017.05.008.

Ferreiro-Vera, C., J. M. Mata-Granados, F. Priego-Capote, J. M. Quesada-Gomez, and M. D. Luque de Castro. 2011. Automated targeting analysis of eicosanoid inflammation biomarkers in human serum and in the exometabolome of stem cells by SPE-LC-MS/MS. Anal. Bioanal. Chem. 399:1093–1103. doi: 10.1007/s00216-010-4400-6.

Fischer, R., A. Konkel, H. Mehling, K. Blossey, A. Gapelyuk, N. Wessel, C. von Schacky, R. Dechend, D. N. Muller, M. Rothe, F. C. Luft, K. Weylandt, and W. H. Schunck. 2014. Dietary omega-3 fatty acids modulate the eicosanoid profile in man primarily via the CYP-epoxygenase pathway. J. Lipid Res. 55:1150–1164. doi: 10.1194/jlr.M047357.

Freeman, L. M., J. E. Rush, P. E. Milbury, and J. B. Blumberg. 2005. Antioxidant Status and Biomarkers of Oxidative Stress in Dogs with Congestive Heart Failure. J. Vet. Intern. Med. 19:537–541. doi: 10.1892/0891-6640(2005)19[537:asaboo]2.0.co;2.

Friedrichs, B., M. Toborek, B. Hennig, L. Heinevetter, C. Müller, and R. Brigelius-Flohé. 1999. 13-HPODE and 13-HODE modulate cytokine induced expression of endothelial cell adhesion molecules differently. Biofactors 9:61–72.

Friend, T. H., C. E. Polan, F. C. Gwazdauskas, and C. W. Heald. 1977. Adrenal glucocorticoid response to exogenous adrenocorticotropin mediated by density and social disruption in lactating cows. J. Dairy Sci. 60:1958–1963. doi: 10.3168/jds.S0022-0302(77)84128-3.

Frijhoff, J., P. G. Winyard, N. Zarkovic, S. S. Davies, R. Stocker, D. Cheng, A. R. Knight, E. L. Taylor, J. Oettrich, T. Ruskovska, A. C. Gasparovic, A. Cuadrado, D. Weber, H. E. Poulsen, T. Grune, H. H. Schmidt, P. Ghezzi. 2015. Clinical Relevance of Biomarkers of Oxidative Stress. Antioxid. Redox Signal. 23: 1144–1170. doi: 10.1089/ars.2015.6317.

Gabbs, M., S. Leng, J. G. Devassy, M. Monirujjaman, and H. M. Aukema. 2015. Advances in our understanding of oxylipins derived from dietary PUFAs. Adv. Nutr. 6:513–540. doi: 10.3945/an.114.007732.

Galano, J. M., Y. Y. Lee, C. Oger, C. Vigor, J. Vercauteren, T. Durand, M. Giera, and J. C. Lee. 2017. Isoprostanes, neuroprostanes and phytoprostanes: An overview of 25years of research in chemistry and biology. Prog Lipid Res. 68:83-108. doi: 10.1016/j.plipres.2017.09.004.

Galano, J. M., J. Roy, T. Durand, J. C. Lee, J. Y. Le Guennec, C. Oger, and M. Demion. 2018. Biological activities of non-enzymatic oxygenated metabolites of polyunsaturated fatty acids (NEO-PUFAs) derived from EPA and DHA: New anti-arrhythmic compounds? Mol. Asp. Med. 64:161–168. doi: 10.1016/j.mam.2018.03.003.

Gan, S. D., and K. R. Patel. 2013. Enzyme Immunoassay and Enzyme-Linked Immunosorbent Assay. J. Investig. Dermatol. 133:1–3. doi: 10.1038/jid.2013.287.

Gaschler, M. M., and B. R. Stockwell. 2017. Lipid peroxidation in cell death. Biochem. Biophys. Res. Commun. 482(3):419-25. doi: 10.1016/j.bbrc.2016.10.086.

Golia, E., G. Limongelli, F. Natale, F. Fimiani, V. Maddaloni, I. Pariggiano, R. Bianchi, M. Crisci, L. D'Acierno, R. Giordano, G. Di Palma, M. Conte, P. Golino, M. G. Russo, R. Calabro, and P. Calabro. 2014. Inflammation and cardiovascular disease: from pathogenesis to therapeutic target. Curr Atheroscler Rep. 16(9):435. doi: 10.1007/s11883-014-0435-z.

Gong, M., X. Zhuo, and A. Ma. 2017. STAT6 Upregulation Promotes M2 Macrophage Polarization to Suppress Atherosclerosis. Med Sci Monit Basic Res. 23:240-249. doi: 10.12659/msmbr.904014.

Gonzalez-Luis, G., F. Perez-Vizcaino, C. E. Blanco, E. Villamor. 2010. Age-related changes in isoprostane-mediated relaxation of piglet blood vessels. Front. Biosci (Elite Ed) 2:369-379. doi: 10.2741/e97.

Gouon-Evans, V., M. E. Rothenberg, and J. W. Pollard. 2000. Post-natal mammary gland development requires macrophages and eosinophils. Development 127:2269–2282.

Halliwell, B., and J. M. C. Gutteridge. 2006. Free Radicals in Biology and Medicine, 4th ed.; Oxford University Press: Oxford, UK.

Hamabata, T., T. Nakamura, S. Masuko, S. Maeda, and T. Murata. 2018. Production of lipid mediators across different disease stages of dextran sulfate sodium-induced colitis in mice. J. Lipid Res. doi: 10.1194/jlr.M079095.

Han, Y., H. Zhao, H. Tang, X. Li, J. Tan, Q. Zeng, and C. Sun. 2013. 20-Hydroxyeicosatetraenoic acid mediates isolated heart ischemia/reperfusion injury by increasing NADPH oxidase-derived reactive oxygen species production. Circ. J. 77:1807–1816. doi: 10.1253/circj.CJ-12-1211.

Han van der Kolk, J. H., J. J. Gross, V. Gerber, and R. M. Bruckmaier. 2017. Disturbed bovine mitochondrial lipid metabolism: A review. Vet. Q. 37:262–273. doi: 10.1080/01652176.2017.1354561.

Hannibal, K. E., and M. D. Bishop. 2014. Chronic stress, cortisol dysfunction, and pain: A psychoneuroendocrine rationale for stress management in pain rehabilitation. Phys. Ther. 94:1816–1825. doi: 10.2522/ptj.20130597.

Hart, C. M., R. J. Karman, T. L. Blackburn, M. P. Gupta, J. G. N. Garcia, and E. R. Mohler. 1998. Role of 8-epi PGF2α, 8-isoprostane, in H2O2-induced derangements of pulmonary artery endothelial cell barrier function. Prostaglandins, Leukotrienes and Essential Fatty Acids. 58(1):9-16. doi: 10.1016/S0952-3278(98)90124-7.

Heemskerk, M. M., H. K. Dharuri, S. A. van den Berg, H. S. Jonasdot-tir, D. P. Kloos, M. Giera, K. W. van Dijk, and V. van Harmelen. 2014. Prolonged niacin treatment leads to increased adipose tissue PUFA synthesis and anti-inflammatory lipid and oxylipin plasma profile. J. Lipid Res. 55:2532–2540. doi: 10.1194/jlr.M051938.

Hellemans J., G. Mortier, A. De Paepe, F. Speleman, and J. Vandesompele. 2007. qBase relative quantification framework and software for management and automated analysis of real-time quantitative PCR data. Genome Biol. 8(2):R19. doi: 10.1186/gb-2007-8-2-r19.

Hinchcliff, K. W., G. A. Reinhart, R. DiSilvestro, A. Reynolds, A. Blostein-Fujii, and R. A. Swenson. 2000. Oxidant stress in sled dogs subjected to repetitive endurance exercise. Am. J. Vet. Res. 61:512–517. doi: 10.2460/ajvr.2000.61.512.

Honkanen, A. M., J. M. Griinari, A. Vanhatalo, S. Ahvenjarvi, V. Toivonen, and K. J. Shingfield. 2012. Characterization of the disappearance and formation of biohydrogenation intermediates during incubations of linoleic acid with rumen fluid in vitro. J. Dairy Sci. 95:1376–1394. doi: 10.3168/jds.2011-4390.

Hughes, K., J. A. Wickenden, J. E. Allen, and C. J. Watson. 2012. Conditional deletion of Stat3 in mammary epithelium impairs the acute phase response and modulates immune cell numbers during post-lactational regression. J. Pathol. 227:106–117. doi: 10.1002/path.3961.

Hydbring, E., A. Madej, E. MacDonald, G. Drugge-Boholm, B. Berglund, and K. Olsson. 1999. Hormonal changes during parturition in heifers and goats are related to the phases and severity of labour. J. Endocrinol. 160:75–85.

Il'Yasova, D., J. D. Morrow, A. Ivanova, and L. E. Wagenknecht. 2004. Epidemiological marker for oxidant status: Comparison of the ELISA and the gas chromatography/mass spectrometry assay for urine 2,3-dinor-5,6-dihydro-15-F2t-isoprostane. Ann. Epidemiol. 14:793–797. doi: 10.1016/j.annepidem.2004.03.003.

Infantino, V., V. Iacobazzi, F. Palmieri, and A. Menga. 2013. ATP-citrate lyase is essential for macrophage inflammatory response. Biochem Biophys Res Commun. 440(1):105-111. doi: 10.1016/j.bbrc.2013.09.037.

Ip, W. K. E., N. Hoshi, D. S. Shouval, S. Snapper, and R. Medzhitov. 2017. Anti-inflammatory effect of IL-10 mediated by metabolic reprogramming of macrophages. Science. 356(6337):513-519. doi: 10.1126/science.aal3535.

Janicka, M., Á. Kot-Wasik, J. Kot, and J. Namieśnik. 2010. Isoprostanes-Biomarkers of Lipid Peroxidation: Their Utility in Evaluating Oxidative Stress and Analysis. Int. J. Mol. Sci. 11:4631–4659. doi: 10.3390/ijms11114631.

Janicka, M., Á. Kot-Wasik, J. Paradziej-Łukowicz, G. Sularz-Peszyńska, A. Bartoszek, and J. Namieśnik. 2013. LC-MS/MS Determination of Isoprostanes in Plasma Samples Collected from Mice Exposed to Doxorubicin or Tert-Butyl Hydroperoxide. Int. J. Mol. Sci. 14:6157–6169. doi: 10.3390/ijms14036157.

Ji, J., D. Shu, M. Zheng, J. Wang, C. Luo, Y. Wang, F. Guo, X. Zou, X. Lv, Y. Li, T. Liu, and H. Qu. 2016. Microbial metabolite butyrate facilitates M2 macrophage polarization and function. Sci Rep. 6:24838. doi: 10.1038/srep24838.

Johnson, D. R., and E. A. Decker. 2015. The Role of Oxygen in Lipid Oxidation Reactions: A Review. Annu. Rev. Food Sci. Technol. 6:171–190. doi: 10.1146/annurev-food-022814-015532.

Joshi, S., A. R. Singh, M. Zulcic, L. Bao, K. Messer, T. Ideker, J. Dutkowski, and D. L. Durden. 2014. Rac2 controls tumor growth, metastasis and M1-M2 macrophage differentiation in vivo. PLoS One. 9(4):e95893. doi: 10.1371/journal.pone.0095893.

Kan, X., G. Hu, B. Huang, W. Guo, Y. Huang, Y. Chen, P. Xu, X. Cai, S. Fu, and J. Liu. 2021. Pedunculoside protects against LPS-induced mastitis in mice by inhibiting inflammation and maintaining the integrity of blood-milk barrier. Aging (Albany NY). 13(15):19460-74. doi: 10.18632/aging.203357.

Kelly, B., L. A. O'Neill. 2015. Metabolic reprogramming in macrophages and dendritic cells in innate immunity. Cell Res. 25(7):771-784. doi: 10.1038/cr.2015.68.

Klawitter, J., M. Haschke, T. Shokati, J. Klawitter, and U. Christians. 2011. Quantification of 15-F2t-isoprostane in human plasma and urine: Results from enzyme-linked immunoassay and liquid chromatography/tandem mass spectrometry cannot be compared. Rapid Commun. Mass Spectrom. 25:463–810. doi: 10.1002/rcm.4871.

Kromer, B. M., and J. R. Tippins. 1996. Coronary artery constriction by the isoprostane 8-epi prostaglandin F2α. Br. J. Pharmacol. 119:1276–1280. doi: 10.1111/j.1476-5381.1996.tb16033.x.

Kuhla, B., C. C. Metges, and H. M. Hammon. 2016. Endogenous and dietary lipids influencing feed intake and energy metabolism of periparturient dairy cows. Domest. Anim. Endocrinol. 56(Suppl.):S2– S10. doi: 10.1016/j.domaniend.2015.12.002.

Kuhn, H., M. Walther, and R. J. Kuban. 2002. Mammalian arachidonate 15-lipoxygenases structure, function, and biological implications. Prostaglandins Other Lipid Mediat. 68–69:263–290. doi: 10.1016/S0090-6980(02)00035-7.

Kuhn, M. J., V. Mavangira, J. C. Gandy, C. Zhang, A. D. Jones, and L. M. Sordillo. 2017. Differences in the oxylipid profiles of bovine milk and plasma at different stages of lactation. J. Agric. Food Chem. 65:4980–4988. doi: 10.1021/acs.jafc.7b01602.

Kuhn, M. J., V. Mavangira, J. C. Gandy, and L. Sordillo. 2018. Production of 15-F-isoprostane as an assessment of oxidative stress in dairy cows at different stages of lactation. J. Dairy Sci. 101:9287–9295. doi: 10.3168/jds.2018-14669.

Kumar, A., E. Kingdon, and J. Norman. 2005. The isoprostane 8-iso-PGF 2α suppresses monocyte adhesion to human microvascular endothelial cells via two independent mechanisms. FASEB J. 19:1–24. doi: 10.1096/fj.03-1364fje.

Kushibiki, S., K. Hodate, H. Shingu, Y. Obara, E. Touno, M. Shinoda, and Y. Yokomizo. 2003. Metabolic and lactational responses during recombinant bovine tumor necrosis factor-α treatment in lactating cows. J. Dairy Sci. 86:819–827. doi: 10.3168/ jds.S0022-0302(03)73664-9.

Lacetera, N., D. Scalia, O. Franci, U. Bernabucci, B. Ronchi, and A. Nardone. 2004. Short communication: Effects of nonesterified fatty acids on lymphocyte function in dairy heifers. J. Dairy Sci. 87:1012–1014. doi: 10.3168/jds.S0022-0302(04)73246-4.

Lawson, J. A., J. Rokach, and G. A. FitzGerald. 1999. Isoprostanes: Formation, analysis and use as indices of lipid peroxidation in vivo. J. Biol. Chem. 274:24441–24444. doi: 10.1074/jbc.274.35.24441.

Lebda, M. A., I. H. Elmassry, N. M. Taha, and M. S. Elfeky. 2022. Nanocurcumin alleviates inflammation and oxidative stress in LPS-induced mastitis via activation of Nrf2 and suppressing TLR4-mediated NF-kappaB and HMGB1 signaling pathways in rats. Environ Sci Pollut Res Int. 29(6):8294-305. doi: 10.1007/s11356-021-16309-9.

Locatelli, A., P. Sartorelli, F. Agnes, G. P. Bondiolotti, and G. B. Picotti. 1989. Adrenal response in the calf to repeated simulated transport. Br. Vet. J. 145:517–522. doi: 10.1016/0007-1935(89)90112-7.

Lushchak, V. I. 2014. Free radicals, reactive oxygen species, oxidative stress and its classification. Chem. Interact. 224:164–175. doi: 10.1016/j.cbi.2014.10.016.

Lykkesfeldt, J., and O. Svendsen. 2007. Oxidants and antioxidants in disease: oxidative stress in farm animals. Vet. J. 173:502-511. doi: 10.1016/j.tvjl.2006.06.005.

Lynch, S. M., J. D. Morrow, L. J. Roberts, and B. Frei. 1994. Formation of non-cyclooxygenase-derived prostanoids (F2-isoprostanes) in plasma and low density lipoprotein exposed to oxidative stress in vitro. J. Clin. Investig. 93:998–1004. doi: 10.1172/JCI117107.

Ma, Y., L. Zhao, M. Gao, and J. J. Loor. 2018. Tea polyphenols protect bovine mammary epithelial cells from hydrogen peroxide-induced oxidative damage in vitro. J. Anim. Sci. 96(10):4159-72. doi: 10.1093/jas/sky278.

Majolee, J., I. Kovacevic, and P. L. Hordijk. 2019. Ubiquitin-based modifications in endothelial cell-cell contact and inflammation. J. Cell Sci. 132(17). doi: 10.1242/jcs.227728.

Malik, A., and T. D. Kanneganti. 2018. Function and regulation of IL-1alpha in inflammatory diseases and cancer. Immunol Rev. 281(1):124-137. doi: 10.1111/imr.12615.

Malko, P., and L. H. Jiang. 2020. TRPM2 channel-mediated cell death: An important mechanism linking oxidative stress-inducing pathological factors to associated pathological conditions. Redox Biol. 37. doi: 10175510.1016/j.redox.2020.101755.

Mantovani, A., A. Sica, S. Sozzani, P. Allavena, A. Vecchi, and M. Locati. 2004. The chemokine system in diverse forms of macrophage activation and polarization. Trends Immunol. 25(12): 677-686. doi: 10.1016/j.it.2004.09.015.

Marshak, R. R. 1956. Studies on parturient paresis in dairy cows with particular reference to udder insufflation. J. Am. Vet. Med. Assoc. 128:423–431.

Mattmiller, S. A., B. A. Carlson, J. C. Gandy, and L. M. Sordillo. 2014. Reduced macrophage selenoprotein expression alters oxidized lipid metabolite biosynthesis from arachidonic and linoleic acid. J. Nutr. Biochem. 25:647–654. doi: 10.1016/j .jnutbio.2014.02.005.

Mavangira, V., J. C. Gandy, C. Zhang, V. E. Ryman, A. Daniel Jones, and L. M. Sordillo. 2015. Polyunsaturated fatty acids influence differential biosynthesis of oxylipids and other lipid mediators during bovine coliform mastitis. J. Dairy Sci. 98:6202–6215. doi: 10.3168/jds.2015-9570.

Mavangira, V., M. J. Mangual, J. C. Gandy, and L. M. Sordillo. 2016. 15-F_{2t}-isoprostane concentrations and oxidant status in lactating dairy cattle with acute coliform mastitis. J. Vet. Intern. Med. 30:339–347. doi: 10.1111/jvim.13793.

Mavangira, V., and L. M. Sordillo. 2018. Role of lipid mediators in the regulation of oxidative stress and inflammatory responses in dairy cattle. Res. Vet. Sci. 116:4–14. doi: 10.1016/j.rvsc.2017.08.002.

Mavangira, V., J. Brown, J. C. Gandy, and L. M. Sordillo. 2020. 20-hydroxyeicosatetraenoic acid alters endothelial cell barrier integrity independent of oxidative stress and cell death. Prostaglandins Other Lipid Mediat. 149:106425. doi: 10.1016/j.prostaglandins.2020.106425.

Mbata, O., N. F. Abo El-Magd, and A. B. El-Remessy. 2017. Obesity, metabolic syndrome and diabetic retinopathy: Beyond hyperglycemia. World J. Diabetes 8:317–329. doi: 10.4239/wjd.v8.i7.317.

McGeachy, M. J., D. J. Cua, and S. L. Gaffen. 2019. The IL-17 Family of Cytokines in Health and Disease. Immunity. 50(4):892-906. doi: 10.1016/j.immuni.2019.03.021.

McMichael, M. A., C. G. Ruaux, W. I. Baltzer, S. C. Kerwin, G. Hosgood, J. M. Steiner, and D. A. Williams. 2006. Concentrations of 15F2tisoprostane in urine of dogs with intervertebral disk disease. Am. J. Vet. Res. 67:1226–1231. doi: 10.2460/ajvr.67.7.1226.

McMichael, M. A. 2007. Oxidative stress, antioxidants, and assessment of oxidative stress in dogs and cats. J. Am. Vet. Med Assoc. 231:714–720. doi: 10.2460/javma.231.5.714.

Menzies, F. M., F. L. Henriquez, J. Alexander, and C. W. Roberts. 2010. Sequential expression of macrophage anti-microbial/inflammatory and wound healing markers following innate, alternative and classical activation. Clin Exp Immunol. 160(3):369-379. doi: 10.1111/j.1365-2249.2009.04086.x.

Miggin, S. M., and B. T. Kinsella. 1998. Expression and tissue distribution of the mRNAs encoding the human thromboxane A2 receptor (TP) alpha and beta isoforms. Biochim. Biophys. Acta 1425:543–559. doi: 10.1016/s0304-4165(98)00109-3.

Mills, E. L., B. Kelly, A. Logan, A. S. H. Costa, M. Varma, C. E. Bryant, P. Tourlomousis, J. H. M. Dabritz, E. Gottlieb, I. Latorre, S. C. Corr, G. McManus, D. Ryan, H. T. Jacobs, M. Szibor, R. J. Xavier, T. Braun, C. Frezza, M. P. Murphy, and L. A. O'Neill. 2016. Succinate Dehydrogenase Supports Metabolic Repurposing of Mitochondria to Drive Inflammatory Macrophages. Cell. 167(2):457-470e13. doi: 10.1016/j.cell.2016.08.064.

Milne, G. L., E. S. Musiek, and J. D. Morrow. 2005. F2-isoprostanes as markers of oxidative stress in vivo: An overview. Biomarkers. 10 (Suppl. 1): S10–S23. doi: 10.1080/13547500500216546.

Milne, G. L., H. Yin, K.D. Hardy, S.S. Davies, and L.J. Roberts 2nd. 2011. Isoprostane generation and function. Chem. Rev. 111:5973–5996. doi: 10.1021/cr200160h.

Milne, G. L., Q. Dai, and L. J. Roberts 2nd. 2015. The isoprostanes--25 years later. Biochim Biophys Acta. 1851(4):433-445. doi: 10.1016/j.bbalip.2014.10.007.

Minuz, P., G. Andrioli, M. Degan, S. Gaino, R. Ortolani, R. Tommasoli, V. Zuliani, A. Lechi, and C. Lechi. 1998. The F2-Isoprostane 8-Epiprostaglandin F2αIncreases Platelet Adhesion and Reduces the Antiadhesive and Antiaggregatory Effects of NO. Arter. Thromb. Vasc. Biol. 18:1248–1256. doi: 10.1161/01.atv.18.8.1248.

Möbert, J., and B. F. Becker, S. Zahler, and E. Gerlach. 1997. Hemodynamic Effects of Isoprostanes (8-Iso-Prostaglandin F2α and E2) in Isolated Guinea Pig Hearts. J. Cardiovasc. Pharmacol. 29:789–794. doi: 10.1097/00005344-199706000-00012.

Moore, K., and L. J. Roberts. 1998. Measurement of Lipid Peroxidation. Free Radic. Res. 28:659–671. doi: 10.3109/10715769809065821.

Morrow, J. D., T. M. Harris, and L. J. Roberts. 1990. Noncyclooxygenase oxidative formation of a series of novel prostaglandins: Analytical ramifications for measurement of eicosanoids. Anal. Biochem. 184:1–10. doi: 10.1016/0003-2697(90)90002-q.

Morrow, J. D., J. A. Awad, H. J. Boss, I. A. Blair, and L. J. Roberts. 1992. Non-cyclooxygenase-derived prostanoids (F2-isoprostanes) are formed in situ on phospholipids. Proc. Natl. Acad. Sci. USA 89:10721–10725. doi: 10.1073/pnas.89.22.10721.

Morrow, J. D., T. Minton, C. R. Mukundan, M. D. Campbell, W. Zackert, V. C. Daniel, K. F. Badr, I. Blair, and L. J. R. Ii. 1994. Free radical-induced generation of isoprostanes in vivo. Evidence for the formation of D-ring and E-ring isoprostanes. J. Biol. Chem. 269:4317–4326.

Morrow, J. D., and L. J. Roberts. 2002. The Isoprostanes. Am. J. Respir. Crit. Care Med. 166:S25–S30. doi: 10.1164/rccm.2206011.

Muck, S., A. A. Weber, J. Meyer-Kirchrath, and K. Schrör. 1997. The bovine thromboxane A2 receptor: Molecular cloning, expression, and functional characterization. Naunyn Schmiedebergs Arch. Pharmacol. 357:10–16. doi: 10.1007/pl00005132.

Mueller, M. J. 2010. Isoprostane nomenclature: Inherent problems may cause setbacks for the development of the isoprostanoid field. Prostaglandins Leukot. Essent. Fat. Acids 82:71–81. doi: 10.1016/j.plefa.2009.11.007.

Musiek, E. S., L. Gao, G. L. Milne, W. Han, M. B. Everhart, D. Wang, M. G.Backlund, R. N. Dubois, G. Zanoni, G. Vidari, T. S. Blackwell, and J. D. Morrow. 2005. Cyclopentenone Isoprostanes Inhibit the Inflammatory Response in Macrophages. J. Biol. Chem. 280:35562–35570. doi: 10.1074/jbc.M504785200.

Musiek, E. S., B. McLaughlin, and J. D. Morrow. 2007. Electrophilic cyclopentenone isoprostanes in neurodegeneration. J. Mol. Neurosci. 33(1):80-6. doi: 10.1007/s12031-007-0042-3.

Noschka, E., S. R. Werre, M. V. Crisman, C. D. Thatcher, G. L. Milne, and L. A. Dahlgren. 2011. Implications of urine F2-isoprostane metabolite concentration in horses with colic and its potential use as a predictor for surgical intervention. Equine Vet. J. 43:34–41. doi: 10.1111/j.2042-3306.2011.00384.x.

Nourooz-Zadeh, J., B. Halliwell, and E. Änggård. 1997. Evidence for the Formation of F3-Isoprostanes during Peroxidation of Eicosapentaenoic Acid. Biochem. Biophys. Res. Commun. 236:467–472. doi: 10.1006/bbrc.1997.6869.

Nourooz-Zadeh, J., E. H. Liu, E. Änggård, and B. Halliwell. 1998. F4-Isoprostanes: A Novel Class of Prostanoids Formed during Peroxidation of Docosahexaenoic Acid (DHA). Biochem. Biophys. Res. Commun. 242:338–344. doi: 10.1006/bbrc.1997.7883.

O'Neill, L. A., and E. J. Pearce. 2016. Immunometabolism governs dendritic cell and macrophage function. J Exp Med. 213(1):15-23. doi: 10.1084/jem.20151570.

Ogletree, M. L., and G. T. Allen. 1992. Interspecies differences in thromboxane receptors: Studies with thromboxane receptor antagonists in rat and guinea pig smooth muscles. J. Pharmacol. Exp. Ther. 260:789–794.

Ohashi, N., and M. Yoshikawa. 2000. Rapid and sensitive quantification of 8-isoprostaglandin F2α in human plasma and urine by liquid chromatography–electrospray ionization mass spectrometry. J. Chromatogr. B Biomed. Sci. Appl. 746:17–24. doi: 10.1016/s0378-4347(00)00201-2.

Ospina, P. A., D. V. Nydam, T. Stokol, and T. R. Overton. 2010. Association between the proportion of sampled transition cows with increased nonesterified fatty acids and beta-hydroxybutyrate and disease incidence, pregnancy rate, and milk production at the herd level. J. Dairy Sci. 93:3595–3601. doi: 10.3168/ jds.2010-3074.

Oyarce, C., A. Vizcaino-Castro, S. Chen, A. Boerma, and T. Daemen. 2021. Re-polarization of immunosuppressive macrophages to tumor-cytotoxic macrophages by repurposed metabolic drugs. Oncoimmunology. 10(1): 1898753. doi: 10.1080/2162402X.2021.1898753.

Parchmann, S., and M. J. Mueller. 1998. Evidence for the Formation of Dinor Isoprostanes E1from α-Linolenic Acid in Plants. J. Biol. Chem. 273:32650–32655. doi: 10.1074/jbc.273.49.32650.

Park, J., H. D. Kim, S. H. Lee, C. H. Kwak, Y. C. Chang, Y. C. Lee, T. W. Chung, J. Magae, and C. H. Kim. 2019. Ascochlorin induces caspase-independent necroptosis in LPS-stimulated RAW 264.7 macrophages. J Ethnopharmacol. 239:111898. doi: 10.1016/j.jep.2019.111898.

Park, S., J. Shin, J. Bae, D. Han, S. R. Park, J. Shin, S. K. Lee, and H. W. Park. 2020. SIRT1 Alleviates LPS-Induced IL-1beta Production by Suppressing NLRP3 Inflammasome Activation and ROS Production in Trophoblasts. Cells. 9(3). doi: 10.3390/cells9030728.

Peek, S., and T. J. Divers. 2008. Milk allergy in diseases of the teats and udder. Page 390 in Rebuhn's Diseases of Dairy Cattle. 2nd ed. Saunders Elsevier, St. Louis, MO.

Pignatelli, P., R. Carnevale, S. Di Santo, S. Bartimoccia, V. Sanguigni, L. Lenti, A. Finocchi, L. Mendolicchio, A. R. Soresina, A. Plebani, and F. Violi. 2010. Inherited Human gp91phoxDeficiency Is Associated With Impaired Isoprostane Formation and Platelet Dysfunction. Arter. Thromb. Vasc. Biol. 31:423–434. doi: 10.1161/ATVBAHA.110.217885.

Poczobutt, J. M., M. Gijon, J. Amin, D. Hanson, H. Li, D. Walker, M. Weiser-Evans, X. Lu, R. C. Murphy, and R. A. Nemenoff. 2013. Eicosanoid profiling in an orthotopic model of lung cancer progression by mass spectrometry demonstrates selective production of leukotrienes by inflammatory cells of the microenvironment. PLoS One 8:e79633. doi: 10.1371/journal.pone.0079633.

Polidori, M. C., D. Praticó, K. Savino, J. Rokach, W. Stahl, and P. Mecocci. 2004. Increased F2 isoprostane plasma levels in patients with congestive heart failure are correlated with antioxidant status and disease severity. J. Card. Fail. 10:334–338. doi: 10.1016/j.cardfail.2003.11.004.

Pratt, D.A., K. A. Tallman, and N. A. Porter. 2011. Free Radical Oxidation of Polyunsaturated Lipids: New Mechanistic Insights and the Development of Peroxyl Radical Clocks. Acc. Chem. Res. 44:458–467. doi: 10.1021/ar200024c.

Proto, J. D., A. C. Doran, G. Gusarova, A. Yurdagul Jr., E. Sozen, M. Subramanian, M. N. Islam, C. C. Rymond, J. Du, J. Hook, G. Kuriakose, J. Bhattacharya, and I. Tabas. 2018. Regulatory T Cells Promote Macrophage Efferocytosis during Inflammation Resolution. Immunity. 49(4):666-667e6. doi: 10.1016/j.immuni.2018.07.015.

Pryor, W. A., and J. P. Stanley. 1975. Suggested mechanism for the production of malonaldehyde during the autoxidation of polyunsaturated fatty acids. Nonenzymic production of prostaglandin endoperoxides during autoxidation. J. Org. Chem. 40:3615–3617. doi: 10.1021/jo00912a038.

Putman, A. K., J. L. Brown, J. C. Gandy, L. Wisnieski, and L. M. Sordillo. 2018. Changes in biomarkers of nutrient metabolism, inflammation, and oxidative stress in dairy cows during the transition into the early dry period. J. Dairy Sci. 101:9350–9359. doi: 10.3168/jds.2018-14591.

Putman, A. K., G. A. Contreras, and L. M. Sordillo. 2021. Isoprostanes in Veterinary Medicine: Beyond a Biomarker. Antioxidants (Basel). 10(2). doi: 10.3390/antiox10020145.

Raphael, W., L. Halbert, G. A. Contreras, and L. M. Sordillo. 2014. Association between polyunsaturated fatty acid-derived oxylipid biosynthesis and leukocyte inflammatory marker expression in periparturient dairy cows. J. Dairy Sci. 97:3615–3625. doi: 10.3168/jds.2013-7656.

Raphael, W., and L. M. Sordillo. 2013. Dietary polyunsaturated fatty acids and inflammation: The role of phospholipid biosynthesis. Int. J. Mol. Sci. 14:21167–21188. doi: 10.3390/ ijms141021167.

Rastani, R. R., R. R. Grummer, S. J. Bertics, A. Gümen, M. C. Wiltbank, D. G. Mashek, and M. C. Schwab. 2005. Reducing dry period length to simplify feeding transition cows: Milk production, energy balance, and metabolic profiles. J. Dairy Sci. 88:1004–1014. doi: 10.3168/jds.S0022-0302(05)72768-5.

Raychowdhury, M. K., M. Yukawa, L. J. Collins, S. H. McGrail, K. C. Kent, and J. A Ware. 1994. Alternative splicing produces a divergent cytoplasmic tail in the human endothelial

thromboxane A2 receptor. J. Biol. Chem. 269:19256–19261. doi: 10.1016/S0021-9258(17)32161-0.

Re, R., N. Pellegrini, A. Proteggente, A. Pannala, M. Yang, and C. Rice-Evans. 1999. Antioxidant activity applying an improved ABTS radical cation decolorization assay. Free Radic. Biol. Med. 26:1231–1237. doi: 10.1016/S0891-5849(98)00315-3.

Rehman, K., and M. S. H. Akash. 2017. Mechanism of Generation of Oxidative Stress and Pathophysiology of Type 2 Diabetes Mellitus: How Are They Interlinked? J. Cell. Biochem. 118:3577–3585. doi: 10.1002/jcb.26097.

Remling, N., S. Riede, P. Lebzien, U. Meyer, M. Höltershinken, S. Kersten, G. Breves, G. Flachowsky, and S. Dänicke. 2014. Effects of fumaric acid on rumen fermentation, milk composition and metabolic parameters in lactating cows. J. Anim. Physiol. Anim. Nutr. (Berl.) 98:968–981. doi: 10.1111/jpn.12152.

Ricote, M., A. C. Li, T. M. Wilson, C. J. Kelly, and C. K. Glass. 1998. The peroxisome proliferator-activated receptor-γ is a negative regulator of macrophage activation. Nature 391:79–82. doi: 10.1038/34178.

Roberts, L. J., 2nd, K. P. Moore, W. E. Zackert, J. A. Oates, and J. D. Morrow. 1996. Identification of the major urinary metabolite of the F2-isoprostane 8-iso-prostaglandin F2alpha in humans. J. Biol. Chem. 271:20617–20620. doi: 10.1074/jbc.271.34.20617.

Roberts, L. J., 2nd, T. J. Montine, W. R. Markesbery, A. R. Tapper, P. Hardy, S. Chemtob, W. D. Dettbarn, and J. D. Morrow. 1998. Formation of isoprostane-like compounds (neuroprostanes) in vivo from docosahexaenoic acid. J. Biol. Chem. 273:13605–13612. doi: 10.1074/jbc.273.22.13605.

Roberts, L. J., and J. D. Morrow. 2000. Measurement of F(2)-isoprostanes as an index of oxidative stress in vivo. Free Radic. Biol. Med. 28:505–513. doi: 10.1016/s0891-5849(99)00264-6.

Roberts, L. J., 2nd and J. P. Fessel. 2004. The biochemistry of the isoprostane, neuroprostane, and isofuran pathways of lipid peroxidation. Chem. Phys. Lipids 128:173–186. doi: 10.1111/j.1750-3639.2005.tb00511.x.

Rokach, J., S. P. Khanapure, S. W. Hwang, M. Adiyaman, J. Lawson, and G. Fitzgerald. 1997. Nomenclature of isoprostanes: A proposal. Prostaglandins 54:853–873. doi: 10.1016/s0090-6980(97)00184-6.

Rund, K. M., A. I. Ostermann, L. Kutzner, J. M. Galano, C. Oger, C. Vigor, S. Wecklein, N. Seiwert, T. Durand, and N. H. Schebb. 2018. Development of an LC-ESI(-)-MS/MS method for the simultaneous quantification of 35 isoprostanes and isofurans derived from the major n3-and n6-PUFAs. Anal. Chim. Acta 1037:63–74. doi: 10.1016/j.aca.2017.11.002.

Rustam, Y. H., and G. E. Reid. 2018. Analytical Challenges and Recent Advances in Mass Spectrometry Based Lipidomics. Anal. Chem. 90:374–397. doi: 10.1021/acs.analchem.7b04836.

Ryman, V. E., N. Packiriswamy, and L. M. Sordillo. 2015. Role of endothelial cells in bovine mammary gland health and disease. Anim Health Res Rev. 16(2):135-49. doi: 10.1017/S1466252315000158.

Ryman, V. E., N. Packiriswamy, and L. M. Sordillo. 2016. Apoptosis of Endothelial Cells by 13-HPODE Contributes to Impairment of Endothelial Barrier Integrity. Mediators Inflamm. 2016:9867138. doi: 10.1155/2016/9867138.

Ryman, V. E., N. Packiriswamy, B. Norby, S. E. Schmidt, A. L. Lock, and L. M. Sordillo. 2017. Supplementation of linoleic acid (C18: 2n -6) or alpha-linolenic acid (C18: 3n -3) changes microbial agonistinduced oxylipid biosynthesis. J. Dairy Sci. 100:1870–1887. doi: 10.3168/jds.2016-11599.

Saeed-Zidane, M., L. Linden, D. Salilew-Wondim, E. Held, C. Neuhoff, E. Tholen, M. Hoelker, K. Schellander, and D. Tesfaye. 2017. Cellular and exosome mediated molecular defense mechanism in bovine granulosa cells exposed to oxidative stress. PLoS One 12:0187569. doi: 10.1371/journal.pone.0187569.

Schirmann, K., N. Chapinal, D. M. Weary, W. Heuwieser, and M. A. von Keyserlingk. 2011. Short-term effects of regrouping on behavior of prepartum dairy cows. J. Dairy Sci. 94:2312–2319. doi: 10.3168/jds.2010-3639.

Schmiel, D. H., and V. L. Miller. 1999. Bacterial phospholipases and pathogenesis. Microbes Infect. 1:1103–1112. doi: 10 .1016/S1286-4579(99)00205-1.

Schmittgen, T. D., and K. J. Livak. 2008. Analyzing real-time PCR data by the comparative C(T) method. Nat Protoc. 3(6):1101-1108. doi: 10.1038/nprot.2008.73.

Scholz, H., A. Yndestad, J. K. Damås, T. Wæhre, S. Tonstad, P. Aukrust, and B. Halvorsen. 2003. 8-Isoprostane increases expression of interleukin-8 in human macrophages through activation of mitogen-activated protein kinases. Cardiovasc. Res. 59:945–954. doi: 10.1016/s0008-6363(03)00538-8.

Sheng, Y. and B. T. Zhou. 2017. High-throughput determination of vancomycin in human plasma by a cost-effective system of two-dimensional liquid chromatography. J. Chromatogr. A. 1499:48–56. doi: 10.1016/j.chroma.2017.02.061.

Signorini, C., S. Perrone, C. Sgherri, L. Ciccoli, G. Buonocore, S. Leoncini, V. Rossi, D. Vecchio, and M. Comporti. 2008. Plasma Esterified F2-Isoprostanes and Oxidative Stress in Newborns: Role of Nonprotein-Bound Iron. Pediatr. Res. 63:287–291. doi: 10.1203/PDR.0b013e318163a1fd.

Signorini, C., C. De Felice, T. Durand, J. M. Galano, C. Oger, S. Leoncini, L. Ciccoli, M. Carone, M. Ulivelli, C. Manna, A. Cortelazzo, J. C. Lee, and J. Hayek. 2018. Relevance of 4-F4t-neuroprostane and 10-F4t-neuroprostane to neurological diseases. Free Radic. Biol. Med. 115:278–287. doi: 10.1016/j.freeradbiomed.2017.12.009.

Sircar, D., and P. V. Subbaiah. 2007. Isoprostane Measurement in Plasma and Urine by Liquid Chromatography–Mass Spectrometry with One-Step Sample Preparation. Clin. Chem. 53:251–258. doi: 10.1373/clinchem.2006.074989.

Skoumalová, A., J. Rofina, Z. Schwippelova, E. Gruys, and J. Wilhelm. 2003. The role of free radicals in canine counterpart of senile dementia of the Alzheimer type. Exp. Gerontol. 38:711–719. doi: 10.1016/s0531-5565(03)00071-8.

Smith, G. L., N. C. Friggens, C. J. Ashworth, and M. G. G. Chagunda. 2017. Association between body energy content in the dry period and post-calving production disease status in dairy cattle. Animal 11:1590–1598. doi: 10.1017/S1751731117000040.

Sodergren, E., B. Vessby, and S. Basu. 2000. Radioimmunological measurement of F2-isoprostanes after hydrolysis of lipids in tissues. Prostaglandins Leukot. Essent. Fat. Acids 63:149–152. doi: 10.1054/plef.2000.0172.

Soffler, C., V. L. Campbell, and D. M. Hassel. 2010. Measurement of Urinary F2-Isoprostanes as Markers of in Vivo Lipid Peroxidation: A Comparison of Enzyme Immunoassays with Gas Chromatography–Mass Spectrometry in Domestic Animal Species. J. Vet. Diagn. Investig. 22:200–209. doi: 10.1177/104063871002200205.

Song, J. H., K. Fujimoto, and T. Miyazawa. 2000. Polyunsaturated (n-3) fatty acids susceptible to peroxidation are increased in plasma and tissue lipids of rats fed docosahexaenoic acid-containing oils. J. Nutr. 130:3028–3033. doi: 10.1093/jn/130.12.3028.

Sordillo, L. M., and S. C. Nickerson. 1988. Morphologic changes in the bovine mammary gland during involution and lactogenesis. Am. J. Vet. Res. 49:1112–1120.

Sordillo, L. M., and S. L. Aitken. 2009. Impact of oxidative stress on the health and immune function of dairy cattle. Vet. Immunol. Immunopathol. 128:104–109. doi: 10.1016/j.vetimm.2008.10.305.

Sordillo, L. M., G. A. Contreras, and S. L. Aitken. 2009. Metabolic factors affecting the inflammatory response of periparturient dairy cows. Anim. Health Res. Rev. 10:53–63. doi: 10.1017/S1466252309990016.

Sordillo, L. 2013. Selenium-Dependent Regulation of Oxidative Stress and Immunity in Periparturient Dairy Cattle. Veter- Med. Int. 2013:1–8. doi: 10.1155/2013/154045.

Sordillo, L. M., and V. Mavangira. 2014. The nexus between nutrient metabolism, oxidative stress and inflammation in transition cows. Anim. Prod. Sci. 54:1204–1214.

Sordillo, L. M. 2018. Oxylipids and the regulation of bovine mammary inflammatory responses. J. Dairy Sci. 101:5629–5641. doi: 10.3168/jds.2017-13855.

Sordillo, L. M. 2018. Mammary gland immunology and resistance to mastitis. Vet Clin North Am Food Anim Pract. 34(3):507-523. doi: 10.1016/j.cvfa.2018.07.005.

Swardfager, W., M. Hennebelle, D. Yu, B. D. Hammock, A. J. Levitt, K. Hashimoto, and A. Y. Taha. 2018. Metabolic/inflammatory/ vascular comorbidity in psychiatric disorders; soluble epoxide hydrolase (sEH) as a possible new target. Neurosci. Biobehav. Rev. 87:56–66. doi: 10.1016/j.neubiorev.2018.01.010.

Taber, D. F., J. D. Morrow, and L. J. Roberts. 1997. A nomenclature system for the isoprostanes. Prostaglandins 53:63–67. doi: 10.1016/s0090-6980(97)00005-1.

Takahashi, K., T. M. Nammour, M. Fukunaga, J. Ebert, J. D. Morrow, L. J. Roberts, R. L. Hoover, and K. F. Badr. 1992. Glomerular actions of a free radical-generated novel prostaglandin, 8-epi-prostaglandin F2 alpha, in the rat. Evidence for interaction with thromboxane A2 receptors. J. Clin. Investig. 90:136–141. doi: 10.1172/JCI115826.

Thompson, D. A., and B. D. Hammock. 2007. Dihydroxyoctadecamonoenoate esters inhibit the neutrophil respiratory burst. J. Biosci. 32:279–291. doi: 10.1007/s12038-007-0028-x.

Trevisi, E., M. Amadori, S. Cogrossi, E. Razzuoli, and G. Bertoni. 2012. Metabolic stress and inflammatory response in high-yielding, periparturient dairy cows. Res. Vet. Sci. 93:695–704. doi: 10.1016/j.rvsc.2011.11.008.

Tsalouhidou, S., C. Argyrou, G. Theofilidis, D. Karaoglanidis, E. Orfanidou, M. G. Nikolaidis, A. Petridou, and V. Mougios. 2006. Mitochondrial phospholipids of rat skeletal muscle are less polyunsaturated than whole tissue phospholipids: Implications for protection against oxidative stress. J. Anim. Sci. 84:2818–2825. doi: 10.2527/jas.2006-031.

Vachier, I., P. Chanez, C. Bonnans, P. Godard, J. Bousquet, and C. Chavis. 2002. Endogenous anti-inflammatory mediators from arachidonate in human neutrophils. Biochem. Biophys. Res. Commun. 290:219–224. doi: 10.1006/bbrc.2001.6155.

Valko, M., D. Leibfritz, J. Moncol, M. T. Cronin, M. Mazur, and J. Telser. 2007. Free radicals and antioxidants in normal physiological functions and human disease. Int. J. Biochem. Cell Biol. 39:44–84. doi: 10.1016/j.biocel.2006.07.001.

van der Sterren, S., and E. Villamor. 2011. Contractile effects of 15-E2t-isoprostane and 15-F2t-isoprostane on chicken embryo ductus arteriosus. Comp. Biochem. Physiol. A Mol. Integr. Physiol. 159:436–444. doi: 10.1016/j.cbpa.2011.04.010.

van Golen, R. F., M. J. Reiniers, N. Vrisekoop, P. B. Olthof, J. van Rheenen, T. M. van Gulik, B. J. Parsons, and M. Heger. 2014. The mechanisms and physiological relevance of glycocalyx

degradation in hepatic ischemia/reperfusion injury. Antioxid. Redox Signal. 21(7):1098-1118. doi: 10.1089/ars.2013.5751.

VanRollins, M., R. L. Woltjer, H. Yin, J. D. Morrow, and T. J. Montine. 2008. F2-Dihomo-isoprostanes arise from free radical attack on adrenic acid. J. Lipid Res. 49:995–1005. doi: 10.1194/jlr.M700503-JLR200.

Van 't Erve, T. J., M. B. Kadiiska, S. J. London, and R. P. Mason. 2017. Classifying oxidative stress by F2-isoprostane levels across human diseases: A meta-analysis. Redox Biol. 12:582–599. doi: 10.1016/j.redox.2017.03.024.

Verma, S., M. R. Buchanan, and T. J. Anderson. 2003. Endothelial Function Testing as a Biomarker of Vascular Disease. Circulation. 108:2054–2059. doi: 10.1161/01.CIR.0000089191.72957.ED.

Villamor, E., and G. González-Luis. 2010. Age-related changes in isoprostane-mediated relaxation of piglet blood vessels. Front. Biosci. 2:369–379. doi: 10.2741/e97.

Viola, A., F. Munari, R. Sanchez-Rodriguez, T. Scolaro, and A. Castegna. 2019. The Metabolic Signature of Macrophage Responses. Front Immunol. 10:1462. doi: 10.3389/fimmu.2019.01462.

Viviano, K., and B. VanderWielen. 2013. Effect of N -Acetylcysteine Supplementation on Intracellular Glutathione, Urine Isoprostanes, Clinical Score, and Survival in Hospitalized Ill Dogs. J. Vet. Intern. Med. 27:250–258. doi: 10.1111/jvim.12048.

Wallace, J. L. 2018. Eicosanoids in the GI tract. Br. J. Pharmacol. doi: 10.1111/bph.14178.

Wang, F., S. Zhang, R. Jeon, I. Vuckovic, X. Jiang, A. Lerman, C. D. Folmes, P. D. Dzeja, and J. Herrmann. 2018. Interferon Gamma Induces Reversible Metabolic Reprogramming of M1 Macrophages to Sustain Cell Viability and Pro-Inflammatory Activity. EBioMedicine. 30:303-316. doi: 10.1016/j.ebiom.2018.02.009.

Wang, Y., Y. Zhang, X. Chi, X. Ma, W. Xu, F. Shi, and S. Hu. 2019. Anti-inflammatory mechanism of ginsenoside Rg1: Proteomic analysis of milk from goats with mastitis induced with lipopolysaccharide. Int Immunopharmacol. 71:382-91. doi: 10.1016/j.intimp.2019.03.048.

Weidinger, A., and A. V. Kozlov. 2015. Biological Activities of Reactive Oxygen and Nitrogen Species: Oxidative Stress versus Signal Transduction. Biomolecules 5:472–484. doi: 10.3390/biom5020472.

Wendelborn, D. F., K. Seibert, and L. J. Roberts. 1988. Isomeric prostaglandin F2 compounds arising from prostaglandin D2: A family of icosanoids produced in vivo in humans. Proc. Natl. Acad. Sci. USA 85:304–308. doi: 10.1073/pnas.85.2.304.

Whitehouse, W., J. Quimby, S. Wan, K. Monaghan, R. Robbins, and L. A. Trepanier. 2017. Urinary F2-Isoprostanes in Cats with International Renal Interest Society Stage 1-4 Chronic Kidney Disease. J. Vet. Intern. Med. 31:449–456. doi: 10.1111/jvim.14634.

Wolfer, A. M., A. J. Scott, C. Rueb, M. Gaudin, A. Darzi, J. K. Nicholson, E. Holmes, and J. M. Kinross. 2017. Longitudinal analysis of serum oxylipin profile as a novel descriptor of the inflammatory response to surgery. J. Transl. Med. 15:83. doi: 10 .1186/s12967-017-1171-2.

Woodward, D. F., R. L. Jones, and S. Narumiya. 2011. International Union of Basic and Clinical Pharmacology. LXXXIII: Classification of Prostanoid Receptors, Updating 15 Years of Progress. Pharmacol. Rev. 63:471–538. doi: 10.1124/pr.110.003517.

Xu, S., B. Jiang, K. A. Maitland, H. Bayat, J. Gu, J. L. Nadler, S. Corda, G. Lavielle, T. J. Verbeuren, A. Zuccollo, and R. A. Cohen. 2006. The thromboxane receptor antagonist S18886 attenuates renal oxidant stress and proteinuria in diabetic apolipoprotein E-deficient mice. Diabetes 55:110–119. doi: 10.2337/diabetes.55.01.06.db05-0831.

Yanting, C., Q. Y. Yang, G. L. Ma, M. Du, J. H. Harrison, and E. Block. 2018. Dose- and type-dependent effects of long-chain fatty acids on adipogenesis and lipogenesis of bovine adipocytes. J. Dairy Sci. 101:1601–1615. doi: 10.3168/jds.2017-13312.

Yeh, Y. C., T. J. Liu, and H. C. Lai. 2020. Pathobiological Mechanisms of Endothelial Dysfunction Induced by tert-Butyl Hydroperoxide via Apoptosis, Necrosis and Senescence in a Rat Model. Int. J. Med. Sci. 17(3): 368-382. doi: 10.7150/ijms.40255.

Yukawa, M., R. Yokota, R. T. Eberhardt, L. Von Andrian, and J. A. Ware. 1997. Differential desensitization of thromboxane A2 receptor subtypes. Circ. Res. 80:551–556. doi: 10.1161/01.res.80.4.551.

Yura, T., M. Fukunaga, R. Khan, G. N. Nassar, K. F. Badr, and A. Montero. 1999. Free-radical-generated F2-isoprostane stimulates cell proliferation and endothelin-1 expression on endothelial cells. Kidney Int. 56(2):471-8. doi: 10.1046/j.1523-1755.1999.00596.x.

Zobel, G., D. M. Weary, K. E. Leslie, and M. A. von Keyserlingk. 2015. Invited review: Cessation of lactation: Effects on animal welfare. J. Dairy Sci. 98:8263–8277. doi: 10.3168/jds.2015-9617.

Zou, Y., Y. Wang, Y. Deng, Z. Cao, S. Li, and J. Wang. 2017. Effects of feeding untreated, pasteurized and acidified waste milk and bunk tank milk on the performance, serum metabolic profiles, immunity, and intestinal development in Holstein calves. J. Anim. Sci. Biotechnol. 8:53. doi: 10.1186/s40104-017-0182-4.